

## Article

# Wind and Solar Energy for Sustainable Energy Production for Family Farms in Coastal Agricultural Regions of Libya Using Measured and Multiple Satellite Datasets

Hamza S. Abdalla Lagili <sup>1,2</sup>, Aşkın Kiraz <sup>2</sup>, Youssef Kassem <sup>3,4,5,\*</sup> and Hüseyin Gökçekuş <sup>4,5</sup>

<sup>1</sup> High and Intermediate Institute of Agricultural Technology, Gheran, Libya; hamzasalem409@gmail.com

<sup>2</sup> Ataturk Faculty of Education, Near East University, Via Mersin 10 Turkey, Nicosia 99138, Cyprus; askin.kiraz@neu.edu.tr

<sup>3</sup> Department of Mechanical Engineering, Engineering Faculty, Near East University, Via Mersin 10 Turkey, Nicosia 99138, Cyprus

<sup>4</sup> Department of Civil Engineering, Civil and Environmental Engineering Faculty, Near East University, Via Mersin 10 Turkey, Nicosia 99138, Cyprus; huseyin.gokcekus@edu.neu.tr

<sup>5</sup> Energy, Environment, and Water Research Center, Near East University, Via Mersin 10 Turkey, Nicosia 99138, Cyprus

\* Correspondence: yousseuf.kassem@neu.edu.tr or youssef.kassem1986@hotmail.com; Tel.: +90-(392)-2236464

**Abstract:** Generating electricity from renewable energy instead of fossil fuels brings great benefits to the environment and sustainable development. Thus, assessing the potential of wind and solar energy in agricultural coastal areas can identify sustainable energy solutions for meeting energy demand and producing fresh water for agricultural applications and domestic use. However, it is difficult to accurately assess the wind and solar energy potential in Libya due to the civil war, lack of measured data, and its limited availability. Consequently, this concise work is unique because it is the first to use daily measurement data from Az-Zāwiyah, Libya, for evaluating wind and solar energy based on one year of measured data for 2022. Moreover, the present study aims to investigate the potential of wind and solar energy as promising renewable sources for meeting energy demand in coastal agricultural regions in Libya using multiple datasets for the first time. In this paper, five satellite products (TerraClimate, ERA5, ERA5-Land, MERRA-2, and CFSR) were assessed and compared against measured data for January 2022–December 2022 to understand their suitability, accuracy, and reliability. The results showed that CFSR and ERA5-Land demonstrate the most favorable performance for assessing the wind resource, while all satellite products can be utilized for preliminary solar resource assessment. Then, the assessment of wind and solar resources was evaluated in five agricultural coastal regions (Aljmail, Az-Zāwiyah, Castelverde, Msallatah, and Sabratah) based on the best satellite product for the period of 2000–2022. Furthermore, the performance of the wind and solar power systems was investigated for typical farms, which were chosen to estimate the required energy demand according to daily electrical consumption. The results show that the positive outcomes of implementing these systems were highlighted, with an emphasis on their potential benefits to the entire Libyan agricultural sector. Accordingly, scaling up and generalizing the proposed systems and generalizing them to include all farms in Libya could have a significant impact on national electricity generation, mitigate greenhouse gases, and contribute to the development of the agricultural sector and the country's economy.



**Citation:** Lagili, H.S.A.; Kiraz, A.; Kassem, Y.; Gökçekuş, H. Wind and Solar Energy for Sustainable Energy Production for Family Farms in Coastal Agricultural Regions of Libya Using Measured and Multiple Satellite Datasets. *Energies* **2023**, *16*, 6725. <https://doi.org/10.3390/en16186725>

Academic Editors: David Borge-Diez and Prafula Pearce

Received: 10 August 2023

Revised: 13 September 2023

Accepted: 18 September 2023

Published: 20 September 2023



**Copyright:** © 2023 by the authors. Licensee MDPI, Basel, Switzerland. This article is an open access article distributed under the terms and conditions of the Creative Commons Attribution (CC BY) license (<https://creativecommons.org/licenses/by/4.0/>).

**Keywords:** Libya; family farm; agricultural coastal region; satellite products; wind energy assessment; solar energy assessment; wind and solar power system

## 1. Introduction

The heavy reliance on conventional fuels, such as coal, oil, and gas, not only dramatically burdens the national economy but also gives rise to various environmental challenges

such as global warming, carbon emissions, and unpredictable weather conditions [1,2]. Excessive use of conventional energy sources, especially for power generation and transportation, has released large amounts of carbon dioxide (CO<sub>2</sub>) into the atmosphere, leading to the depletion of natural resources [3]. Furthermore, the rising energy demand, the impacts of global warming and climate change, and growing fossil fuel consumption have prompted a transition from conventional fuels to renewable energy sources. Renewable energy resources represent the most promising and effective approach to reducing greenhouse gases and related environmental issues [4]. Recently, numerous studies have focused on evaluating the potential of renewable energy, particularly wind and solar energy, as a clean and sustainable source for electricity generation in various regions/countries around the world. For instance, Potić et al. [5] explored the electricity production potential from wind energy in the Municipality of Knjaževac, located in East Serbia, by employing a combination of the Analytic Hierarchy Process (AHP) and Geographic Information Systems (GISs). Mohamadi et al. [6] investigated the potential of wind energy for electricity production in eastern parts of Iran. Dehghani-Sanij et al. [7] evaluated wind energy potential in terms of installed capacity, generation, capacity factor, and levelized cost of energy in Canada. Kassem et al. [8] evaluated the potential of the solar power system at Near East University Hospital, Northern Cyprus, as an energy source to meet the energy demand during the daytime to reduce energy bills. Maammour et al. [9] investigated the performance of solar power systems for farming families in the northwest of Algeria to reduce national electricity consumption. Ayadi et al. [10] investigated the techno-economic feasibility of a grid-connected solar power system for the University of Jordan to decrease electricity consumption and costs associated with the university's energy usage. Additionally, Al-Najideen and Alrwashdeh [11] designed a solar power system to cover the electricity demand for Mu'tah University in Jordan. Elnaggar et al. [12] evaluated the economic viability of wind energy potential in Gaza, Palestine, for solving the shortage of energy supplies.

In the end, limited energy resources have led to exploring alternative energy sources for solving the energy crisis, especially in developing countries. Renewable energy consumption is widely regarded as less environmentally harmful than the consumption of non-renewable energy. As a result, there is a growing recognition of the importance of transitioning towards sustainable energy solutions to mitigate environmental impacts and ensure long-term energy availability.

### *1.1. Electrical Energy Situation in Libya*

Libya is located in North Africa. Libya's main source of energy has been its vast reserves of oil. The country possesses significant oil reserves, making it one of the largest oil producers in Africa. Libya's electricity sector is dominated by fossil fuels, particularly natural gas and oil. The General Electricity Company of Libya (GECOL) holds the responsibility for overseeing the electricity system in Libya. As a state-owned entity, GECOL manages and supervises various aspects, including generation, transmission, distribution, and network systems [13]. However, GECOL faces substantial challenges in fulfilling its mission, with the most pressing issue being its inability to consistently provide customers with the required quantity and quality of electricity [14]. According to Sorensen [15], Libya heavily relies on fossil fuels as the primary source of electricity generation. Libya possesses significant reserves of both natural gas and oil, making them the key energy sources for electricity production [15].

In 2018, electricity generation in Libya relied heavily on natural gas, accounting for about 98% of the total, while the remaining 2% was sourced from oil-fired power facilities according to the International Energy Agency. Additionally, the country has large reserves of natural gas, which are mainly used to operate power plants and provide household heating and cooking needs.

In general, there are eight major thermal power plants distributed across the country [16]. Among these, the largest is Al-Khoms, located along the Mediterranean coast east of Tripoli,

and it has a large capacity of 2500 megawatts. Other important thermal power plants include the Zawiya station near the city of Zawiya with a capacity of 1200 MW and the West Tripoli station with a capacity of 1000 MW. Besides these major facilities, smaller power plants, including diesel and gas turbine units, are spread across different regions of the country.

Recently, Libya has witnessed rapid population growth and large-scale construction activities, resulting in high energy demand. As per GECOL, the country's installed generation capacity in 2020 stood at approximately 7.5 GW, with a peak demand of around 7 GW [17]. In addition, electricity consumption in Libya varies depending on the region and level of economic development. According to the World Bank, Libya's per capita electricity consumption in 2019 was about 1100 kilowatt hours per year, which is relatively low compared to neighboring countries. This can be partly attributed to the challenges faced by the country's electricity sector, including frequent power outages and unreliable supply [18].

Furthermore, the cost of electricity for households in Libya fluctuates depending on regional disparities and consumption levels. The Libyan government extends substantial subsidies to ensure affordable electricity for households, fostering economic growth. Nonetheless, these subsidies strain the government's budget, raising concerns about their long-term viability amid persistent economic challenges. In Libya, the cost of domestic electricity stands at approximately LYD 0.09 per kWh, roughly equivalent to USD 0.06 per kWh. This cost is comparatively low compared to neighboring countries with lesser government subsidies, where electricity expenses tend to be higher.

Moreover, the ongoing conflict and instability in Libya have disrupted natural gas production and distribution, resulting in shortages and electricity supply disruptions [19]. Furthermore, the deterioration of oil infrastructure and a decline in oil production have significantly constrained the availability of fuel for oil-fired power plants [16]. Consequently, Libya's power plants operate significantly below their capacity, leading to frequent power outages and load shedding [19].

### *1.2. Renewable Energy Situation in Libya*

Libya has significant potential in renewable energy resources, especially solar and wind energy. The country benefits from abundant year-round sunshine and consistent coastal winds. However, the full realization of Libya's renewable energy potential has been hampered by political instability, security issues, and entrenched dependence on fossil fuels. Nevertheless, there have been noteworthy endeavors to harness renewable energy sources in Libya.

Wind energy shows promise, especially along Libya's coastal areas, which enjoy favorable wind conditions. The eastern coastal areas boast wind speeds of up to 10 m per second, making them ideal for efficient electricity generation. This renewable source has the potential to significantly boost Libya's energy mix, given the country's continued heavy reliance on fossil fuels. The European Union Joint Research Center (JRC) estimates that Libya's wind energy potential is 35 GW, with 10 GW being sufficient to meet the country's current electricity demand, according to the Renewable Energy and Energy Efficiency Authority (REEEA) of Libya. In 2018, Libya opened its first wind farm, the 1.25 MW Al-Fattayah Wind Farm, with plans underway to establish additional wind farms along the coast and elsewhere [20–22].

Furthermore, Libya's position within the Sahara desert region endows it with extensive solar energy potential. The National Renewable Energy Authority (NREA) reveals a daily solar energy potential of 6.5 kWh/m<sup>2</sup>, among the highest in the world. Also, the European Commission's Joint Research Centre (JRC) estimates that Libya contributes 20% to the Mediterranean region's total solar energy potential of 332 TWh/year [23]. Additionally, the International Renewable Energy Agency (IRENA) calculates North Africa's solar potential at 2600 TWh/year, with Libya accounting for 1050 TWh/year [24]. Private-sector initiatives have also entered the scene, with companies like Solar Energy Solutions (SES) planning a

50 MW solar power plant in Sabha and the LEC aiming for a colossal 500 MW solar power plant in Sebha, both poised to significantly augment Libya's electricity mix while reducing its fossil fuel dependency [25,26].

Numerous scientific researchers have investigated the potential of renewable energy including wind and solar energy in different sites in Libya as shown in Table 1. Based on the findings, it can be concluded that:

- Most of the scientific researchers have focused on addressing the current and future situation of renewable energy in the country.
- Most scientific researchers have analyzed the characteristics of wind speed at a specific region based on the NASA dataset or actual data measured before 2012.
- Several studies have investigated the economic viability of a grid-connected PV/wind/hybrid renewable system.
- Regarding the literature review, it is found that Libya has high wind and solar energy potential. Nevertheless, Libya's renewable energy potential is hampered by challenges such as legal, political, economic, and financial barriers.

**Table 1.** Summary of previous studies related to renewable energy in Libya.

Reference	Year	Location	Description of the Study	Main Finding
[27]	1995	Zwara	Analyzing the wind speed characteristics using WASP software for wind farm installation	The mean wind speed and wind power density at the selected region are 6.9 m/s and 399 W/m <sup>2</sup> , respectively
[28]	2003	Libya's coastal region	Design of seawater reverse osmosis desalination plants driven by wind and solar energy	The levelized water cost was estimated to be 1.8 EUR/m <sup>3</sup> and 1.9 EUR/m <sup>3</sup> for scenario 1 (Grid + Wind energy conversion) and scenario 2 (Grid + PV)
[29]	2003	Zwara	Evaluation of the preliminary feasibility study for the proposed pilot wind farm with a capacity of 6 MW	The project demonstrates economic viability and feasibility
[30]	2006	Libya	Highlighting the applications of renewable energy, the available resources, and prospects for the use of renewable energy resources in the country	Photovoltaic systems have great potential for diverse applications, especially for supplying electricity to remote areas, supported by economic and technical justifications
[31]	2010	Ghariat, Obari, Tazerbo, Derna, Sebha, Shahat, Ghat, Misurata, Jaghboub, Hon, Agedabia, Alkomes, Elkufra, Benina, Jalo, Zuara, Sirt, Tubrk, Ghadames, Tripoli, Airport, Nalut, Yefran	Analyzing statistically the wind speed data of 22 metrological stations using Type I extreme value probability distribution	The country can be divided into four zones with a 50-year return period
[32]	2011	Mrair-Gabis Village	Investigating the potential of utilizing the renewable power system with various configuration options for small-scale seawater reverse osmosis desalination units using HOMWER software	PV/diesel generators/batteries are the best options to generate electricity for small-scale seawater reverse osmosis desalination units
[33]	2012	Libya	Developing renewable hybrid energy systems as power sources for mosques using HOMER software	PV/diesel generators/batteries are the best options to generate electricity

Table 1. Cont.

Reference	Year	Location	Description of the Study	Main Finding
[34]	2012	Dernah, Tolmetha, Al-maqrum, Sirt, and Misratah	Addressing the impact of the penetration of wind power on the Libyan power system. Additionally, investigating the wind energy potential using Weibull distribution functions during the period of 1979–1989.	The inclusion of wind generation has been proven to enhance the reliability of power systems
[35]	2013	Libya	Investigating the present and future utilization of renewable energy (wind and solar) in the country	The country has high wind and solar energy potential. Nevertheless, Libya’s renewable energy potential is hampered by challenges such as legal, political, economic, and financial barriers.
[36]	2013	Derna	Evaluating the wind speed characteristics using the Weibull distribution function from 2000 to 2009	Using small-scale wind turbines with lower rated speeds will produce more power than higher-rated speeds at the same hub height
[37]	2013	Libya	Presenting analytical data on the current and future energy conditions and discussing the challenges and obstacles facing the renewable energy sector in Libya	Libya has huge potential to harness renewable energy through home grid-connected PV systems, large-scale grid-connected wind farms, and concentrated PV systems
[38]	2014	Misurata	Assessing the economic viability of a hybrid system (PV/diesel generator/battery) as a power source for the school using HOMER software	Excess power from the proposed system in spring, summer, and autumn can be used to reduce the cost of energy or can be sold to the grid
[39]	2014	Dernah, Musrata, Zuara, and Sebha	Assessing the wind energy potential using the Weibull distribution function	Dernah has the highest maximum energy production compared to other locations
[40]	2014	Benina-Benghazi	Analyzing the wind speed data statistically using the Weibull distribution function for the year 2008	The energy density of wind is estimated at 415.82 W/m <sup>2</sup> at a height of 10 m, which corresponds to wind energy class 4
[41]	2015	Dernah	Evaluate the environmental impact of the wind farm in the selected region	Wind energy stands out for producing the lowest levels of carbon dioxide emissions when compared to fossil fuels and other renewable energy sources
[42]	2015	Libya	Providing analytical data for the current and future energy situation in the country as well as addressing the challenges and obstacles faced by the renewable energy sector	Solar resources offer immense potential in comparison to wind energy, particularly after considering oil and natural gas
[43]	2016	Libya	Investigating what is available to the energy sector regarding the use of renewable energy (wind and solar energy) as an alternative energy source	The renewable energy sector could help to cover the energy demand and reduce the amount of CO <sub>2</sub> in the country

Table 1. Cont.

Reference	Year	Location	Description of the Study	Main Finding
[44]	2016	AL-Maqrun Town	Investigating the wind energy potential and the performance of large-scale wind turbines based on year data (2002–2003)	Utilizing wind turbines with power rated higher than 1 MW could help reduce the energy demand and greenhouse gas emissions
[45]	2016	Al-Zawiya	Studying the impact of wind energy integration on the refinery's energy system to meet the refinery's demand	The integrated system would help to cover the energy demand, reduce CO <sub>2</sub> emissions, and improve the economy
[46]	2016	Libya	Examining the existing utilization and prospects of renewable energy in Libya, alongside exploring the challenges and opportunities for investment in this sector	The availability of renewable energy complements peak loads and current energy demand, making wind and solar projects attractive for Libya
[47]	2016	Al-Fattaih-Darnah	Studying the wind energy potential using the Weibull distribution function during the year 2003	The annual wind power density of the region is categorized as class 3
[48]	2017	Tarhuna, Misalatha, Goterria, Assaba, Assaba, EL-Magrun, and Dernah	Analyzing statistically the wind speed data from seven locations using the Weibull distribution function from 2007 to 2008 and 2002 to 2004	Misalatha and Asaaba are suitable regions for the installation of the wind farm based on the economic feasibility results
[49]	2017	Benina-Benghazi	Investigating the technical and economic feasibility of a solar water heating system using RETScreen software	Solar water heating systems are economically viable and can lead to fuel savings and a reduction in CO <sub>2</sub> emissions
[50]	2018	Libya	Evaluating the potential implementation of concentrating solar power plants for electric production	The results are promising for implementing economically competitive concentrating solar power plants in the country
[51]	2018	Libya	Assessing the present state of energy resources and exploring the future potential of renewable energy sources, along with discussing upcoming projects aimed at harnessing these sustainable resources	Libya has great potential for renewable energy, especially in solar and wind energy resources
[52]	2019	University of Al-Marj	Design a wind–solar hybrid power generation system in Libya using HOMER software	The most feasible economical design to supply an average load connected to the grid was identified as the installation of ten wind turbines and solar PV with capacities of 100 kW and 150 kW, respectively
[53]	2019	Zwara	Estimating the monthly and annual wind power density for 2007 using the Weibull distribution function	Small-scale wind turbines can be considered suitable for generating electricity from wind energy

Table 1. Cont.

Reference	Year	Location	Description of the Study	Main Finding
[54]	2019	Hun	Analyzing the wind energy resource potential using the Weibull distribution function and investigating the performance of wind turbines during the period of 2011–2012	The selected region is suitable for developing wind farms using class III/B wind.
[55]	2019	Tripoli, Nault, and Esspeea	Analyzing the characteristics of wind speed using ten distribution functions based on monthly data for the period of 1981–2010	Small-scale wind turbines can be utilized for producing electricity from wind energy
[56]	2020	Libya	Review the future of solar and wind energy as alternative sources in Libya	The country has high wind and solar energy potential. However, the implementation and development of renewable energy technologies in Libya face a range of challenges and barriers, including legal, political, economic, and financial obstacles.
[57]	2020	Libya	Providing the status of renewable energy and benefits from it and explaining strategies to enhance future applications and electricity generation to support the energy sector	Libya has a huge potential for solar and wind energy, but the use of renewable energy in consumption is almost non-existent
[58]	2020	Libya	Analyzing the potential of solar and wind energy for producing hydrogen	The northeastern and southern parts of the country are advised to exploit wind and solar energy, respectively, for hydrogen production
[59]	2020	Libya	Addressing the status of renewable energy and its benefits and explaining strategies to enhance its future applications	Solar energy can be considered as the best possible renewable energy source, but it is very difficult to develop and improve its use as a clean energy source in the country
[60]	2020	Tripoli, Nalut, Espiaa, Al bayda, Benghazi, Al-kufrah, Misratah, Sabha, Darnah	Evaluating the wind and solar energy at nine locations as well as the techno-economic feasibility of wind and solar projects based on the NASA dataset	Al Kufra is the best place for installing solar plants due to the high value of solar radiation. Benghazi and Darnah are suitable places for large-scale wind farm installations in the future.
[61]	2020	Al Butnan, Al Jabal al Akhdar, Al Jabal al Gharbi, Al Jifarah, Al Jufrah, Al Kufrah, Al Marj, Al Marqab, Al Wahat, An Nuqat al Khams, Az Zawiyah, Benghazi, Darnah, Ghat, Misratah, Murzuq, Nalut, Sabha, Surt, Tripoli, Wadi al Hayat, and Wadi ash Shati'	Evaluating solar energy potential based on the NASA dataset and developing solar systems using RETScreen software	The southern part of Libya has high solar potential compared to other parts. Al Kufrah demonstrated the best option for the construction of a large-scale solar plant to generate electricity from solar energy compared to other regions.

Table 1. Cont.

Reference	Year	Location	Description of the Study	Main Finding
[62]	2021	Benghazi	Evaluating the techno-economic feasibility of small-scale PV/storage/diesel distributed generation for reliable electric power supply in local communities using HOMER software	The most feasible economical design system was found to be the PV-battery system as compared to the diesel generator option
[63]	2021	Libya	Providing a broad review of the energy situation in Libya and evaluating the potential of available renewable energy (wind, solar, biomass, wave, and geothermal energy)	Wind and solar energy are major contributors to the displacement of fossil fuels for energy production
[64]	2021	Libya	Providing solar photovoltaic status, utilization, and proposed strategies to enhance future applications and electricity generation	The country has a high potential for solar energy and government strategy is crucial to support PV market growth
[65]	2021	Espiaa, Msallata, Alqatrun, and Adirsiyah	Evaluating the wind energy potential using Weibull distribution. Three approaches were used to estimate the Weibull parameters.	The highest and lowest values of wind power density were obtained at Msallata and Adirsiyah with a value of 418.502 W/m <sup>2</sup> and 77.993 W/m <sup>2</sup> , respectively, at a height of 20 m
[66]	2021	Zawia	Developing a utility-scale wind farm with a total estimated power of 20 MW to reduce the GHG emissions associated with oil refinery facilities in the selected region	The wind farm could potentially avoid around 2 MtCO <sub>2</sub> of CO <sub>2</sub> emissions
[67]	2021	Tobruk, Derna, Benghazi, Ajdabiya, Sirt, Misrata, and Tripoli	Assessing the wind potential at seven locations using the Weibull distribution function based on simulation data	The highest energy production and capacity factors are obtained from Derna, Tobruk, and Misrata
[68]	2021	Sabha, Obari, Alqtroun, and Hun	Evaluate the potential of wind energy as a power source using the Weibull distribution function	Sabha demonstrated the best option for generating electricity from wind compared to other regions
[69]	2021	Aljofra	Assessing the economic feasibility of solar energy using SAM software	PV and concentrated solar power systems can be considered the most promising technologies for generating electricity
[70]	2021	Libya	Addressing the necessity of replacing fossil fuels with renewables and providing a detailed analysis of the cost of solar and wind power, along with future trends	Wind and solar energy play a significant role in displacing fossil fuels for energy production
[71]	2023	Azzizia, Assabaa, Tarhuna, Mslata, Misurata, Sirte, Magrun, Tulmitha, Derna, Ejdabia, Bennina, Surman, Zwara, and Triboli	Selecting the best site for the installation of a wind farm using a hybrid multi-criteria approach	Derna and Tarhuna were suitable regions for wind farm installation in the country

Table 1. Cont.

Reference	Year	Location	Description of the Study	Main Finding
[72]	2023	Kufra, Benghazi, Tripoli, Tobruk, Sabha, and Mesrata	Finding the best location for installing solar plants in the country using the Grey-TOPSIS method	Mesrata is a suitable location for installing the solar plant

### 1.3. Scope of Present Work

Regarding the literature review, agricultural production was greatly reduced due to the civil war and restrictions on the supply network for pumping groundwater. In addition, the limited availability of suitable water for irrigation and domestic use has exacerbated the challenges faced by farmers. Moreover, implementing renewable energy systems can offer a potential solution to address the challenges mentioned based on the literature review on this subject [73–75]. Renewable energy systems have been recognized as a cost-effective alternative that is relatively easy to maintain and operates without emitting harmful greenhouse gases.

According to the authors' review, no research has been carried out on the utilization of renewable energy systems to fulfill the energy demands of irrigation water pumping systems and households in Libya. Therefore, the main purpose of this study is to evaluate wind and solar energy systems in coastal agricultural areas in Libya to meet the energy needs of family farms for electricity generation and fresh water for crop irrigation. Moreover, in the majority of the existing literature (Table 1), the primary focus lies in the assessment of wind and solar energy using either the NASA dataset or pre-2012 actual measurements. Nevertheless, it is crucial to note that no study to date has undertaken an evaluation of satellite-derived data for conducting technical and economic analyses of wind and solar systems in Libya. Therefore, this research seeks to address this gap by systematically evaluating the suitability, accuracy, and reliability of data obtained from different satellite sources and comparing them with measured data. Furthermore, a comprehensive technical and economic analysis of wind and solar energy systems in coastal areas of Libya is proposed. This analysis relies on measured data and multiple satellite datasets, providing a comprehensive perspective on the feasibility and efficiency of these renewable energy solutions.

To achieve these objectives, the following strategies and methodologies have been implemented.

- For evaluating the wind energy potential:
  - The wind speed characteristics in Az-Zāwiyah were analyzed using measured wind speed data for January 2022–December 2022. The data were measured with an Ambient Weather WS-2902 Home WiFi Weather Station. It should be noted that the device was placed in a treeless, unshaded area to ensure unobstructed exposure to the full range of ambient weather conditions. This unobstructed positioning ensures accurate measurements and a reliable collection of weather data.
  - The analysis of wind speed distribution plays a crucial role in assessing the wind energy potential in a particular area. However, evaluating wind energy potential can be challenging in areas without sufficient measurements. Therefore, utilizing data coming from satellite measurements and reanalysis datasets becomes essential in investigating wind resource assessment. The study's objective is to assess the accuracy and reliability of five satellite-based wind products by comparing them against observed data obtained from the Az-Zāwiyah region.
  - Utilizing the most reliable satellite-based wind product, the assessment of wind resources in five agricultural coastal regions was conducted by analyzing the average monthly data for a long period.

In this study, thirteen distribution models were employed to analyze the wind speed characteristics and evaluate the wind energy potential at the selected locations. The parameters of the distribution functions were calculated using the maximum likelihood method. The power law model was applied to determine the average wind speed at different heights. Additionally, the wind power density was estimated for each location. Furthermore, the technical performance of various types of wind turbines was evaluated. The assessment of the wind turbine's technical performance involves determining factors such as energy production, capacity factor, simple payback period, and levelized cost of electricity.

- For evaluating the solar energy potential:
  - The solar radiation data in Az-Zāwiyah were analyzed using measured wind speed data for January 2022–December 2022. The data were measured using an Ambient Weather WS-2902 Home WiFi Weather Station.
  - Solar radiation is an essential factor for assessing the potential and estimating the power output of solar PV applications. Satellite data can be used as an alternative for solar resource assessment in areas where measured data are unavailable. Thus, it is essential to evaluate the performance of these alternative data sources to ensure their accuracy and reliability. The study aims to evaluate the accuracy and reliability of five satellite-based wind products by comparing them with the observed data obtained from the Az-Zāwiyah region.
  - Utilizing the most reliable satellite-based solar products, the assessment of solar resources in five agricultural coastal regions was conducted by analyzing the average monthly long-period dataset.

This study introduces a novel contribution by focusing on evaluating the feasibility of implementing wind and PV systems to generate electricity for domestic consumption and simultaneously produce freshwater for crop irrigation in coastal agricultural areas in Libya.

## 2. Materials and Methods

The proposed methodology aims to assess the wind and solar energy potential in agricultural coastal regions in Libya. Additionally, the study aims to determine the viability of utilizing these renewable energy sources to meet the energy needs of family farms in these areas. By reducing reliance on fossil fuel-based energy sources, the agricultural sector can transition towards a more sustainable energy system. Figures 1 and 2 illustrate the proposed methodology and diagram of the PV/wind system for family farms, respectively.

### 2.1. Study Area

Libya (Figure S1 in the Supplementary Materials) is a country located in North Africa on the Mediterranean coast. It has a diverse climate influenced by its geographical location and the Sahara Desert to the south. In general, the northern coastal region experiences a Mediterranean climate. Moreover, the southern part of Libya is covered by the vast expanse of the Sahara Desert. In this study, five coastal agricultural regions in Libya, particularly along the Mediterranean coast, were selected. These locations are Az-Zāwiyah, Sabratah, Castelverde, Tajoura, Msallatah, Janzur, and Aljmail. They are located on the northwestern coast of Libya. They experience a Mediterranean climate with some influences from the Sahara Desert. The weather is generally mild, with hot summers and mild winters. Also, they receive most of their rainfall between October and March. However, the amount of rainfall is generally low. The geographic locations and comprehensive geographic details of the selected locations are presented in Figure 3 and Table 2, respectively. It should be noted that all the selected locations have agricultural potential for vegetable planting due to their moderate climate and access to water resources. Farmers cultivate a range of crops, including vegetables, fruits, and grains in these locations.

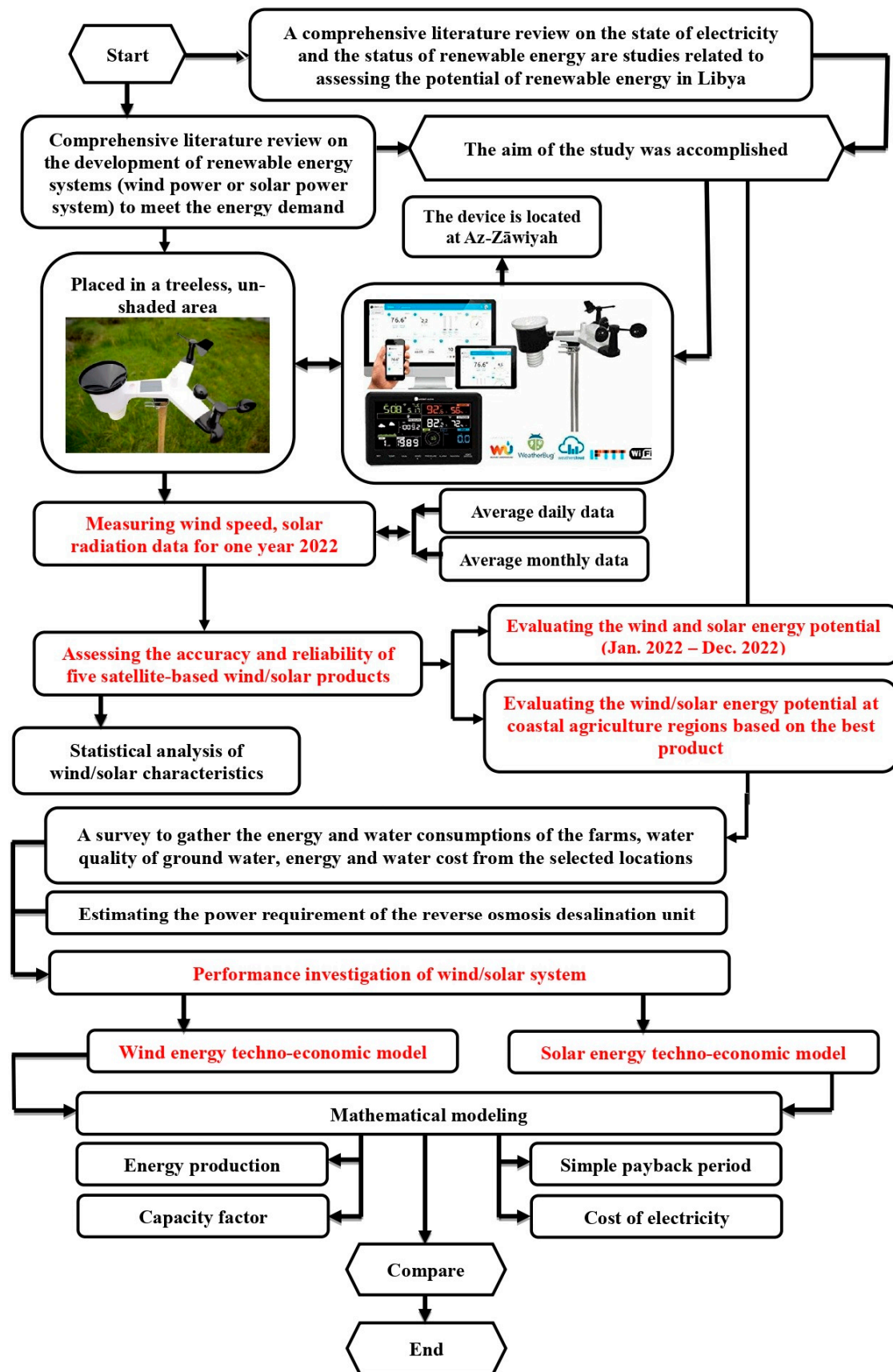


Figure 1. Flowchart of the proposed methodology.

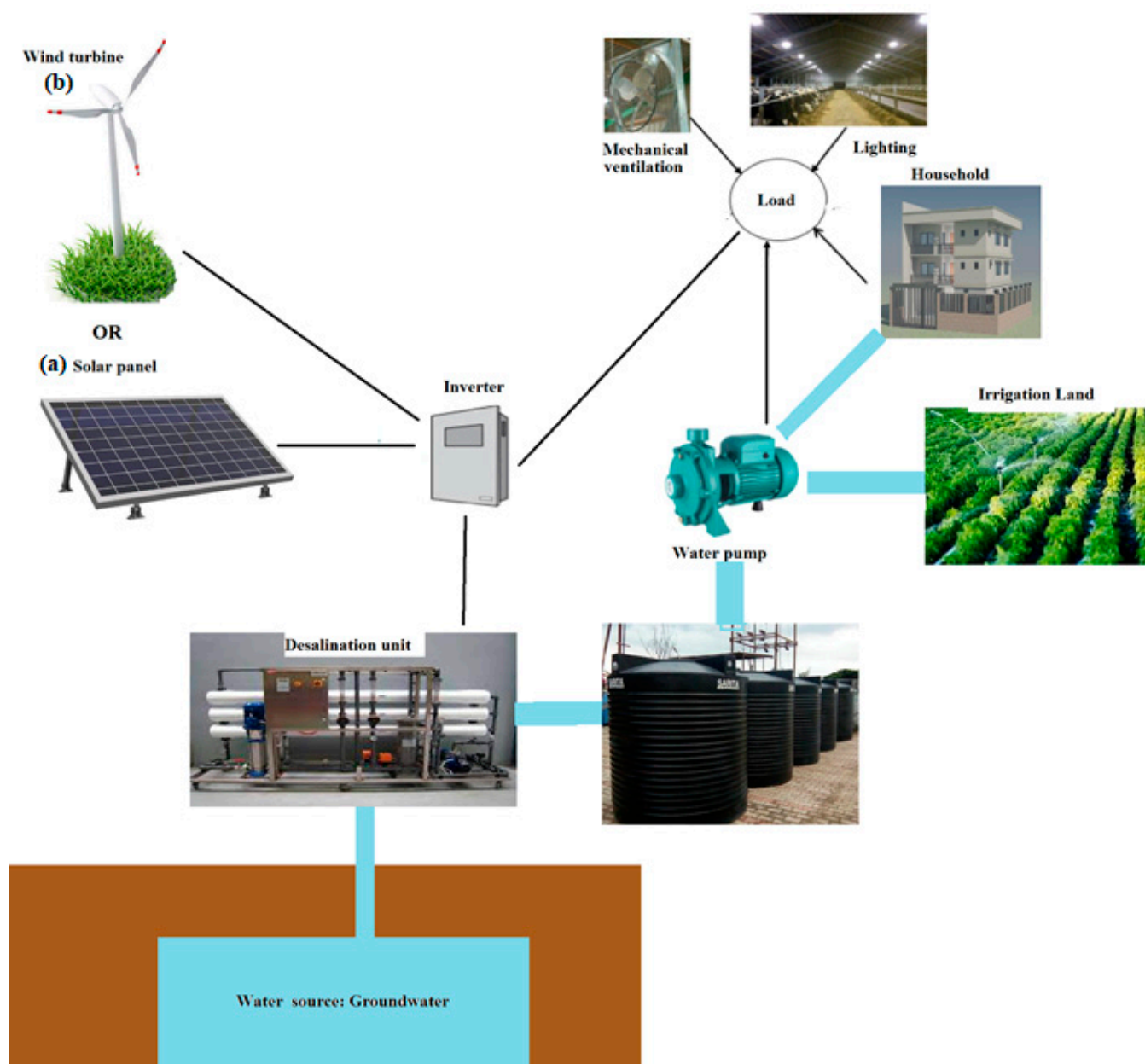


Figure 2. Diagram of (a) PV and (b) wind system for agriculture farms.

Table 2. Geographic details of the selected locations.

Location	Latitude (° N)	Longitude (° E)	Elevation (m)
Aljmail	32.856	12.058	2
Az-Zāwiyah	32.763	12.736	20
Castelverde	32.750	13.717	40
Msallatah	32.582	14.151	166
Sabratah	32.781	12.450	4

## 2.2. Data on Agricultural Farms through the Survey

After a comprehensive analysis of the existing literature, a simple survey was conducted in the selected sites to evaluate data on agricultural farms and collect insights from farm owners. A mixed-methods survey was employed, combining qualitative and quantitative approaches, to gather data. The survey included direct questions, incorporating both multiple-choice options and open-ended inquiries. Due to the civil war, the data

collection of load, water quality, and cost in Libya relies on farmers, which makes obtaining individual data for each farm directly from the government companies impractical. It is important to acknowledge that in Libya, the collection of data including load, water quality, and cost depends on the farmers themselves. As a result, obtaining individual data of farms directly from state companies is challenging and impractical due to the ongoing civil war situation. It is important to mention that the authors chose the largest farm in the selected location for analysis, and it is worth noting that most of the farms in the country share similar specifications. The following are the main characteristics of most farms in the coastal regions of Libya which are discussed below.

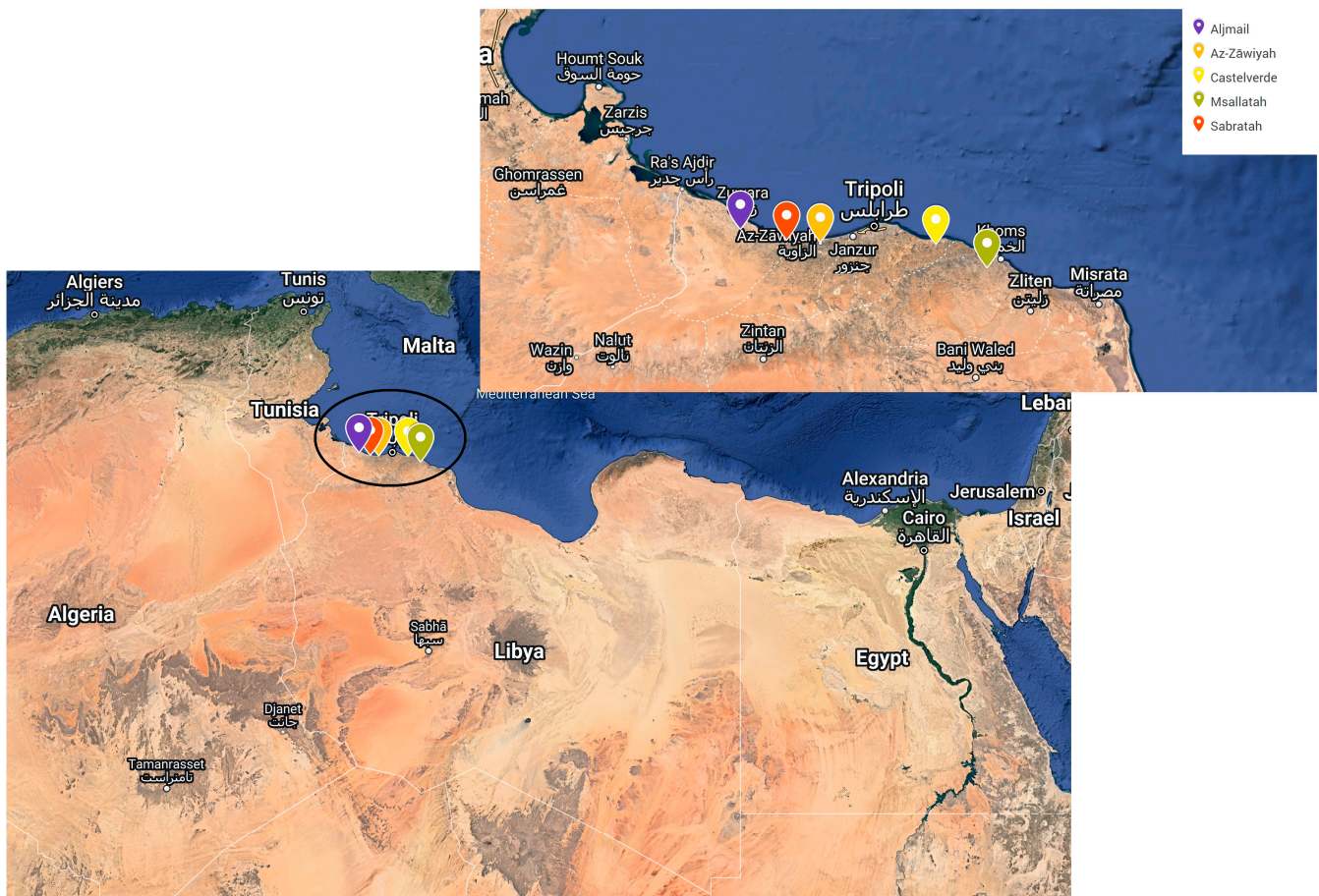


**Figure 3.** Libya map and geographic locations of regions.

### 2.2.1. Case 1: Farm 1

Farm 1 encompasses an area of 15 hectares and consists of various components, including 1500 orange trees, 400 olive trees, clover, and multiple types of crops. The farm also features dedicated sheds for poultry, cows, and sheep. Additionally, there are four water wells on the farm, each with different depths and purposes. The farm has a clayey soil composition with a partially sandy component. It is divided into five sections:

- **Section 1:** It occupies a total area of 5 hectares. The main crop grown on the farm is orange trees. The well used for irrigation has a depth of 190 m. The Total Dissolved Solids (TDSs) in the water is 1800, indicating the mineral content. The pH level of the water is 8, indicating its acidity/alkalinity balance. Additionally, the farm employs a submersible well pump with a capacity of 12 horsepower (12 hp). This pump is responsible for drawing water from the well and supplying it to the irrigation system. It operates for an average of 15 h per day. It also has a diesel electricity generator with a capacity of 500 kilovolt-amperes (kVA). This generator is used to generate electricity

for various farm operations. On average, it operates for a range of 5 to 6 h per day. The generator requires approximately 120 L of diesel per day.

- **Section 2:** This section occupies an area of 5 hectares. It cultivates a variety of crops. The well in this section has a depth of 185 m with a pH level of 7.5 and a TDS value of 1700. The farm uses a pump with a capacity of 7.5 hp to extract water from the well for irrigation purposes. The pump operates for an average of 10 to 15 h per day, indicating the duration for which it is active in supplying water to the crops. The farm has a diesel electricity generator with a capacity of 60 kVA. This generator provides electrical power for various farm operations. The generator operates for an average of 5 to 6 h per day, indicating the duration for which it is in use. The farm requires approximately 20 L of diesel per day to fuel the generator.
- **Section 3:** The farm spans a 2-hectare area and is primarily dedicated to cultivating clover. It utilizes a well with a depth of 210 m, containing water with a TDS value of 1950 and a pH level of 8.5. To facilitate irrigation, a pump with a capacity of 8.5 hp is employed to extract water from the well. This pump operates for an average of 15 to 20 h per day, ensuring a consistent water supply for the clover crop. In addition, the farm is equipped with a diesel electricity generator boasting a capacity of 78 kVA. This generator serves as a power source for various farm operations. It operates for an average of 5 to 6 h per day. To sustain its operation, the generator consumes approximately 30 L of diesel fuel daily.
- **Section 4:** The farm encompasses a 1-hectare area and is primarily dedicated to cultivating olive trees. It relies on a well with a depth of 225 m, containing water with a TDS value of 2100 and a pH level of 8.5. To facilitate irrigation, a pump with a capacity of 5.5 hp is utilized to extract water from the well. The pump operates for an average of 5 h per day, providing water to the olive trees during this period. Moreover, the farm is equipped with a diesel electricity generator boasting a capacity of 40 kVA. This generator serves as a power source for various farm operations. It operates for an average of 5 to 6 h per day. To sustain its operation, the generator consumes approximately 5 L of diesel fuel daily.
- **Section 5:** It occupies an area of 1 hectare and consists of sheds designed to house chickens, poultry, cows, and sheep. These sheds are equipped with a total of 21 mechanical ventilation fans, each with a capacity of 3.5 horsepower, enabling efficient air circulation. It should be noted that these fans operate for 24 h in summer and an average of 4 to 5 h per day in the winter. Additionally, the sheds are fitted with 20 lights, each having a capacity of 100 Watts, to provide illumination. The farm is equipped with two diesel electricity generators, serving as a backup or alternative power source, with a capacity of 615 kVA to supply electricity. Operating the generator requires approximately 150 L/d of diesel fuel.
- **Section 6:** Four houses are located on a 1-hectare plot of land. Each house has a specific area measurement: house #1 covers 250 m<sup>2</sup>, house #2 covers 180 m<sup>2</sup>, house #3 covers 300 m<sup>2</sup>, and house #4 covers 150 m<sup>2</sup>. The daily electric consumption for each house falls within the range of 15–25 kWh. Specifically, house #1 consumes 25 kWh/d, house #2 consumes 20 kWh/d, house #3 consumes 30 kWh/d, and house #4 consumes 15 kWh/d.

The farmers' feedback on electricity amount and cost is presented in Figure 4. Additionally, the total fuel consumption and cost are illustrated in Figure 4. It is found that the total amounts of the electricity demand and fuel consumption are 612 kWh/day and 476 L/day, respectively.

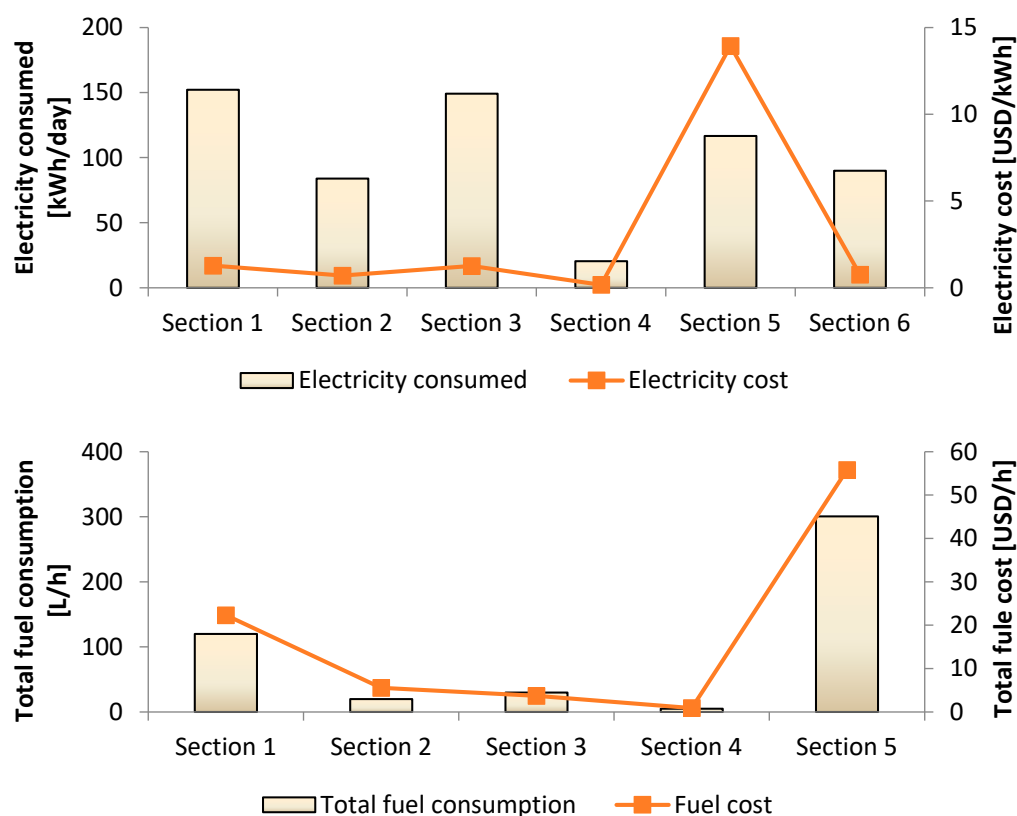


Figure 4. Electricity amount, fuel consumption, and cost for Farm 1.

#### 2.2.2. Case 2: Farm 2

Farm 2 has an area of about 2 hectares and encompasses a diverse range of components. The farm's soil composition is characterized as semi-sandy with a small amount of clay. Within its boundaries:

- There are 30 greenhouses, each spanning an area of 400 m<sup>2</sup>. The farm features a diverse range of 2000 trees, including pomegranate trees, grapevines, and peach trees. These trees collectively occupy an area of 7000 m<sup>2</sup>.
- It has 10 LED searchlights with a capacity of 1000 W.
- The farm has accommodation for workers (5 rooms). The area of the rooms is approximately 90 m<sup>2</sup>.

These greenhouses and trees rely on a well with a depth of 200 m, containing water with a TDS value of 1800 and a pH level of 8. To facilitate irrigation, a pump with a capacity of 15 hp is employed to extract water from the well. The pump operates for an average of 10 h per day. Additionally, the farm is equipped with a diesel electricity generator boasting a capacity of 400 kVA. This generator serves as a power source for various farm operations and typically operates for an average of 5 h/d for a greenhouse, 12 h/d for lighting, and 19 h/d for rooms. To sustain its operation, the generator consumes approximately 90 L of diesel fuel daily.

Figure 5 presents the feedback from farmers regarding the amount and cost of electricity.

It should be noted that the TDS and pH values of water are measured in the field using a handheld water quality meter. This device is designed to provide accurate readings of TDS and pH levels, allowing farmers to monitor and assess the water quality for various purposes, such as irrigation. By using it on site, farmers can obtain real-time measurements and make informed decisions regarding water usage and management on their farms.

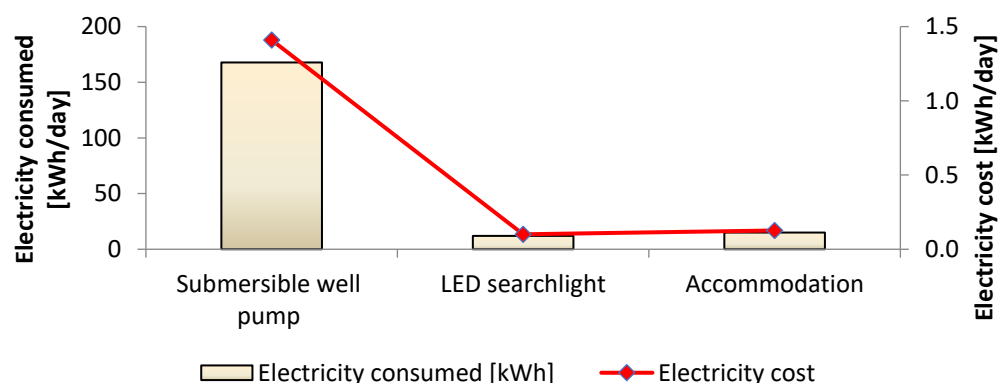


**Figure 5.** Electricity amount, fuel consumption, and cost for farm 2.

Generally, according to the survey findings, the following has been found:

- Regarding the education variable, the majority of farmers have completed middle school, while only a few of them have not received formal education. The income of the farmers ranges from USD 105 to USD 315, which depends on the size of the farm, crop type, and so on.
- The total volume of freshwater needed for irrigation, drinking purposes, and domestic use is within the range of 20,000–24,000 L per week, with an associated cost of around USD 24–30. It is important to note that groundwater is not suitable for all types of crops, which necessitates the need to obtain fresh water by purchasing it from water tankers.

### 2.3. Weather Data

#### 2.3.1. Measured Data

As mentioned previously, this paper evaluated the wind and solar energy potential for agricultural farms on the northwestern coast of Libya. Due to the civil war and limited availability of meteorological stations in Libya, an Ambient Weather WS-2902 Home WiFi Weather Station was used to measure the weather data including wind speed and solar radiation at Az-Zāwiyah. The device was installed in a location devoid of trees or shading. This ensures that the station is exposed to the full extent of ambient weather conditions without any obstructions. This unobstructed placement allows for accurate measurements and reliable weather data collection. It can be utilized to measure daily data for various weather parameters. Additionally, it can be connected to a computer through a data logger device to collect and store the measured data. It is equipped with sensors to measure parameters such as temperature, wind speed, and solar radiation. It provides the capability to record and display these measurements on its built-in console or through the Ambient Weather online platform. To collect and store the data for further analysis, it can connect to a computer using a data logger device. The data logger acts as an intermediary device that allows the weather station to interface with the computer and transfer the collected data. It captures and saves the measurements at regular intervals. The data was collected over one year, specifically from January 2022 to December 2022. The data were measured at a height of 2 m.

#### 2.3.2. Reanalysis and Analysis of Datasets

In light of the limited availability of measurement instruments in most developing countries like Libya, it is crucial to evaluate satellite products (SPs), such as reanalysis and analysis datasets, using locally measured data before utilizing them as a source of meteorological information. This evaluation ensures the reliability and accuracy of the satellite products in providing valuable meteorological data for the given region.

In general, reanalysis and analysis of datasets refer to comprehensive sets of meteorological data that are generated through advanced data assimilation techniques [76].

These datasets are created by combining various sources of observations, including weather station measurements, satellite data, and other relevant sources, using sophisticated mathematical models [76,77]. Many scientific researchers have utilized the satellite database for evaluating the potential of wind energy [78–96] as shown in Table S1 in the Supplementary Materials. In this study, five SPs were selected based on their high spatial resolution, coverage domain, and periods of availability as shown in Table 3.

**Table 3.** Major characteristics of SPs used in the study.

Products	Description/Full Name of the Dataset	Resolution	Period
TerraClimate	Global gridded dataset of meteorological and water balance for global terrestrial surfaces	$0.042^\circ \times 0.042^\circ$	1958–present
ERA5	Fifth-generation reanalysis product of the European Centre for Medium-Range Weather Forecasts	$0.05^\circ / 1 \text{ d}$	1979–present
ERA5-Land	ERA5-Land has been produced by replaying the land component of the ECMWF ERA5 climate reanalysis	$0.125^\circ \times 0.125^\circ$	11 July 1963–present
MERRA-2	Second-generation Modern-ERA Retrospective Analysis for Research and Applications	$0.5^\circ \times 0.625^\circ$	1981–present
CFSR	NCEP (NOAA NWS National Centers for Environmental Prediction) Climate Forecast System Reanalysis dataset	$1/5^\circ$	1979–present

### 2.3.3. Statistical Indices

The performance of the reanalysis and analysis datasets was evaluated using different statistical metrics, including coefficient of determination ( $R^2$ ), root mean squared error (RMSE), and mean absolute error (MAE). Moreover, the performance of the model can be described based on the ranges of the relative root mean square error (RRMSE) as given in Table S2 in the Supplementary Material. In this study, the mathematical expressions for the employed statistical metrics are shown in Equations (1)–(4).

$$R^2 = 1 - \frac{\sum_{i=1}^n (a_{a,i} - a_{p,i})^2}{\sum_{i=1}^n (a_{p,i} - a_{a,ave})^2} \quad (1)$$

$$RMSE = \sqrt{\frac{1}{n} \sum_{i=1}^n (a_{a,i} - a_{p,i})^2} \quad (2)$$

$$MAE = \frac{1}{n} \sum_{i=1}^n |a_{a,i} - a_{p,i}| \quad (3)$$

$$RRMSE = \frac{\sqrt{\frac{1}{n} \sum_{i=1}^n (a_{a,i} - a_{p,i})^2}}{\frac{1}{n} \sum_{i=1}^n (a_{p,i})^2} \quad (4)$$

where  $n$  is the amount of data,  $a_{p,i}$  is the predicted value,  $a_{a,i}$  is the actual value,  $a_{a,ave}$  is the average actual value, and  $i$  is the number of input variables.

## 2.4. Assessment of Wind Energy Potential

### 2.4.1. Extrapolation of Wind Speed Data

As mentioned before, the wind speed data were measured and recorded continuously at a hub height of 2 m above the ground. Therefore, the power law model is utilized to extrapolate the wind speed to various hub heights. The model is represented by the following equation [76].

$$\frac{v}{v_2} = \left( \frac{z}{z_2} \right)^\alpha \quad (5)$$

where  $v$  is the wind speed at the wind turbine hub height  $z$ ,  $v_2$  is the wind speed at the original height  $z_2$ , and  $\alpha$  is the surface roughness coefficient, which depends on the characteristics of the region. The value of  $\alpha$  can be determined using Equation (6).

$$\alpha = \frac{0.37 - 0.088 \ln(v_2)}{1 - 0.088 \ln(z_2/2)} \quad (6)$$

#### 2.4.2. Modeling the Distribution of Wind Frequencies

Wind speed characteristics play a crucial role in the design and operation of wind energy systems. Probability distribution models are commonly used to analyze wind speed data and estimate the probability of different wind speeds occurring at a particular location. Generally, examining the wind speed characteristics (WSCs) is considered the first step for evaluating the wind energy potential at a specific location. Therefore, finding suitable probability distribution models is essential for describing the WSCs. Several probability distribution models were evaluated for their suitability in wind energy applications worldwide. According to Refs. [97–100], the 2-parameter Weibull (2p-W) and 1-parameter Rayleigh (1p-R) are commonly utilized for studying the distribution of wind speed of specific regions [97–100]. For instance, Celik [97] studied the wind speed characteristics at Iskenderun in Turkey using 2p-W and 1p-R. Hussain et al. [98] estimated the wind power density for Gwadar, Jiwani, Ormara, and Pasni in Pakistan using 2p-W. Serban et al. [99] evaluated the wind power potential at two locations in Romania using 2p-W and 1p-R. Ali et al. [100] utilized 2p-W and 1p-R for evaluating the WSCsd at Deokjeok-do Island, Incheon, in South Korea. Moreover, several scientific researchers have analyzed the WSCs using various distribution functions (DFs) to determine the best-fit probability distribution [101–115]. Table S3 in the Supplementary Materials summarizes the previous studies associated with studying the WSCs using various DFs. It should be noted that the choice of model depends on the available data on wind speed at specific regions. Based on the findings (Table S3 in the Supplementary Materials), it can be concluded that (1) the most common distribution functions for WSCs are exponential, gamma, generalized extreme value, inverse Gaussian, log-logistic, lognormal, Nakagami, Rayleigh, and Weibull; (2) two studies found that Wakeby distribution was the best distribution to describe the WSCs at specific regions; and (3) two studies used Kumaraswamy distribution for analyzing the wind speed characteristics in India and Lebanon.

In this study, 13 distribution functions (DFs) were used for analyzing the wind characteristics at the selected locations. The probability density function ( $f(v)$ ) and cumulative distribution function ( $F(v)$ ) expressions for the selected DFs are expressed as shown in Table 4.

In this study, the maximum likelihood method (MLM) was used to calculate the distribution parameters. Moreover, the Kolmogorov–Smirnov (K-S) test was employed to find the best distribution model.

The Kolmogorov–Smirnov (K-S) test is as follows [108]:

$$D = \max_{1 \leq i \leq n} \left( F(x_i) - \frac{i-1}{n}, \frac{i}{n} - F(x_i) \right) \quad (7)$$

where

$$F_n(x) = \frac{1}{n} \times (\text{Number of observation} \leq x) \quad (8)$$

where  $F(x)$  is probability distribution function of the normal distribution,  $x_i$  is the  $i$ th order statistics of a random sample,  $1 \leq i \leq n$ , and  $n$  is the sample size.

**Table 4.** Expression of the probability density function and cumulative distribution function used in the present study.

Distribution Function			Probability Density Function			Cumulative Distribution Function		
Normal (N)			$f(v) = \frac{1}{\sqrt{2\pi\sigma^2}} \exp\left(-\frac{v-\mu}{2\sigma^2}\right)$			$F(v) = \frac{1}{2} \left[1 + \operatorname{erf}\left(\frac{v-\mu}{\sigma\sqrt{2}}\right)\right]$		
Gamma (G)			$f(v) = \frac{R^{\alpha-1}}{\beta^\alpha \Gamma(\alpha)} \exp\left(-\left(\frac{v}{\beta}\right)\right)$			$F(v) = \frac{\Gamma_{R/\beta}(\alpha)}{\Gamma(\alpha)}$		
Generalized Extreme Value (GEV)			$f(v) = \begin{cases} \frac{1}{\sigma} \left[ \left(1 + \zeta \left(\frac{v-\mu}{\sigma}\right)\right)^{-1/\zeta} \right]^{\zeta+1} \exp\left(-\left(1 + \zeta \left(\frac{v-\mu}{\sigma}\right)\right)^{-1/\zeta}\right) & k \neq 0 \\ \frac{1}{\sigma} \left[ \exp\left(-\left(\frac{v-\mu}{\sigma}\right)\right) \right]^{\zeta+1} \exp\left(\exp\left(-\left(\frac{v-\mu}{\sigma}\right)\right)\right) & k = 0 \end{cases}$			$F(v) = \begin{cases} \exp\left(-\exp\left(-\left(\frac{v-\mu}{\sigma}\right)\right)\right) & k \neq 0 \\ \exp\left(-\exp\left(-\frac{v-\mu}{\sigma}\right)\right) & k = 0 \end{cases}$		
Nakagami (Na)			$f(v) = \frac{2m^m}{\Gamma(m)\Omega^m} v^{2m-1} e^{(-\frac{m}{\Omega}G^2)}$			$F(v) = \frac{\gamma(m, \frac{m}{\Omega}v^2)}{\Gamma(m)}$		
Inverse Gaussian (IG)			$f(v) = \sqrt{\frac{\lambda}{2\pi(R-\gamma)}} \exp\left(-\frac{\lambda(v-\mu)^2}{2\mu^2R}\right)$			$F(v) = \Phi\left(\sqrt{\frac{\lambda}{R-\gamma}}\left(\frac{v}{\mu} - 1\right)\right) + \Phi\left(-\sqrt{\frac{\lambda}{R-\gamma}}\left(\frac{v}{\mu} + 1\right)\right) \exp\left(\frac{2\lambda}{\mu}\right)$		
Log-normal (LN)			$f(v) = \frac{1}{v\sigma\sqrt{2\pi}} \exp\left[-\frac{1}{2}\left(\frac{\ln(v)-\mu}{\sigma}\right)^2\right]$			$F(v) = \frac{1}{2} + \operatorname{erf}\left[\frac{\ln(v)-\mu}{\sigma\sqrt{2}}\right]$		
Log-Logistic (LL)			$f(v) = \left(\frac{\left(\frac{\beta}{\alpha}\left(\frac{v}{\alpha}\right)^{\beta-1}\right)}{\left(1 + \frac{v}{\alpha}\right)^\beta}\right)^2$			$F(v) = \frac{1}{\left(1 + \frac{v}{\alpha}\right)^{-\beta}}$		
Rayleigh (R)			$f(v) = \frac{v}{\sigma^2} \exp\left(-\frac{1}{2}\left(\frac{v}{\sigma}\right)^2\right)$			$F(v) = 1 - \exp\left(-\frac{1}{2}\left(\frac{v}{\sigma}\right)^2\right)$		
Weibull (W)			$f(v) = \left(\frac{\alpha}{\sigma}\right)\left(\frac{v}{\sigma}\right)^{\alpha-1} \exp\left(-\left(\frac{v}{\sigma}\right)^\alpha\right)$			$F(v) = 1 - \exp\left(-\left(\frac{v}{\sigma}\right)^\alpha\right)$		
Three-Parameter Weibull (W-3P)			$f(v) = \left(\frac{\alpha}{\beta}\right)\left(\frac{v-\gamma}{\beta}\right)^{\alpha-1} \exp\left(-\left(\frac{v-\gamma}{\beta}\right)^\alpha\right)$			$F(v) = 1 - \exp\left(-\left(\frac{v-\gamma}{\beta}\right)^\alpha\right)$		
Kumaraswamy (K)			$f(v) = \frac{abe^{-\frac{1-(1-v^a)^b}{\beta(1-v^a)^b}}}{\Gamma(\alpha)\beta^\alpha} \frac{1}{(1-v^a)^2} \left(\frac{1-(1-v^a)^b}{\beta(1-v^a)^b}\right)^{\alpha-1}$			$F(v) = \int_0^{\frac{1-(1-v^a)^b}{\beta(1-v^a)^b}} \frac{e^{-\omega}}{\Gamma(\alpha)\beta^\alpha} d\omega = \frac{\Gamma(\alpha, z)}{\Gamma(\alpha)\beta^\alpha} \left(\alpha, \frac{1-(1-v^a)^b}{\beta(1-v^a)^b}\right)$		
Birnbaum-Saunders (BS)			$f(v) = \frac{\sqrt{\frac{v-\mu}{\beta} + \sqrt{\frac{\beta}{v-\mu}}}}{2\gamma(v-\mu)} \Phi\left(\frac{\sqrt{\frac{v-\mu}{\beta} - \sqrt{\frac{\beta}{v-\mu}}}}{\gamma}\right)$			$F(v) = \Phi\left(\frac{\sqrt{v} - \sqrt{\frac{\beta}{v}}}{\gamma}\right)$		
Logistic (L)			$f(v) = \frac{\exp\left(-\frac{v-\mu}{\sigma}\right)}{\sigma\left\{1 + \exp\left(-\frac{v-\mu}{\sigma}\right)\right\}^2}$			$F(v) = \frac{1}{1 + \exp(-v)}$		
N	$\sigma$	Standard deviation	Na	$m$	Shape parameter	LL	$\beta$	Shape parameter
	$\mu$	Mean parameter		$\Omega$	Scale parameter		$\alpha$	Scale parameter
G	$\beta$	Shape parameter	IG	$\lambda$	Shape parameter	W	$\alpha$	Shape parameter
	$\alpha$	Scale parameter		$\mu$	Mean parameter		$\sigma$	Scale parameter
GEV	$\mu$	Location parameter	LN	$\sigma$	Shape parameter	W-3P	$\alpha$	Shape parameter
	$\alpha$	Scale parameter		$\mu$	Scale parameter		$\sigma$	Scale parameter
	$\zeta$	Shape parameter	R	$\sigma$	Scale parameter		$\gamma$	Location parameter
	$a$	Shape parameter	BS	$\mu$	Location parameter	L	$\mu$	Location parameter
	$b$	Shape parameter		$\beta$	Scale parameter		$\sigma$	Scale parameter
K	$\alpha$	Shape parameter		$\gamma$	Shape parameter			
	$\beta$	Scale parameter						

### 2.4.3. Wind Power Density

Wind power density (WPD) is a measure of the amount of power that can be harnessed from the wind at a specific location. It is defined as the ratio of the power present in the wind to the area swept by the wind turbine. WPD is also referred to as wind power potential or wind power per unit area, and it provides a numerical representation of the energy potential in a given region. It can be expressed as follows [102]:

$$\frac{P}{A} = \frac{1}{2}\rho v^3 \quad (9)$$

where  $P$  is the wind power density in W,  $A$  is a swept area in  $m^2$ ,  $\rho$  is the air density ( $\rho = 1.225 \text{ kg/m}^3$ ), and  $v$  is the wind speed in m/s

Moreover, the average WPD for a period measurement can be determined using the equation below [102].

$$\frac{\bar{P}}{A} = \frac{1}{2}\rho\bar{v}^3 \quad (10)$$

where  $\bar{P}$  is the mean wind power density in W and  $\bar{v}$  is the mean wind speed in m/s.

Moreover, it can be estimated as a function of the probability density function ( $f(v)$ ) as shown below [102].

$$\frac{P}{A} = \frac{1}{2}\rho v^3 f(v) \quad (11)$$

### 2.4.4. Output Energy of Wind Turbines

Equation (12) can be utilized to estimate the power generated by the wind turbine. Additionally, the power curve of the wind turbines can be approximated using a parabolic function, as shown by Equation (10) [102].

$$E_{wt} = \sum_{i=1}^n P_{wt(i)} t \quad (12)$$

$$P_{wt(i)} = \begin{cases} P_r \frac{v_i^2 - v_{ci}^2}{v_r^2 - v_{ci}^2} & (v_{ci} \leq v_i \leq v_r) \\ \frac{1}{2}\rho A C_p v_r^2 & (v_r \leq v_i \leq v_{co}) \\ 0 & (v_i \leq v_{ci} \text{ and } v_i \geq v_{co}) \end{cases} \quad (13)$$

where  $E_{wt}$  is total power output,  $t$  is the number of hours in the period under consideration,  $v_i$  is the vector of possible wind speed at a given site,  $P_{wt(i)}$  is the vector of the corresponding wind turbine output power (W),  $P_r$  is the rated power of the turbine (W),  $v_{ci}$  is the cut-in wind speed (m/s),  $v_r$  is the rated wind speed (m/s), and  $v_{co}$  is the cut-out wind speed (m/s) of the wind turbine.  $C_p$  is the coefficient of performance of the turbine (Equation (14)), and it is a function of the tip-speed ratio and the pitch angle.

$$C_p = 2 \frac{P_r}{\rho A v_r^3} \quad (14)$$

Moreover, the capacity factor (CF) of the wind turbine is estimated by Equation (15) [102].

$$CF = \frac{E_{wt}}{8760 P_R} \quad (15)$$

### 2.4.5. Techno-Economic Analysis of Wind Turbines

Recently, wind systems have faced common economic challenges. The cost of electricity generated by a wind turbine is influenced by several factors. The economic feasibility of a wind power plant hinges on specific local conditions that can differ significantly from one location to another. Consequently, conducting a thorough economic evaluation becomes vital, especially when making substantial investments in large-scale wind turbine

installations for power generation. In the current study, the mathematical equations used to evaluate the economic viability of wind turbines can be expressed as follows.

- (a) The total investment cost is

$$C_{TI} = C_{WT} + C_{ST} + C_{EN} + C_{CI} + C_{TR} + C_{EL} + C_M \quad (16)$$

$$C_{WT} = C_{CWT} \times P_R \quad (17)$$

where  $C_{WT}$  is the cost of the wind turbine in USD,  $C_{ST}$  is 2% of  $C_{WT}$ ,  $C_{CI}$  is the civil work and installation cost in USD (8% of  $C_{WT}$ ),  $C_{EN}$  is the engineering cost in USD (5% of  $C_{WT}$ ),  $C_{TR}$  is the transport cost (2% of  $C_{WT}$ ),  $C_{EL}$  is the electrical connection cost in USD (7% of  $C_{WT}$ ),  $C_M$  is the miscellaneous cost (1% of  $C_{WT}$ ),  $C_{CWT}$  is the specific cost of the wind turbine in USD/kW, and  $P_R$  is rated power of the turbine in kW.

- (b) The net present value (NPV)

$$NPV = \sum_{n=0}^N \frac{C_n}{(1+r)^n} \quad (18)$$

where  $N$  is the project life,  $C_n$  is the after-tax cash flow in year  $n$ , and  $r$  is the discount rate.

- (c) The present value of costs (PVC) method estimates the cost of production. As part of this method, the annual operating cost of the wind turbine is calculated using Equation (19).

$$PVC = 1 + C_{omr} \left[ \frac{1+i}{r-i} \right] \times \left[ 1 - \left( \frac{1+i}{1+r} \right)^n \right] - S \left( \frac{1+i}{1+r} \right)^n \quad (19)$$

where  $C_{omr}$  is the operation and maintenance (O&M) cost,  $r$  is the interest rate,  $i$  is the inflation rate, and  $n$  is machine life as designed by the manufacturer.

- (d) Cost of electricity generated by a wind turbine in USD/kWh

$$CEG = \frac{PVC}{AEP} \quad (20)$$

$$AEP = 8760 \times P_R \times CF \quad (21)$$

- (e) Annual greenhouse gas (GHG) savings in CO<sub>2</sub>/Year

$$GHG = \frac{\text{Average national electricity generation mix} \times AEP}{1000000} \quad (22)$$

- (f) Simple payback period (SPP) in years

$$SPP = \frac{I}{AEP \times P_e} \quad (23)$$

where  $I$  is the installed capital cost of the wind turbine plus the costs of civil works and  $P_e$  is the price of electricity (USD/kWh).

## 2.5. Assessment of Solar Energy Potential

### 2.5.1. Classification of Solar Potential

The assessment of solar energy potential was conducted by categorizing it according to the annual value of global solar radiation (GSR). Global solar radiation is widely used as a parameter for evaluating the energy generation potential of photovoltaic (PV) systems. The classification of solar energy based on the GSR annual value is presented in Table 5.

**Table 5.** Classification of solar energy [116].

Class	Annual GSR [kWh/m <sup>2</sup> ]
1 (poor)	<1191.8
2 (marginal)	1191.8–1419.7
3 (fair)	1419.7–1641.8
4 (good)	1641.8–1843.8
5 (excellent)	1843.8–2035.9
6 (outstanding)	2035.9–2221.8
7 (superb)	>2221.8

### 2.5.2. Estimating Solar PV Energy Output

The monthly energy output ( $E_M$ ) from a solar PV system can be determined by considering factors such as the peak sun hours of the location, the installed capacity of the system, and the derate factor that accounts for component efficiencies and environmental conditions. Mathematically, the monthly energy output in kWh from a solar PV system can be estimated using Equation (24).

$$E_M = N_d \times f_m \times \frac{H_c}{1 \text{ kW/m}^2} \times P_{IC} \quad (24)$$

where  $f_m$  is the average monthly derate factor or performance ratio,  $N_d$  is the number of days in the month,  $H_c$  is solar radiation on the plane of the solar PV array in kWh/m<sup>2</sup>/day, and  $P_{IC}$  is solar PV installed capacity in kW.

### 2.5.3. Technical Indices

In this study, the technical performance of the installation is assessed by evaluating several performance parameters: final energy output, final energy yield, performance ratio, and capacity factor. These parameters serve as indicators of the overall performance of the solar PV system, taking into account factors such as the available solar resources and other environmental variables.

- (a) Final Energy Output ( $E_{AC}$ ): This parameter represents the total amount of energy produced by the solar PV system over a given period, typically measured in kWh. It provides an overall measure of the system's energy generation capability.

$$E_{AC} = \sum_{d=1}^N E_{AC(m)} \quad (25)$$

where  $E_{AC}$  is the monthly energy output at the time ( $t$ ) and  $N$  is the number of days in a month.

- (b) Final Energy Yield ( $Y_f$ ): It is calculated by dividing the final energy output by the installed capacity of the solar PV system. It represents the average energy production per unit of installed capacity and helps assess the system's efficiency in converting sunlight into usable electricity.

$$Y_f = \frac{E_{AC}}{P_{IC}} \quad (26)$$

- (c) Performance Ratio ( $PR$ ): The performance ratio is determined by dividing the actual energy yield by the theoretical energy yield. The theoretical energy yield is calculated based on the available solar resource and is an estimation of the maximum energy the system could produce under ideal conditions. The performance ratio reflects the efficiency of the system in converting available sunlight into electricity, taking into account losses due to factors such as shading, temperature, and system degradation.

$$PR = \frac{E_{AC}}{P_{IC}} \frac{G_{STC}}{H_C} \quad (27)$$

where  $G_{STC}$  is the reference irradiance.

- (d) Capacity Factor (CF): It is the ratio of the actual energy output of the solar PV system to the maximum possible energy output if the system operated at its maximum capacity for a given period. It indicates the extent to which the system is utilized and provides insight into its operational efficiency. A higher capacity factor indicates better utilization of the installed capacity.

$$CF = \frac{E_{AC(d)}}{P_{IC}} \frac{1}{T_h} \quad (28)$$

where  $T_h$  is the total expected number of hours of operation in a given period.

#### 2.5.4. Economic Viability

To evaluate the economic feasibility of the installation, several financial indicators are utilized in this analysis. These indicators include discounted payback period, simple payback period, internal rate of return (IRR), net present value (NPV), and levelized cost of energy (LCOE) of the generated electricity.

- (a) The NPV is expressed as:

$$NPV = \sum_{t=0}^n \frac{NCF_t}{(1+i)^t} = -C_o + \sum_{t=1}^n \frac{NCF_t}{(1+i)^t} \quad (29)$$

where  $C_o$  is the investment cost,  $n$  is the project economic life, and  $NCF_t$  is the annual net cash flow (which is annual revenue minus annual expenses (such as operation cost, maintenance, and replacement)) for a year. From a monetary benefit viewpoint, the NPV of a project needs to have a positive value ( $NPV > 0$ ).

- (b) The internal rate of return is the value of the discount rate (IRR) that would result in an NPV of zero, and it can be determined from Equation (30):

$$-C_o + \sum_{t=1}^n \frac{NCF_t}{(1+IRR)^t} = 0 \quad (30)$$

To calculate the IRR, Equation (30) needs to be solved using an iteration or trial-and-error approach. In this study, the IRR calculation is performed using the built-in IRR function available in Microsoft Excel.

- (c) The levelized cost of energy (LCOE) is a metric used to assess the economic viability of a solar PV installation. It represents the average cost of generating each unit of electricity over the lifetime of the project. The LCOE takes into account the total costs associated with building, operating, and maintaining the solar PV system, divided by the total energy output generated by the system throughout its lifetime. Mathematically, the LCOE can be expressed as follows:

$$LCOE = \frac{C_o + \sum_1^n \frac{C_{i,t} + C_{O\&M,t}}{(1+i)^t}}{\sum_1^n \frac{E_t}{(1+i)^t}} \quad (31)$$

where  $C_{i,t}$ ,  $C_{O\&M,t}$ , and  $E_t$  are the investment cost (such as replacement cost), operation and maintenance cost, and electricity generated each year, respectively.

- (d) The payback period is a financial metric used to evaluate the time required to recover the initial investment costs through revenue generated by an investment. It represents the length of time it takes for the investment to reach a break-even point. The simple payback period provides a straightforward measure of the time required to recover an investment. Mathematically, the SPP period can be calculated using Equation (32).

$$SPP = \frac{C_o}{A_s} \quad (32)$$

where  $A_s$  is the annual saving.

### 3. Results

#### 3.1. Assessment of Wind and Solar Energy Potential for Az-Zāwiyah

##### Wind Speed Characteristics and Wind Power Density Using Daily and Monthly Data

As aforementioned, the wind speed (WS) data were measured at a height of 2 m. Thus, the power law method is employed to synthesize the actual data collected at a height of 2 m to a height of 10 m to compare it with the reanalysis and analysis datasets. The statistical description of average daily wind speed includes the standard deviation (SD), coefficient of variation (CV), minimum (Min.), maximum (Max.), kurtosis (K), and skewness (S), which are summarized in Table 6 for the selected location.

Considering the measured dataset, it is noticed that the mean wind speeds were low. It was found that the mean wind speed ranged from 2.50 m/s (October) to 4.33 m/s (April). Generally, the mean and SD values indicate a high level of consistency in wind behavior. Moreover, it can be seen that the lowest CV value is 17.45% (September), suggesting that the dataset has relatively low variation around its mean value. On the other hand, the highest CV value is 41.54% (January), indicating a slightly higher level of variation compared to the mean. Furthermore, it is noticed that the minimum wind speeds with values of 1.60 m/s and 2.24 m/s were recorded in December and May, respectively. Moreover, the maximum values of wind speeds were recorded in January and October with values of 7.34 m/s and 4.06 m/s, respectively. Additionally, skewness values for most months are positive, indicating that all distributions are right-skewed, indicating a longer or fatter tail on the right side of the distribution. The skewness values for February, April, July, October, and November are negative, indicating that the tail of the distribution is skewed to the left. Moreover, the kurtosis values, ranging from  $-0.83$  to  $1.84$ , indicate the degree of the flatness of the distributions of the data. In this case, the range of kurtosis values suggests that the distributions of the data vary in terms of their flatness. A negative kurtosis value ( $-0.83$ ) indicates a distribution that is slightly flatter or less peaked than a normal distribution, while a positive kurtosis value ( $1.84$ ) suggests a distribution that has heavier tails than a normal distribution. Figure 6 illustrates the daily wind speed for Az-Zāwiyah. It is noticed that the maximum wind speed of 7.34 m/s was recorded on 8 January 2022, while the minimum value of 1.60 m/s was obtained on 5 December 2022.

Considering reanalysis and analysis datasets, Table 6 and Figure 6 give the following findings.

- The mean wind speed is within the range of 2.86–4.34 m/s for CFSR, 1.58–3.90 m/s for ERA5, 1.87–4.09 m/s for ERA5-Land, and 3.79–6.01 m/s for MERRA-2. Additionally, the highest and lowest values of mean and SD were obtained from MERRA-2 and ERA5.
- ERA5 exhibits the highest CV value (CV = 64.31%), while CFSR yields the lowest value (CV = 14.44%).
- The minimum wind speed occurred in January (1.53 m/s) for CFSR, July (0.08 m/s) for ERA5, June (0.18 m/s) for ERA5-Land, and October (1.73 m/s) for MERRA-2.
- The maximum wind speeds are observed in different months: November (8.96 m/s) for CFSR, January (7.92 m/s) for ERA5, January (8.39 m/s) for ERA5-Land, and November (14.50 m/s) for MERRA-2.
- The skewness values for most months are positive, indicating that all distributions are right-skewed.

**Table 6.** Statistical estimators of the daily wind speed using various datasets for Az-Zāwiyah.

Month	Dataset	Mean	SD	CV	Min.	Max.	S	K	Month	Dataset	Mean	SD	CV	Min.	Max.	S	K
Jan	Measured	3.47	1.44	41.54	1.99	7.34	1.31	0.76	Jul	Measured	3.03	0.64	21.11	1.95	4.39	0.06	−0.83
	CFSR	3.22	1.48	45.95	1.53	6.90	1.21	0.56		CFSR	3.60	0.59	16.47	2.46	4.63	0.00	−1.02
	ERA5	3.20	1.79	56.02	1.35	7.92	1.26	0.70		ERA5	2.55	1.16	45.67	0.08	4.52	−0.37	−0.66
	ERA5-Land	3.50	1.89	54.03	1.59	8.39	1.22	0.67		ERA5-Land	2.74	1.25	45.74	0.21	4.75	−0.43	−0.76
	MERRA-2	5.97	2.52	42.23	2.75	12.31	0.92	0.24		MERRA-2	4.46	1.27	28.56	2.64	7.12	0.40	−0.92
Feb	Measured	3.49	1.22	34.82	2.00	6.23	0.92	−0.07	Aug	Measured	2.88	0.79	27.50	1.76	4.94	1.26	1.19
	CFSR	3.21	0.87	27.26	1.95	5.23	0.90	0.14		CFSR	3.51	0.68	19.32	2.53	5.12	0.90	0.15
	ERA5	2.84	1.78	62.48	0.28	6.69	0.75	−0.37		ERA5	2.05	1.15	56.03	0.19	4.91	0.99	0.98
	ERA5-Land	3.04	1.88	61.76	0.37	7.04	0.74	−0.40		ERA5-Land	2.31	1.18	51.24	0.24	5.33	0.95	1.15
	MERRA-2	5.35	2.39	44.74	2.38	10.69	0.85	−0.33		MERRA-2	4.31	1.18	27.41	2.62	7.46	1.20	0.93
Mar	Measured	3.82	1.25	32.82	2.09	7.20	1.09	0.94	Sep	Measured	3.01	0.53	17.45	2.13	4.27	0.72	0.59
	CFSR	3.85	1.39	35.95	2.04	8.09	1.51	2.75		CFSR	3.61	0.52	14.44	2.92	4.65	0.34	−0.98
	ERA5	3.34	1.66	49.72	0.51	6.59	0.07	−0.79		ERA5	2.27	1.06	46.58	0.47	4.85	0.39	0.02
	ERA5-Land	3.68	1.72	46.83	0.78	7.00	0.06	−0.92		ERA5-Land	2.43	1.08	44.57	0.65	5.08	0.43	0.05
	MERRA-2	5.86	1.87	32.00	2.75	9.82	0.29	−0.83		MERRA-2	4.63	0.96	20.73	3.34	7.23	1.05	0.89
Apr	Measured	4.33	1.21	28.00	2.22	6.77	0.39	−0.83	Oct	Measured	2.50	0.62	24.64	1.80	4.06	0.89	−0.04
	CFSR	4.34	1.28	29.44	2.70	7.48	1.04	0.70		CFSR	2.86	0.54	18.89	1.79	4.42	1.13	2.06
	ERA5	3.90	1.84	47.29	1.00	6.95	0.07	−1.23		ERA5	1.58	1.01	64.03	0.41	3.84	0.98	−0.22
	ERA5-Land	4.09	1.87	45.79	1.24	7.19	0.15	−1.09		ERA5-Land	1.87	1.20	64.31	0.38	4.28	0.81	−0.68
	MERRA-2	5.92	1.88	31.65	2.36	9.77	0.19	−0.44		MERRA-2	3.79	1.46	38.42	1.73	7.47	0.99	0.52
May	Measured	3.39	1.02	30.13	2.24	6.52	1.37	1.84	Nov	Measured	3.55	1.44	40.45	1.76	7.14	0.80	−0.08
	CFSR	3.83	1.07	27.97	2.21	7.27	1.22	2.21		CFSR	4.00	1.51	37.65	2.41	8.96	1.44	2.62
	ERA5	2.19	1.35	61.59	0.27	6.18	1.14	1.62		ERA5	3.13	1.75	55.91	0.64	7.19	0.52	−0.34
	ERA5-Land	2.38	1.49	62.57	0.21	6.04	1.05	0.79		ERA5-Land	3.39	1.87	55.15	0.91	7.77	0.56	−0.43
	MERRA-2	4.38	1.60	36.45	2.45	9.03	1.50	2.17		MERRA-2	6.01	3.15	52.48	1.84	14.50	0.55	0.00
Jun	Measured	3.31	0.70	21.07	2.15	5.03	0.57	0.02	Dec	Measured	3.33	1.08	32.35	1.60	6.31	0.37	0.40
	CFSR	3.86	0.79	20.52	2.49	5.21	0.05	−1.00		CFSR	3.26	1.28	39.21	1.62	5.83	0.56	−1.01
	ERA5	2.72	1.13	41.38	0.13	5.13	−0.33	0.55		ERA5	2.52	1.43	56.65	0.46	6.13	0.36	−0.47
	ERA5-Land	2.92	1.22	41.91	0.18	5.40	−0.40	0.33		ERA5-Land	2.84	1.58	55.55	0.24	6.24	0.06	−0.98
	MERRA-2	4.55	1.15	25.22	2.73	7.61	0.56	0.58		MERRA-2	5.05	1.93	38.18	1.74	9.64	0.29	−0.53

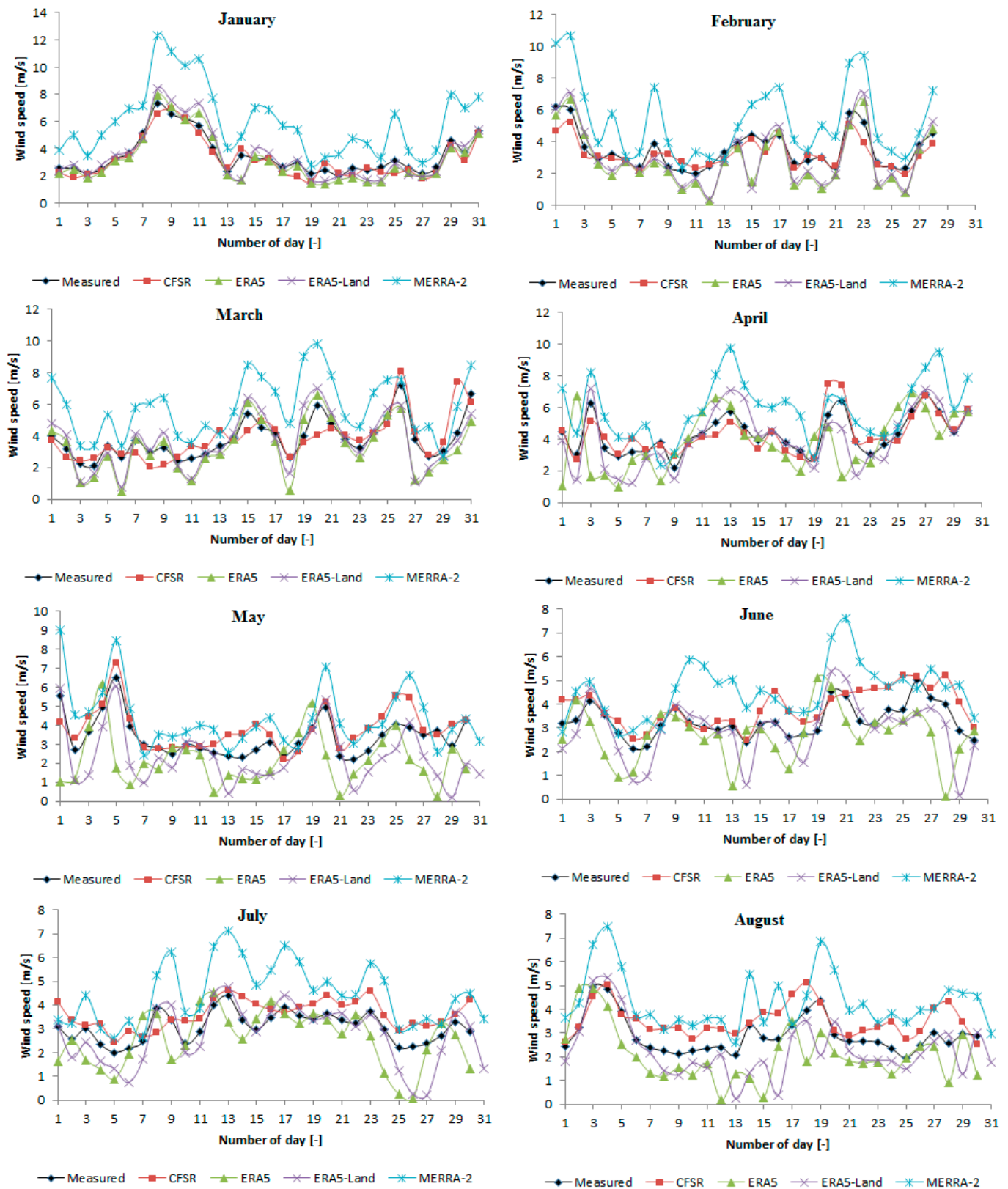


Figure 6. Cont.

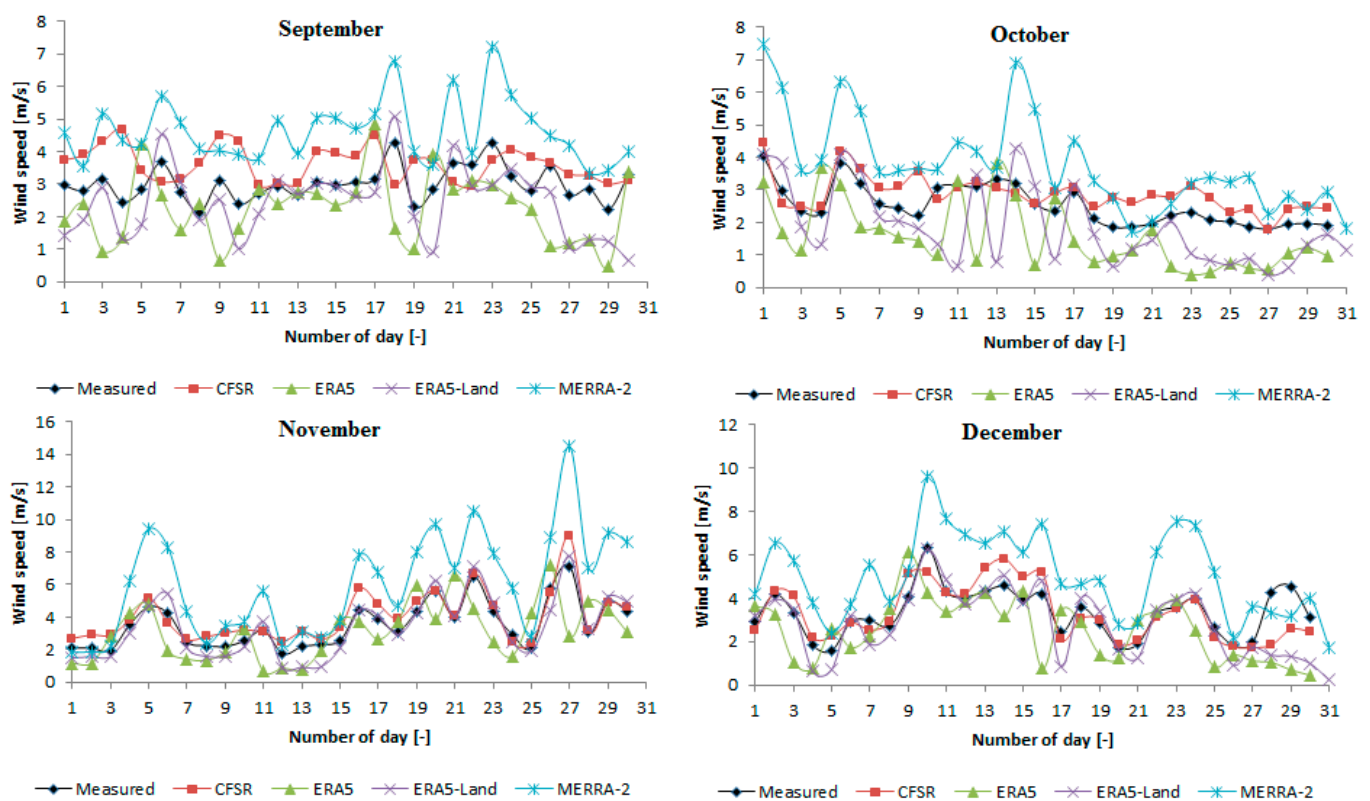


Figure 6. Average daily wind speed for Az-Zāwiyah during 2022.

Generally, the differences in the statistical description of wind speed among the measured dataset and various satellite products can be attributed to several factors related to data sources, measurement methods, physical phenomena, and the characteristics of each dataset. The measured wind data originates directly from on-site observations, potentially reflecting distinctive wind behaviors characteristic of that location. In contrast, satellite-derived data rely on remote sensing technology, which may introduce errors due to atmospheric conditions, sensor limitations, and data processing algorithms. Different satellites and sensors could contribute to variations in satellite products covering more extensive areas, and the resolution might vary between products. This could lead to discrepancies when compared to the localized measured data. Therefore, it is crucial to assess the performance of reanalysis or analysis data by comparing it with that of the measured dataset.

In this study, statistical indices such as R-squared, RMSE, MAE, and RRMSE were employed to assess the performance of the estimated data. The findings are presented in Table 7, which gives the following results:

- Based on the R-squared value, the best dataset varies from month to month. It is important to note that higher R-squared values do not necessarily indicate that one dataset is superior to another. The coefficient of determination, R-squared, only represents the strength of the linear relationship between the observed and modeled values. Therefore, RMSE, MAE, and RRMSE were employed to find the best dataset.
- Among the available datasets, CFSR consistently demonstrates the best performance across all months, as indicated by the lower values of RMSE and MAE when compared to the other datasets.
- For all months, the RRMSE value for the CFSR model ranges from 20% to 30%, suggesting a good performance rate. This finding is supported by the results presented in Table S2 in the Supplementary Materials.
- For a whole year, it is noticed that ERA5-Land and MERRA-2 produced the highest value of R-squared compared to CFSR and ERA5. Based on the value of RMSE and

MAE, CFSR gives the best performance compared to other datasets. In addition, the performance of the utilized dataset was assessed using RRMSE. The RRMSE value for CFSR falls within the range of 20% to 30%, indicating a good performance rate for the CFSR model, as demonstrated in Table S2 in the Supplementary Materials. Moreover, the performance rate for ERA5-Land can be considered fair based on Table S2 in the Supplementary Materials. However, the performance rates for ERA5 and MERRA-2 are deemed poor (Table S2 in the Supplementary Materials).

**Table 7.** Statistical parameters using average daily data for Az-Zāwiyah.

Month	Variable	Dataset				Month	Variable	Dataset			
		CFSR	ERA5	ERA5-Land	MERRA-2			CFSR	ERA5	ERA5-Land	MERRA-2
Jan	R-squared	0.93	0.93	0.91	0.89	Jul	R-squared	0.53	0.41	0.87	0.79
	RMSE	0.46	0.60	0.65	2.79		RMSE	0.73	1.01	0.74	1.61
	MAE	0.39	0.47	0.49	2.50		MAE	0.65	0.82	0.54	1.42
	RRMSE	12.99	16.41	16.49	43.12		RRMSE	19.93	36.20	24.80	34.73
Feb	R-squared	0.86	0.77	0.74	0.88	Aug	R-squared	0.54	0.45	0.57	0.75
	RMSE	0.58	1.11	1.11	2.27		RMSE	0.83	1.18	0.96	1.56
	MAE	0.46	0.88	0.83	1.88		MAE	0.70	0.96	0.72	1.43
	RRMSE	17.55	33.36	31.30	38.80		RRMSE	23.25	50.16	36.96	34.98
Mar	R-squared	0.62	0.71	0.68	0.65	Sep	R-squared	0.03	0.05	0.45	0.57
	RMSE	0.86	1.01	0.98	2.33		RMSE	0.99	1.28	1.00	1.75
	MAE	0.60	0.78	0.78	2.06		MAE	0.86	1.06	0.78	1.62
	RRMSE	21.08	27.09	24.19	37.92		RRMSE	27.26	51.49	37.74	36.97
Apr	R-squared	0.77	0.11	0.79	0.69	Oct	R-squared	0.59	0.40	0.51	0.71
	RMSE	0.61	1.86	0.99	1.92		RMSE	0.53	1.20	1.07	1.62
	MAE	0.45	1.42	0.76	1.69		MAE	0.45	1.07	0.87	1.31
	RRMSE	13.57	43.34	22.05	31.01		RRMSE	18.30	64.13	48.22	39.90
May	R-squared	0.65	0.06	0.61	0.72	Nov	R-squared	0.88	0.28	0.92	0.93
	RMSE	0.78	1.89	1.37	1.33		RMSE	0.68	1.60	0.64	3.03
	MAE	0.62	1.46	1.13	1.11		MAE	0.55	1.36	0.53	2.49
	RRMSE	19.70	73.61	48.96	28.64		RRMSE	15.85	44.76	16.59	44.80
Jun	R-squared	0.60	0.10	0.62	0.38	Dec	R-squared	0.57	0.15	0.56	0.56
	RMSE	0.74	1.25	0.88	1.52		RMSE	0.83	1.61	1.14	2.16
	MAE	0.59	0.94	0.64	1.30		MAE	0.60	1.29	0.75	1.95
	RRMSE	18.87	42.76	27.75	32.51		RRMSE	23.84	55.95	35.31	40.11
Whole year	R-squared	0.66	0.43	0.74	0.74						
	RMSE	0.74	1.35	0.98	2.05						
	MAE	0.58	1.04	0.73	1.73						
	RRMSE	19.53	43.47	29.24	38.01						

Additionally, this study presents a comprehensive evaluation of WS from five SPs. These SPs are CFSR, ERA5, ERA5-Land, MERRA-2, and TerraClimate. It should be noted that TerraClimate is a dataset of monthly climate and climatic water balance for global terrestrial surfaces from 1958 to the present. Figure 7 illustrates the variation in monthly data for all datasets used in this study. Based on the findings, TerraClimate, ERA5, and ERA5-Land have higher R-squared values compared to MERRA-2 and CFSR. As mentioned earlier, it is crucial to note that higher R-squared values do not necessarily imply that one dataset is superior to another. Thus, the analysis reveals that CFSR has exhibited superior performance compared to other datasets, as evidenced by the lower values of RMSE, MAE, and RRMSE. Following CFSR, ERA5-Land demonstrated the next-best performance.

As mentioned above, 13 distribution functions were utilized to describe the wind speed characteristics of Az-Zāwiyah from January 2022 to December 2022. Moreover, the analysis indicates that CFSR demonstrated superior performance compared to other datasets, as indicated by lower values of RMSE, MAE, and RRMSE. ERA5-Land follows CFSR with the next-best performance.

Additionally, the parameters of ten distribution functions were estimated using daily, monthly, and whole-year wind speed data with the maximum likelihood method. The best distribution among the ten distribution functions for each location was evaluated based on the results of the Kolmogorov–Smirnov test. Tables S4–S8 in the Supplementary Materials tabulate the estimated distribution parameters for all selected models based on the average

daily and monthly wind speed data. Furthermore, they provide the goodness-of-fit statistic and distribution model rankings for average daily wind speed using different datasets (measured, CFSR, and ERA5-Land). Additionally, Table 8 displays the top five distribution models that achieved the highest rankings to analyze the average daily wind speed data during the investigation period. Based on the results of the K-S tests, it was found that the W-3P, GEV, and BS distribution functions demonstrated the lowest values, indicating that they are better fits for the wind speed data.

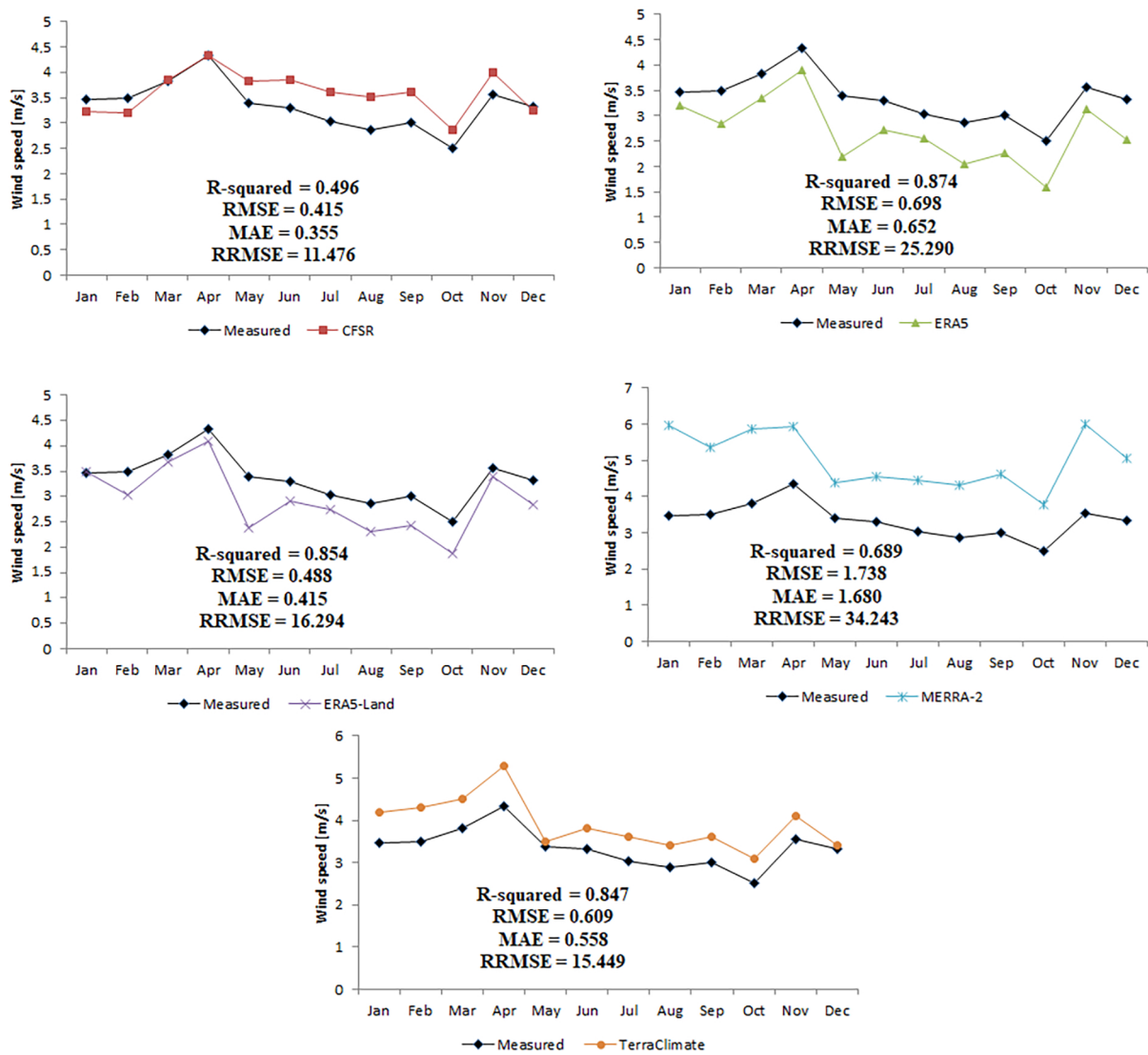


Figure 7. Average monthly wind speed for Az-Zāwiyah during 2022.

Table 8. Ranking of the best five distribution models based on the K-S test.

	Actual			CFSR			ERA5-Land		
	Model	Statistic	Rank	Model	Statistic	Rank	Model	Statistic	Rank
January	W-3P	0.112	1	BS	0.100	1	W-3P	0.081	1
	BS	0.134	2	W-3P	0.101	2	GEV	0.093	2
	K	0.135	3	GEV	0.114	3	BS	0.098	3
	GEV	0.158	4	IG	0.127	4	IG	0.102	4
	IG	0.169	5	LL	0.128	5	LL	0.107	5

Table 8. Cont.

	Actual			CFSR			ERA5-Land		
	Model	Statistic	Rank	Model	Statistic	Rank	Model	Statistic	Rank
February	K	0.083	1	GEV	0.105	1	BS	0.087	1
	W-3P	0.084	2	BS	0.108	2	W	0.088	2
	GEV	0.095	3	LL	0.112	3	LN	0.089	3
	LL	0.101	4	W-3P	0.122	4	GEV	0.091	4
	BS	0.105	5	IG	0.142	5	G	0.091	5
March	GEV	0.083	1	LL	0.090	1	GEV	0.084	1
	LL	0.083	2	GEV	0.092	2	N	0.097	2
	BS	0.084	3	BS	0.093	3	W-3P	0.098	3
	W-3P	0.091	4	W	0.095	4	BS	0.101	4
	LN	0.093	5	LN	0.102	5	R	0.109	5
April	GEV	0.101	1	LL	0.076	1	GEV	0.082	1
	G	0.106	2	GEV	0.082	2	R	0.088	2
	Na	0.108	3	BS	0.099	3	W	0.091	3
	W-3P	0.109	4	LN	0.107	4	N	0.093	4
	BS	0.109	5	IG	0.111	5	BS	0.098	5
May	W	0.071	1	LL	0.080	1	IG	0.089	1
	IG	0.081	2	BS	0.080	2	BS	0.099	2
	G	0.091	3	GEV	0.083	3	GEV	0.101	3
	K	0.093	4	IG	0.085	4	G	0.108	4
	Na	0.094	5	W-3P	0.085	5	R	0.109	5
June	LL	0.089	1	GEV	0.092	1	W-3P	0.125	1
	GEV	0.102	2	W	0.095	2	GEV	0.126	2
	BS	0.105	3	K	0.103	3	L	0.139	3
	LN	0.114	4	BS	0.106	4	Na	0.144	4
	W-3P	0.114	5	N	0.107	5	BS	0.146	5
July	GEV	0.092	1	GEV	0.089	1	GEV	0.092	1
	W	0.097	2	K	0.091	2	W-3P	0.117	2
	N	0.103	3	N	0.099	3	N	0.134	3
	K	0.106	4	W	0.099	4	K	0.134	4
	BS	0.107	5	W-3P	0.101	5	BS	0.135	5
August	GEV	0.072	1	GEV	0.111	1	GEV	0.108	1
	LL	0.081	2	BS	0.113	2	BS	0.118	2
	BS	0.085	3	W-3P	0.115	3	G	0.119	3
	W-3P	0.105	4	LL	0.137	4	IG	0.119	4
	LN	0.116	5	Na	0.155	5	W-3P	0.135	5
September	LN	0.081	1	W	0.123	1	L	0.113	1
	BS	0.087	2	Na	0.134	2	GEV	0.129	2
	GEV	0.093	3	G	0.137	3	Na	0.135	3
	G	0.095	4	N	0.140	4	N	0.135	4
	LL	0.097	5	LN	0.143	5	BS	0.146	5
October	K	0.112	1	GEV	0.105	1	Na	0.113	1
	W-3P	0.122	2	BS	0.121	2	W-3P	0.113	2
	LN	0.127	3	LN	0.125	3	G	0.116	3
	GEV	0.131	4	LL	0.130	4	BS	0.116	4
	LL	0.134	5	W	0.133	5	LL	0.118	5
November	K	0.096	1	W-3P	0.106	1	GEV	0.118	1
	W-3P	0.111	2	GEV	0.117	2	R	0.127	2
	Na	0.121	3	IG	0.126	3	Na	0.128	3
	LL	0.126	4	LL	0.128	4	W	0.131	4
	GEV	0.132	5	BS	0.129	5	G	0.134	5

Table 8. Cont.

	Actual			CFSR			ERA5-Land		
	Model	Statistic	Rank	Model	Statistic	Rank	Model	Statistic	Rank
December	GEV	0.100	1	GEV	0.107	1	GEV	0.127	1
	N	0.101	2	W-3P	0.109	2	K	0.129	2
	Na	0.113	3	IG	0.112	3	N	0.132	3
	BS	0.121	4	LN	0.112	4	BS	0.145	4
	W-3P	0.122	5	LL	0.116	5	L	0.146	5
Whole year	BS	0.025	1	GEV	0.033	1	K	0.034	1
	GEV	0.030	2	BS	0.035	2	W	0.036	2
	LL	0.050	3	IG	0.038	3	Na	0.037	3
	IG	0.054	4	LN	0.044	4	W-3p	0.038	4
	W-3p	0.056	5	W-3p	0.047	5	GEV	0.043	5
Monthly	L	0.139	1	GEV	0.117	1	GEV	0.098	1
	Na	0.152	2	N	0.133	2	G	0.109	2
	BS	0.155	3	W-P3	0.139	3	Na	0.110	3
	GEV	0.157	4	Na	0.140	4	W-P3	0.111	4
	G	0.157	5	IG	0.141	5	N	0.116	5

To evaluate the wind potential in the selected location, the wind power density is computed. In this study, the air density is assumed to be  $1.23 \text{ kg/m}^3$ . The value of WPD for each location is tabulated in Table 9.

Table 9. Mean in m/s and WPD in  $\text{W/m}^2$  for each month, whole year, and average monthly.

	Actual			CFSR			ERA5-Land		
	Model	Mean	WPD	Model	Mean	WPD	Model	Mean	WPD
January	Actual	3.47	25.72	Actual	3.47	25.72	Actual	3.47	25.72
	W-3P	3.57	27.99	BS	3.2171	20.51	W-3P	3.4988	26.38
	BS	3.47	25.74	W-3P	3.2161	20.49	GEV	3.498	26.37
	K	3.55	27.58	GEV	3.2168	20.50	BS	3.474	25.83
	GEV	3.47	25.72	IG	3.2168	20.50	IG	3.498	26.37
	IV	3.47	25.72	LL	3.1821	19.85	LL	3.4771	25.90
February	Actual	3.49	26.19	Actual	3.49	26.19	Actual	3.49	26.19
	K	3.49	26.08	GEV	3.2057	20.29	BS	3.0429	17.36
	W-3P	3.49	26.10	BS	3.2056	20.29	W	2.954	15.88
	GEV	3.49	26.19	LL	3.1651	19.53	LN	3.1321	18.93
	LL	3.45	25.40	W-3P	3.2041	20.26	GEV	3.0436	17.37
	BS	3.49	26.14	IG	3.2057	20.29	G	3.0436	17.37
March	Actual	3.82	34.26	Actual	3.82	34.26	Actual	3.82	34.26
	GEV	3.82	34.27	LL	3.7693	32.99	GEV	3.6782	30.65
	LL	3.76	32.66	GEV	3.8535	35.25	N	3.6782	30.65
	BS	3.82	34.26	BS	3.8535	35.25	W-3P	3.681	30.72
	W-3P	3.81	34.19	W	3.7104	31.47	BS	3.6782	30.65
	LN	3.81	34.11	LN	3.8431	34.96	R	3.6782	30.65
April	Actual	4.33	50.08	Actual	4.33	50.08	Actual	4.33	50.08
	GEV	4.33	50.08	LL	4.2838	48.42	GEV	4.0858	42.02
	G	4.33	50.08	GEV	4.342	50.43	R	4.0858	42.02
	Na	4.33	49.88	BS	4.3412	50.40	W	4.0253	40.18
	W-3P	4.33	50.12	LN	4.3364	50.23	N	4.0858	42.02
	BS	4.33	50.08	IG	4.342	50.43	BS	4.0858	42.02

Table 9. Cont.

	Actual			CFSR			ERA5-Land		
	Model	Mean	WPD	Model	Mean	WPD	Model	Mean	WPD
May	Actual	3.39	24.02	Actual	3.39	24.02	Actual	3.39	24.02
	W	3.29	21.90	LL	3.7544	32.60	IG	2.3815	8.32
	IG	3.39	24.03	BS	3.8313	34.64	BS	2.3815	8.32
	G	3.39	24.03	GEV	3.8313	34.64	GEV	2.3815	8.32
	K	3.64	29.66	IG	3.8313	34.64	G	2.3815	8.32
	Na	3.35	23.08	W-3P	3.8309	34.63	R	2.3815	8.32
June	Actual	3.31	22.32	Actual	3.31	22.32	Actual	3.31	22.32
	LL	3.27	21.59	GEV	3.8607	35.45	W-3P	2.9195	15.33
	GEV	3.31	22.32	W	3.8071	33.99	GEV	2.9205	15.34
	BS	3.31	22.32	K	3.9165	37.01	L	2.9205	15.34
	L	3.31	22.31	BS	3.8607	35.45	Na	2.977	16.25
	W-3P	3.31	22.28	N	3.8607	35.45	BS	2.9227	15.38
July	Actual	3.03	17.19	Actual	3.03	17.19	Actual	3.03	17.19
	GEV	3.03	17.18	GEV	3.6035	28.82	GEV	2.7356	12.61
	W	2.98	16.35	K	3.6001	28.74	W-3P	2.7494	12.80
	N	3.03	17.18	N	3.6035	28.82	N	2.7356	12.61
	K	3.03	17.15	W	3.5615	27.83	K	2.553	10.25
	BS	3.03	17.18	W-3P	3.6069	28.91	BS	2.7388	12.65
August	Actual	2.88	14.65	Actual	2.88	14.65	Actual	2.88	14.65
	GEV	2.88	14.65	GEV	3.5129	26.70	GEV	2.3074	7.57
	LL	2.83	14.00	BS	3.5128	26.70	BS	2.3074	7.57
	BS	2.88	14.65	W-3P	3.5117	26.68	G	2.3074	7.57
	W-3P	2.88	14.67	LL	3.4779	25.91	IG	2.3074	7.57
	LN	2.87	14.58	Na	3.5033	26.49	W-3P	2.3034	7.53
September	Actual	3.01	16.80	Actual	3.01	16.80	Actual	3.01	16.80
	LN	3.01	16.79	W	3.5707	28.04	L	2.4296	8.83
	BS	3.01	16.80	Na	3.61	28.98	GEV	2.4296	8.83
	GEV	3.01	16.80	G	3.612	29.03	Na	2.4316	8.86
	G	3.01	16.80	N	3.612	29.03	N	2.4296	8.83
	LL	2.98	16.30	LN	3.6118	29.02	BS	2.4296	8.83
October	Actual	2.50	9.63	Actual	2.50	9.63	Actual	2.50	9.63
	K	2.52	9.84	GEV	2.8597	14.41	Na	1.8844	4.12
	W-3P	2.51	9.72	BS	2.8597	14.41	W-3P	1.8675	4.01
	LN	2.50	9.60	LN	2.8586	14.39	G	1.8702	4.03
	GEV	2.50	9.62	LL	2.8225	13.85	BS	1.8685	4.02
	LL	2.47	9.31	W	2.8039	13.58	LL	1.9805	4.79
November	Actual	3.55	27.65	Actual	3.55	27.65	Actual	3.55	27.65
	K	3.54	27.35	W-3P	4.0756	41.70	GEV	3.3942	24.09
	W-3P	3.55	27.51	GEV	3.9967	39.33	R	3.3942	24.09
	Na	3.52	26.93	IG	3.9967	39.33	Na	3.4171	24.58
	LL	3.53	27.19	LL	3.8996	36.53	W	3.2903	21.94
	GEV	3.55	27.65	BS	3.9853	38.99	G	3.3942	24.09
December	Actual	3.33	22.64	Actual	3.33	22.64	Actual	3.33	22.64
	GEV	3.33	22.65	GEV	3.2542	21.23	GEV	2.8371	14.07
	N	3.33	22.65	W-3P	3.2466	21.08	K	2.85	14.26
	Na	3.32	22.53	IG	3.2542	21.23	N	2.8371	14.07
	BS	3.33	22.65	LN	3.2538	21.22	BS	2.8371	14.07
	W-3P	3.32	22.56	LL	3.265	21.44	L	2.8371	14.07

Table 9. Cont.

	Actual			CFSR			ERA5-Land		
	Model	Mean	WPD	Model	Mean	WPD	Model	Mean	WPD
Whole year	Actual	3.34	25.72	Actual	3.34	26.12	Actual	3.34	26.18
	BS	3.34	26.38	GEV	3.60	26.13	K	2.93	26.19
	GEV	3.34	26.37	BS	3.60	26.14	W	2.92	26.19
	LL	3.34	25.83	IG	3.60	26.15	Na	2.93	26.20
	IG	3.34	26.37	LN	3.59	26.16	W-3p	2.93	26.21
	W-3p	3.34	25.90	W-3p	3.60	26.17	GEV	2.93	26.22
Monthly	Actual	3.34	25.72	Actual	3.34	26.12	Actual	3.34	26.18
	L	3.34	26.38	GEV	3.60	26.13	GEV	2.93	26.19
	Na	3.34	26.37	N	3.60	26.14	G	2.93	26.19
	BS	3.34	25.83	W-P3	3.60	26.15	Na	2.93	26.20
	GEV	3.34	26.37	Na	3.59	26.16	W-P3	2.93	26.21
	G	3.34	25.90	IG	3.60	26.17	N	2.93	26.22

Using the average measured dataset for evaluating the wind potential, it shows that the value of WPD ranges from 9.31 W/m<sup>2</sup> to 50.12 W/m<sup>2</sup> with an average value of 24.25 W/m<sup>2</sup>. Moreover, the value of WPD is within the range of 9.63–50.43 W/m<sup>2</sup> with an average value of 28.53 W/m<sup>2</sup> using the CFSR dataset. Furthermore, it was found that the WPD values varied between 4.01 W/m<sup>2</sup> and 50.08 W/m<sup>2</sup> with an average value of 18.65 W/m<sup>2</sup> by utilizing the ERA5-Land dataset.

In general, the wind energy generation potential of sites is classified according to average power density values at a height of 10 m as follows [117,118]:

- Fair (WPD < 100 W/m<sup>2</sup>)
- Fairly good (100 W/m<sup>2</sup> < WPD < 300 W/m<sup>2</sup>)
- Good (300 W/m<sup>2</sup> < WPD < 700 W/m<sup>2</sup>)
- Very good (WPD > 700 W/m<sup>2</sup>)

Based on the value of WPD, the selected locations can be considered as power class 1, which indicates poor wind energy potential. Therefore, small-scale wind turbines are suitable to be used in the selected regions for exploiting the available wind energy potential. Furthermore, it can be concluded that high-capacity wind turbines (MWs) with a height of 90 m and above can be suitable for gathering the wind energy potential in the selected locations.

This is investigated using the power law model, i.e., the collected data at 10 m height is synthesized to the 90 m height, the height at which most of the 1 MW capacity or above wind turbines are located.

### 3.2. Assessment of Solar Energy Potential for Az-Zāwiyah

Table S9 in the Supplementary Materials presents a statistical summary of the average solar radiation, including various descriptive measures such as mean, standard deviation (SD), coefficient of variation (CV), minimum (Min.), maximum (Max.), kurtosis (K), and skewness (S) for the selected location. Moreover, the daily solar radiation for Az-Zāwiyah is illustrated in Figure S2 in the Supplementary Materials. Based on the findings, the following can be noticed:

- By considering the measured data, the mean values for all months are within the range of 118.86–327.83 W/m<sup>2</sup>. The minimum value of 38.37 W/m<sup>2</sup> and maximum value of 343.39 W/m<sup>2</sup> were recorded in March and June, respectively.
- Based on the CFSR dataset, the mean values fall within the range of 124.16–329.77 W/m<sup>2</sup>. April had the lowest recorded value of 16.00 W/m<sup>2</sup>, while August had the highest recorded value of 378.0 W/m<sup>2</sup>.

- By analyzing the ERA5 dataset, it is found that the mean values for all months varied from 121.51 W/m<sup>2</sup> to 328.80 W/m<sup>2</sup>. Moreover, it is noticed that the lowest value of 38.30 W/m<sup>2</sup> was observed in March, while the highest value of 342.2 W/m<sup>2</sup> was recorded in June.
- By considering the ERA5-Land dataset, it is observed that the mean value ranged from 118.58 W/m<sup>2</sup> to 325.95 W/m<sup>2</sup>. Moreover, the maximum and minimum solar radiation values were recorded in March and June with values of 39.10 W/m<sup>2</sup> and 341.90 W/m<sup>2</sup>, respectively.
- Based on the MERRA-2 dataset, the WPD values varied from 130.98 to 339.85 W/m<sup>2</sup>. March had the lowest recorded value of 59.20 W/m<sup>2</sup>, while June had the highest recorded value of 360.90 W/m<sup>2</sup>.

Furthermore, it is essential to assess the performance of the estimated data; thus, this study employed statistical indices, including R-squared, RMSE, MAE, and RRMSE, to evaluate their performance. The results of the analysis are summarized in Table 10, presenting the following findings:

- The selection of the best dataset varies for each month based on the R-squared value. However, it is crucial to note that higher R-squared values do not automatically indicate the superiority of one dataset over another. R-squared merely reflects the strength of the linear relationship between the observed and modeled values. Therefore, to determine the best dataset, the analysis also considered RMSE, MAE, and RRMSE, as these metrics provide additional insights beyond the R-squared value.
- Among the available datasets, ERA5-Land consistently demonstrated the best performance when the data for the whole year were used, as indicated by the lower values of RMSE and MAE when compared to the other datasets.
- For the whole year, the RRMSE values for all datasets ranged from 20% to 30%, suggesting a good performance rate. This finding is supported by the results presented in Table S2 in the Supplementary Materials.

**Table 10.** Statistical parameters using average daily solar radiation data for Az-Zāwiyah.

Month	Variable	Dataset				Month	Variable	Dataset			
		CFSR	ERA5	ERA5-Land	MERRA-2			CFSR	ERA5	ERA5-Land	MERRA-2
January	R-squared	0.38	0.76	0.97	0.86	July	R-squared	0.09	0.88	0.99	0.03
	RMSE	30.82	15.41	5.08	21.50		RMSE	10.81	5.40	3.56	17.26
	MAE	22.68	11.34	3.67	18.40		MAE	5.36	2.68	3.30	12.99
	RRMSE	23.76	12.30	4.14	15.35		RRMSE	3.32	1.66	1.11	5.14
February	R-squared	0.43	0.74	0.98	0.58	August	R-squared	0.06	0.46	0.99	0.16
	RMSE	41.02	20.51	4.72	27.80		RMSE	20.88	10.44	3.32	19.09
	MAE	30.24	15.12	3.68	23.72		MAE	11.34	5.67	3.04	16.96
	RRMSE	23.84	12.33	2.87	15.54		RRMSE	6.97	3.55	1.16	6.29
March	R-squared	0.62	0.88	0.99	0.39	September	R-squared	0.74	0.94	0.99	0.72
	RMSE	33.88	16.94	4.10	42.62		RMSE	13.61	6.80	2.45	14.70
	MAE	21.16	10.58	3.15	32.33		MAE	7.81	3.90	1.94	10.88
	RRMSE	14.77	7.41	1.78	19.18		RRMSE	5.40	2.72	0.99	5.80
April	R-squared	0.08	0.39	0.99	0.56	October	R-squared	0.44	0.87	0.99	0.56
	RMSE	57.74	28.87	3.87	37.04		RMSE	22.22	11.11	2.16	24.52
	MAE	23.30	11.65	2.46	26.09		MAE	17.80	8.90	1.56	20.71
	RRMSE	21.14	10.48	1.38	13.86		RRMSE	10.92	5.69	1.16	11.80
May	R-squared	0.67	0.86	0.99	0.56	November	R-squared	0.40	0.84	0.99	0.76
	RMSE	32.23	16.12	3.50	29.24		RMSE	23.72	11.86	3.25	20.51
	MAE	20.24	10.12	2.91	24.56		MAE	13.71	6.86	2.37	16.44
	RRMSE	10.28	5.24	1.16	9.27		RRMSE	15.18	7.83	2.21	12.61
June	R-squared	0.53	0.85	0.97	0.30	December	R-squared	0.60	0.90	0.85	0.49
	RMSE	8.40	4.20	2.63	17.75		RMSE	12.80	6.40	6.88	13.84
	MAE	4.61	2.30	2.32	14.88		MAE	9.78	4.89	4.10	10.33
	RRMSE	2.55	1.28	0.80	5.22		RRMSE	9.59	4.97	5.39	10.49

Table 10. Cont.

Month	Variable	Dataset				Month	Variable	Dataset			
		CFSR	ERA5	ERA5-Land	MERRA-2			CFSR	ERA5	ERA5-Land	MERRA-2
Whole year	R-squared	0.88	0.97	0.99	0.91						
	RMSE	28.98	14.49	4.00	25.30						
	MAE	15.59	7.79	2.87	19.01						
	RRMSE	11.78	5.96	1.67	10.15						

Moreover, the variation in monthly solar radiation data for all datasets used in this study is illustrated in Figure 8. Based on the findings, the R-squared value is within the range of 0.981–0.997, which indicates a strong linear relationship between the observed and modeled values. Additionally, the RRMSE value for all datasets falls within the range of 20% to 30%, indicating a good performance rate for all datasets, as demonstrated in Table 4. Additionally, Figure 9 shows the annual value of solar radiation (SR) for the selected region. It is observed that the SR value is within the range of 1882–2070 kWh/m<sup>2</sup>. Generally, the solar energy generation potential of sites is classified according to the annual value of SR as shown in Table 5. It is found that the selected region exhibits abundant solar resources and is classified as class 5 (excellent). Consequently, the region is suitable for the future installation of PV systems, primarily due to its significantly high SR value.

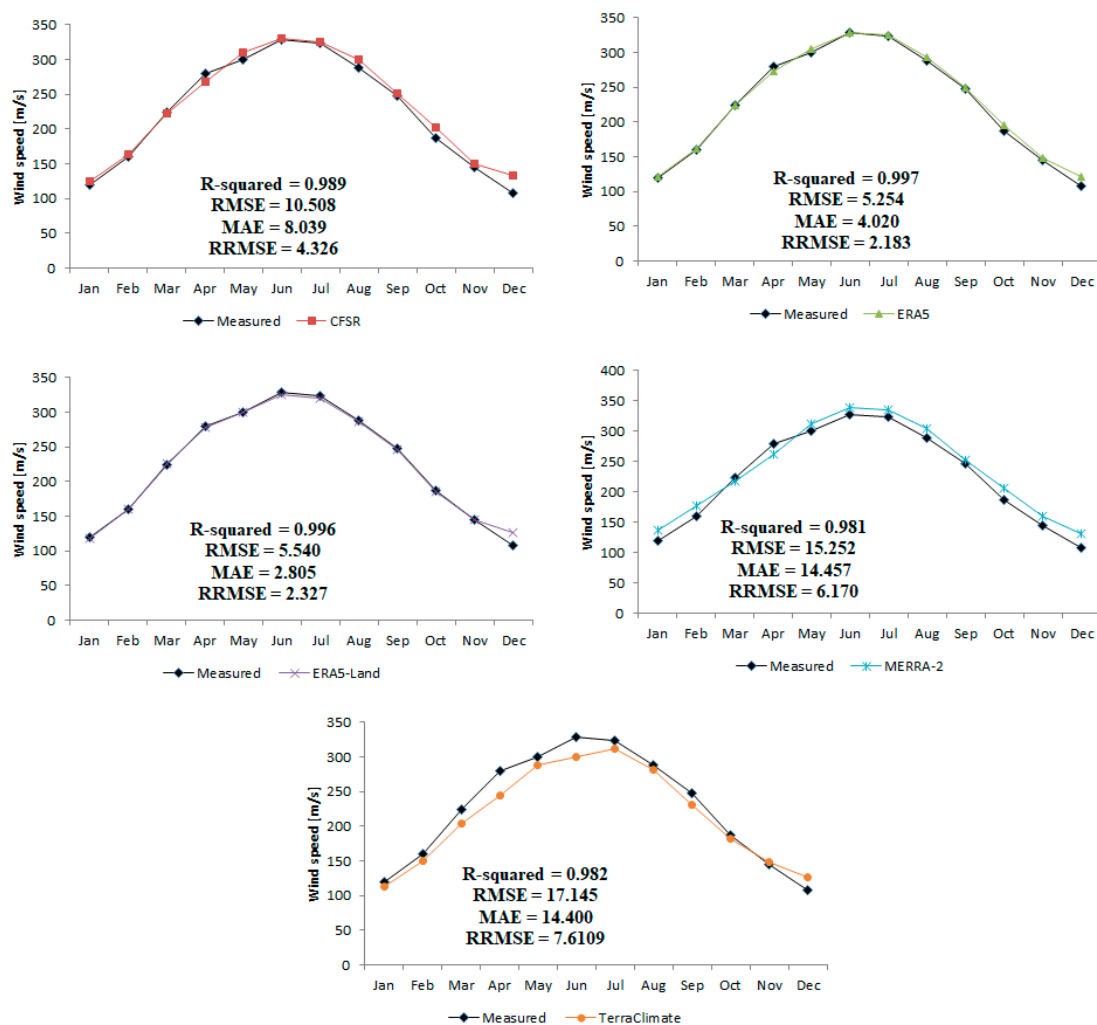
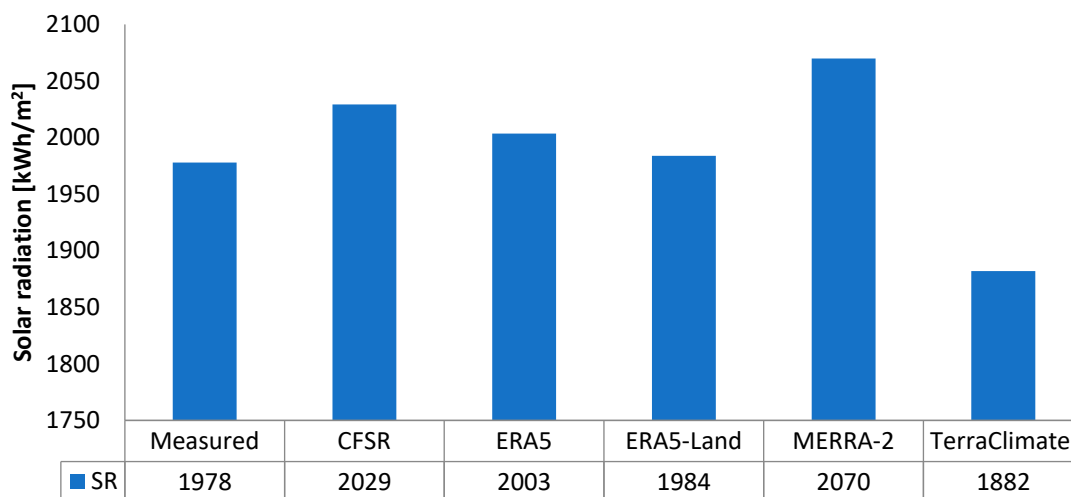


Figure 8. Average monthly solar radiation for Az-Zāwiyah during 2022.



**Figure 9.** Annual value of solar radiation for Az-Zāwiyah during 2022.

### 3.3. Assessment of Wind and Solar Energy Potential Based on the Long Period of 2000–2022

In this study, the wind energy potential was evaluated at agricultural and coastal locations, namely, Az-Zāwiyah, Aljmail, Castilverde, Janzur, Msallatah, Sabratah, and Tajoura. These regions have economies that heavily depend on agriculture. The productive land in these areas supports diverse agricultural activities, including crop cultivation and livestock farming. Moreover, based on the previous section, it has been determined that the ERA5-Land and ERA5 datasets exhibit superior performance compared to other datasets for wind speed and solar radiation, respectively. Therefore, average daily wind speed and solar radiation data have been used to estimate the wind and solar potential in the selected regions. The data were collected from CFSR, ERA5-Land, and ERA5 from 2000 to 2022.

#### 3.3.1. Wind Speed Characteristics and Wind Power Density at a Height of 10 m

Table 11 provides the descriptive statistics for the wind speed data for all selected locations. Considering the ERA5-Land dataset, it is found that the mean value of wind speed is within the range of 4.75–5.19 m/s. The highest and lowest mean wind speeds were recorded at Aljmail and Msallatah, respectively. Furthermore, the CV values observed in the data range from 30.72% (Msallatah) to 34.29% (Aljmail), indicating a moderate level of variability in the measured wind speeds. Moreover, it is found that the maximum wind speed of 8.40 m/s was recorded at Msallatah. Additionally, skewness values for all locations are positive, indicating that all distributions are right-skewed, indicating a longer or fatter tail on the right side of the distribution. Based on the CFSR dataset, the average wind speed falls within the 4.85 (Aljmail)–5.49 (Msallatah) m/s range. The data show moderate variability in wind speeds, with coefficient of variation (CV) values ranging from 20.68% (Msallatah) to 25.81% (Az-Zāwiyah). The highest maximum wind speed was recorded at Msallatah with a value of 7.69 m/s. Furthermore, the skewness values for most locations (Castilverde, Msallatah, and Sabratah) are positive, indicating that all distributions are right-skewed, implying a longer or fatter tail on the right side of the distribution.

To demonstrate the suitability of the distribution functions (DFs), the Kolmogorov–Smirnov test was used. Tables S10 and S11 in the Supplementary Materials list the parameter values estimated for various distribution functions for all selected locations based on the ERA5-Land and CFSR datasets, respectively. It is shown that GEV matches well with the observed wind speed data. Additionally, it is found that the Rayleigh DF seems to be unsuitable for describing the wind speed for all locations. Moreover, Table 12 lists the mean wind speed and WPD for the observed data and each DF. The analysis reveals that the WPD values fall within the range of 65.41–86.32 W/m<sup>2</sup> and 69.73–101.9.3 W/m<sup>2</sup> based on the ERA5-Land and CFSR datasets, respectively. Based on the ERA5-Land dataset, all

selected locations exhibit a favorable wind resource, which can be effectively utilized for various applications, including the deployment of small-scale wind turbines.

**Table 11.** Statistical estimators of the daily wind speed using ERA5-Land and CFSR for all locations.

Dataset	Location	Mean	SD	CV	Min	Max	S	K
ERA5-Land	Aljmail	4.75	1.63	34.29	2.37	7.58	0.14	−0.88
	Az-Zāwiyah	5.19	1.64	31.55	2.72	7.95	0.00	−0.94
	Castelverde	4.86	1.62	33.26	2.58	7.86	0.36	−0.64
	Msallatah	5.19	1.60	30.72	3.09	8.40	0.62	−0.22
	Sabratah	4.85	1.63	33.66	2.46	7.67	0.11	−0.91
CFSR	Aljmail	4.84	1.24	25.52	2.71	6.78	−0.28	−0.69
	Az-Zāwiyah	4.85	1.25	25.81	2.80	6.81	−0.16	−0.91
	Castelverde	4.98	1.19	23.85	3.12	7.05	0.13	−0.65
	Msallatah	5.49	1.14	20.68	3.89	7.69	0.57	−0.29
	Sabratah	5.25	1.18	22.52	3.37	7.27	0.08	−0.71

**Table 12.** Mean in m/s and WPD in  $W/m^2$  for each location.

Location	ERA5-Land			CFSR			Location	ERA5-Land			CFSR		
	Model	Mean	WPD	Model	Mean	WPD		Model	Mean	WPD	Model	Mean	WPD
Aljmail	Observed	4.75	65.81	Observed	4.84	69.76	Az-Zāwiyah	Observed	5.19	86.07	Observed	4.85	70.10
	GEV	4.74	65.74	GEV	4.84	69.73		GEV	5.19	86.08	GEV	4.85	70.13
	N	4.74	65.74	W-3P	4.85	70.25		N	5.19	86.08	N	4.85	70.13
	G	4.74	65.74	N	4.84	69.73		BS	5.19	86.09	BS	4.84	70.02
	W-3P	4.74	65.41	BS	4.84	69.74		G	5.19	86.08	W-3P	4.86	70.58
	Na	4.75	65.83	L	4.84	69.73		W-3P	5.19	86.15	Na	4.85	70.27
Castelverde	Observed	4.86	70.62	Observed	4.98	76.08	Msallatah	Observed	5.19	86.32	Observed	5.49	101.87
	GEV	4.86	70.60	Na	4.97	75.82		GEV	5.19	86.28	W-3P	5.48	101.56
	K	4.80	68.12	G	4.98	76.12		Na	5.16	84.80	BS	5.49	101.92
	Na	4.84	70.01	BS	4.98	76.12		G	5.19	86.28	GEV	5.49	101.93
	N	4.86	70.60	W-3P	4.98	76.14		W-3P	5.18	85.55	LL	5.35	94.49
	G	4.86	70.60	GEV	4.98	76.12		IG	5.19	86.28	W	5.27	90.10
Sabratah	Observed	4.85	70.06	Observed	5.25	88.93							
	GEV	4.85	70.13	GEV	5.25	88.88							
	N	4.85	70.13	N	5.25	88.88							
	K	4.76	66.53	Na	5.24	88.60							
	G	4.85	70.13	BS	5.25	88.88							
	W-3P	4.84	69.82	W-3P	5.25	88.98							

Considering the CFSR dataset, Msallatah has the highest annual WPD compared to other locations. This location can be considered a location for installing large-scale wind turbines. However, four locations with an annual WPD of less than  $100 W/m^2$  may be considered good candidates for installing small-scale wind turbines.

### 3.3.2. Solar Radiation Characteristics

Based on the previous section, Az-Zāwiyah has been assessed to possess abundant solar resources, classified as class 5 (excellent). As a result, the region is highly suitable for the future installation of photovoltaic (PV) systems. This is primarily due to the region's significantly high solar resource (SR) value, indicating favorable conditions for solar energy generation. Also, it is possible to assume that solar radiation remains relatively constant over large areas, disregarding the impact of cloud absorption on solar radiation according to Bhatia [78]. Moreover, according to the World Bank Group (Global Solar Atlas), SR in coastal locations is within the range of  $1900\text{--}2100 kWh/m^2$ . Thus, this study examines the potential of solar energy across five different locations over 13 years from 2010 to 2020, using a monthly database provided by ERA5 (best SP). The variations in average monthly solar radiation (SR) and air temperature (AT) are illustrated in Figure 10. The maximum SR value is recorded in July while the minimum value is recorded in December.

The annual value of SR is within the range of 1970.21–2028.46 kWh/m<sup>2</sup>. Based on these values, the selected locations exhibit abundant solar resources and are classified as class 5 (excellent). Consequently, these locations are suitable for the future installation of PV systems, primarily due to their significantly high SR value. Figure 8 also presents the average air temperature, revealing that Sabratah and Msallatah have the maximum and minimum mean AT values at 21.17 °C and 20.06 °C, respectively.

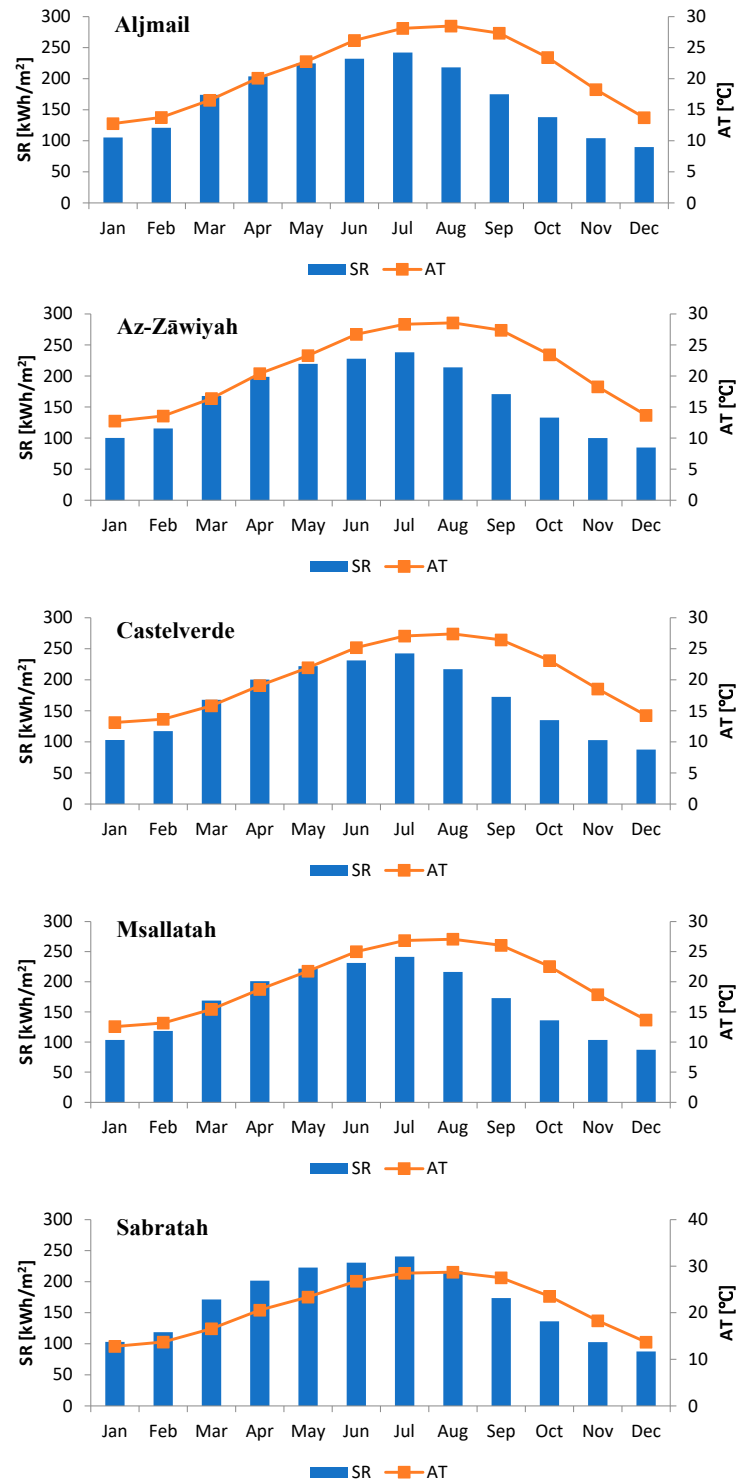


Figure 10. Monthly variation in solar radiation (SR) and air temperature (AT) for all selected locations.

### 3.4. Economic Analysis of Wind and Solar Project in Az-Zāwiyah during 2022

In the previous sections, it was noted that the frames have identical conditions and similar daily loads. Furthermore, the analysis indicated that the chosen locations have a higher potential for solar energy in comparison to wind energy. Consequently, the authors have developed two renewable energy systems with different capacities based on the value of the peak power output ( $P_{max}$ ) of the PV system (Equation (33)) [9]. Subsequently, the performance of both the PV and wind projects was assessed by evaluating the energy production capacity factor (CF), simple payback period (SPP), and the levelized cost of electricity (LCOE).

$$P_{max} = \frac{E_{AC}P_i}{G_{SR}f_{PV}\eta_{inv}} \quad (33)$$

where  $P_i$  is the solar radiation at STC in  $\text{kW}/\text{m}^2$ ,  $G_{SR}$  is the maximum monthly value of global solar radiation ( $\text{kWh}/\text{m}^2/\text{d}$ ),  $f_{PV}$  is the PV derating factor (assumed to be 80%),  $E_{AC}$  is the daily power consumption in  $\text{kWh}/\text{d}$ , and  $\eta_{inv}$  is the inverter yield.

Moreover, the energy requirement of a saline water reverse osmosis (RO) system must be calculated to evaluate its power needs and incorporate it into a renewable energy system. The total power requirement of an RO plant takes into account the power needed for desalination (i.e., mechanically pushing water through membranes), as well as the electricity required to pump the feed water to the plant and the treated water into the water system. The primary water source for the desalination plant is the saline groundwater extracted from the existing well. As mentioned before, the total volume of water needed for irrigation, drinking purposes, and domestic use is approximately 24,000 L/week ( $3428.57 \text{ L}/\text{day} = 3.4 \text{ m}^3/\text{day}$ ). Thus, the energy requirements for the RO desalination plant can be determined using Equation (34) [119].

$$P_D = \frac{SEC \cdot q}{CF_D} \quad (34)$$

where  $P_D$  is the power requirement of the RO in kW,  $CF_D$  is the capacity factor of the plant, which is assumed to be 95%,  $q$  is the flow rate for the feed water in  $\text{m}^3/\text{h}$ , and  $SEC$  is the specific energy consumption of desalination in  $\text{kWh}/\text{m}^3$ , which can range from 0.5 to 3  $\text{kWh}/\text{m}^3$ , depending on factors such as the salinity of the feed water, the operational characteristics of the plant, the type of membranes used, and other relevant factors [119]. In this study, it is assumed to be 1.75  $\text{kWh}/\text{m}^3$ .

By using Equations (33) and (34), the maximum output power of the system was calculated to be 104 kW for Farm 1 and 34 kW for Farm 2, based on the measured maximum solar radiation value.

The economic data required for the techno-economic model include the cost of electricity per kWh, the annual interest rate, the capital cost of acquisition, and the operation and maintenance costs associated with the wind turbine. In this study, the following assumptions were taken into consideration:

- The lifetime of the turbine and PV is assumed to be 20 years and 25 years, respectively.
- The interest rate and inflation rate were taken as 7% and 8%, respectively.
- The engineering cost, civil work cost, installation cost, cost of transport, cost of the electrical connection, and miscellaneous costs were assumed to be 2%, 5%, 8%, 2%, 7%, and 1%, respectively, of the cost of the wind turbine.
- The scrap value was assumed to be 10% of the turbine price and civil work cost.
- The price of the electricity was taken as USD 0.10 to ensure the economic viability and feasibility of the project.
- The capacity of the RO plant is 200 L/h and it costs about USD 2000 based on the available literature. Calculations consider that the plant is under operation 17 h/day.

### 3.4.1. Economic Analysis of Wind Turbines for the Period of January 2022–December 2022

In general, wind turbines can be classified into horizontal axis wind turbines (HAWTs) and vertical axis wind turbines (VAWTs). The horizontal axis wind turbine, equipped with propeller blades, commonly achieves an efficiency of 60% and is widely deployed. In contrast, vertical axis wind turbines can surpass 70% efficiency. In this section, the performance of different types of wind turbines is compared. The specification of the selected wind turbine is presented in Table S12 in the Supplementary Materials. Also, the power curves of these turbines are illustrated in Figure S3 in the Supplementary Materials.

Figures S4 and S5 in the Supplementary Materials present the monthly variation of EP for all selected turbines. It is found that the EP values are within the range of 3257.9–10,870.0 kWh for VAWTs and 2049.7–19,275.5 kWh for HAWTs. The highest and lowest values of EP were obtained by using MERRA-2 and ERA5, respectively. The highest coefficient of correlation was found between the measured data and ERA5-Land when VAWTs and HAWTs were used, respectively, with ERA5 showing the next highest correlation as shown in Figures S4 and S5 in the Supplementary Materials. On the other hand, the lowest correlation was observed between the actual data and MERRA-2 and CFSR when VAWTs and HAWTs were used, respectively.

Moreover, the monthly variation in CF for all selected turbines is presented in Figures S6 and S7 in the Supplementary Materials. The CF values range from 9.0% to 29.2% for VAWTs and from 5.7% to 51.8% for HAWTs. The highest CF value was obtained when using MERRA-2, while the lowest value was obtained with ERA5. Additionally, Figures S6 and S7 in the Supplementary Materials show that the highest coefficient of correlation is found between the actual data and ERA5-Land when VAWTs and HAWTs are used, respectively. Additionally, ERA5 exhibits the next highest correlation. On the other hand, the lowest correlation is observed between the actual data and MERRA-2 and CFSR when VAWTs and HAWTs are used, respectively.

Furthermore, Figure 11 shows the estimated results in terms of annual energy produced (AEP), annual capacity factor (ACF), electricity generated cost (LCOE), and simple payback period (SPP) for all used datasets.

Based on the measured data illustrated in Figure 11, it is evident that the annual energy production (EP) was estimated to be 102,533 kWh for the VAWT and 104,595 kWh for the HAWT. Moreover, the analysis revealed that the annual CF for the VAWT was 23.4%, while for the HAWT, it was slightly higher at 23.9%. These findings suggest that the CF of wind turbines tends to increase as the hub height of the turbines rises. Moreover, the calculated SPP for the wind turbines in the chosen region indicates that both the VAWTs and HAWTs will be able to recoup their initial costs within their lifetimes, which is 20 years. Specifically, the VAWT has the longest SPP of 14.14 years, while the HAWT has a shorter SPP of 11.95 years. The LCOE using HAWTs was found to be 0.117 USD/kWh, while for the VAWTs, it was slightly higher at 0.138 USD/kWh.

Based on the dataset collected from various satellite products (Figure 9), it is noticed that MERRA-2 has the highest EP values, with an EP of 121,591 kWh for VAWTs and 180,608 kWh for HAWTs. Conversely, ERA5 presents the lowest EP values, amounting to 74,028 kWh for VAWTs and 58,948 kWh for HAWTs, across both wind turbine types. Additionally, it is seen that the comparison reveals that the EP values obtained using the CFSR dataset slightly exceed the EP values estimated from the measured data. Similarly, the maximum annual value of CF is obtained from MERRA-2, while the minimum one is obtained from ERA5. Moreover, the comparison highlights that the CF values obtained using the CFSR dataset slightly exceed the CF values estimated from the measured data (i.e., the CF value for VAWTs is 25.2% with the CFSR dataset compared to 23.4% with the measured data, while the CF value for HAWTs is 24.8% with the CFSR dataset, slightly higher than the 23.9% estimated from the measured data). Additionally, the calculated SPP for the wind turbines in the selected region, based on the CFSR, MERRA-2, and TerraClimate datasets, indicates that both the VAWTs and HAWTs will be able to recover their initial costs within their lifetimes. However, the longest SPP values are obtained from the ERA5

and ERA5-Land datasets, exceeding 15 years. This suggests that installing the wind turbines in the selected location using the ERA5 and ERA5-Land datasets may not be economically viable for energy production. In addition, the MERRA-2 dataset has the lowest value of the LCOE, while the ERA5 dataset results in the highest LCOE value. Additionally, the LCOE values obtained using the CFSR dataset are close to the LCOE value derived from the measured data.

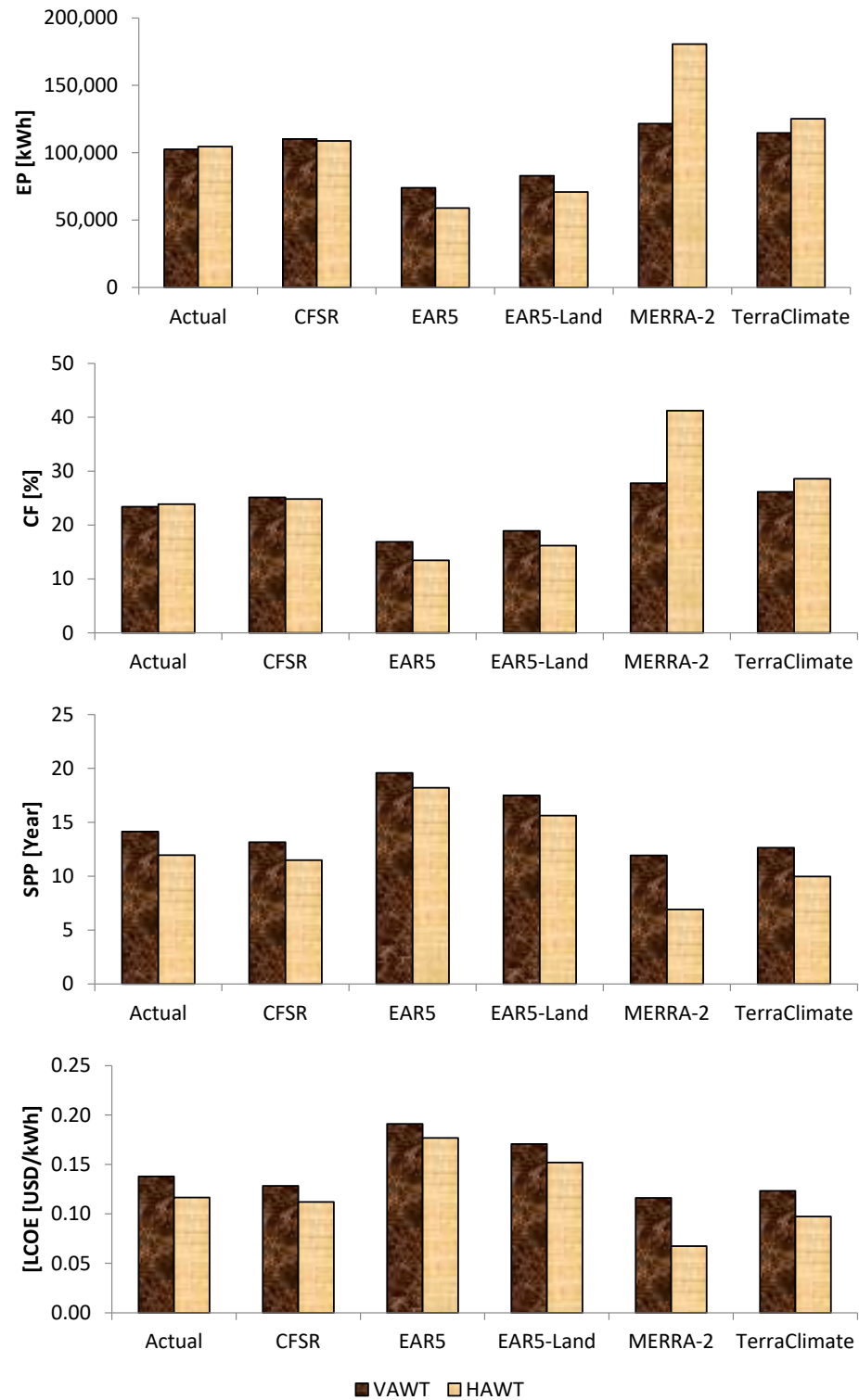


Figure 11. Performance of wind projects in terms of EP, CF, LCO, and SPP for all selected turbines.

It is important to acknowledge that these results were derived for a single turbine (either a VAWT or HAWT) with a capacity of 50 kW. Extrapolating these results can provide insights into the expected performance of wind farms with capacities of 102.3 kW for Farm 1 and 32 kW for Farm 2.

#### 3.4.2. Economic Analysis of PV System for the Period of January 2022–December 2022

Based on the available information and research conducted by the authors regarding PV technology companies or manufacturers in Libya, PV system components including the PV modulus and inverters may not be widely available in the Libyan market in all regions. In general, solar energy has gained global attention due to its renewable and sustainable nature in many African countries including Libya (see Table 1). Considering the global availability of solar technology, it is expected that PV panels will be available in the market. However, the extent of availability and adoption can be influenced by factors such as local regulations, government incentives, infrastructure, and market demand as shown in Table 1.

For the developed PV system, a mono-Si 545 W PV module manufactured by JinKO Solar Company was selected as it is an efficient PV module. The specification of the selected module is tabulated in Table S13 in the Supplementary Materials. To construct the proposed PV project in each farm, a total of 188 and 60 of the selected modules are required for Farm 1 and Farm 2, respectively. Furthermore, the estimated area occupied by these modules is approximately 484 m<sup>2</sup> for Farm 1 and 154 m<sup>2</sup> for Farm 2. Four units of a Multisolar 30 kW Hybrid Inverter with a capacity of 30 kW were utilized for Farm 1. For Farm 2, a Pure Sine Wave Inverter with capacities of 30 kW and 10 kW was employed. The specification of the selected inverters can be found in Refs. [120,121].

Figures 12 and 13 illustrate the economic performance of the PV system for Farm 1 and Farm 2, respectively, across different datasets. The analysis encompasses various parameters such as annual energy production (AEP), annual capacity factor (ACF), performance ratio (PR), system efficiency, electricity generation cost (LCOE), and simple payback period (SPP). The key findings from the study are as follows:

- The annual energy production (AEP) for Farm 1 falls within the range of 154,055 to 169,422 kWh, while for Farm 2, it ranges from 49,086 to 53,982 kWh.
- Both farms exhibit similar ranges for annual capacity factor (ACF), performance ratio (PR), and system efficiency, which are approximately 17.2% to 18.9%, 79.88% to 79.92%, and 69.35% to 69.38%, respectively.
- The electricity generation cost (LCOE) for Farm 1 varies from 0.0161 to 0.0178 USD/kWh, whereas for Farm 2, it ranges between 0.0200 and 0.0222 USD/kWh.
- The simple payback period (SPP) for Farm 1 is estimated to be between 10.89 and 11.12 years, while for Farm 2, it falls within the range of 14.20 to 14.60 years.
- These findings provide insights into the economic viability and performance of the PV systems at Farm 1 and Farm 2 across the considered datasets.
- The analysis suggests that the solar potential is relatively consistent across different datasets, as the values obtained are similar or closely aligned with the measured data. This indicates that the solar energy generation potential remains relatively uniform regardless of the specific dataset used for evaluation.

#### 3.5. Economic Analysis of Wind and Solar Projects in All Selected Locations during the Period of 2000–2022

Table 13 summarizes the annual value of EP, CF, LCOE, and SPP for each wind turbine. The findings indicate that using horizontal axis wind turbines (HAWTs) leads to an increase in the annual EP and CF compared to VAWTs. The results reveal that Msallatah exhibited the highest annual EP and CF among the selected regions. For VAWTs, the EP was 143,662.34 kWh with a CF of 32.8%. On the other hand, for HAWTs, the EP was 176,174.20 kWh with a CF of 40.22%. Sabratah was identified as the second most suitable location for wind power generation. Moreover, the values obtained for all regions

are relatively close, indicating that all selected areas are suitable for future wind farm installations. Moreover, it is observed that the SPP values varied from 6.51 to 6.24 years for HAWTs and from 10.09 to 10.65 years for VAWTs. These results indicate that both types of turbines have SPP values within the lifetime of 20 years. In other words, both turbines can cover the initial investment cost before the end of their expected lifetime. Furthermore, the analysis reveals that the LCOE values obtained using HAWTs range from 0.1039 to 0.0953 USD/kWh. In contrast, the LCOE values obtained using VAWTs range from 10.6476 to 10.0931 USD/kWh. The LCOE value for HAWTs is lower compared to VAWTs. This indicates that the cost of producing electricity using HAWTs is more economical than using VAWTs.

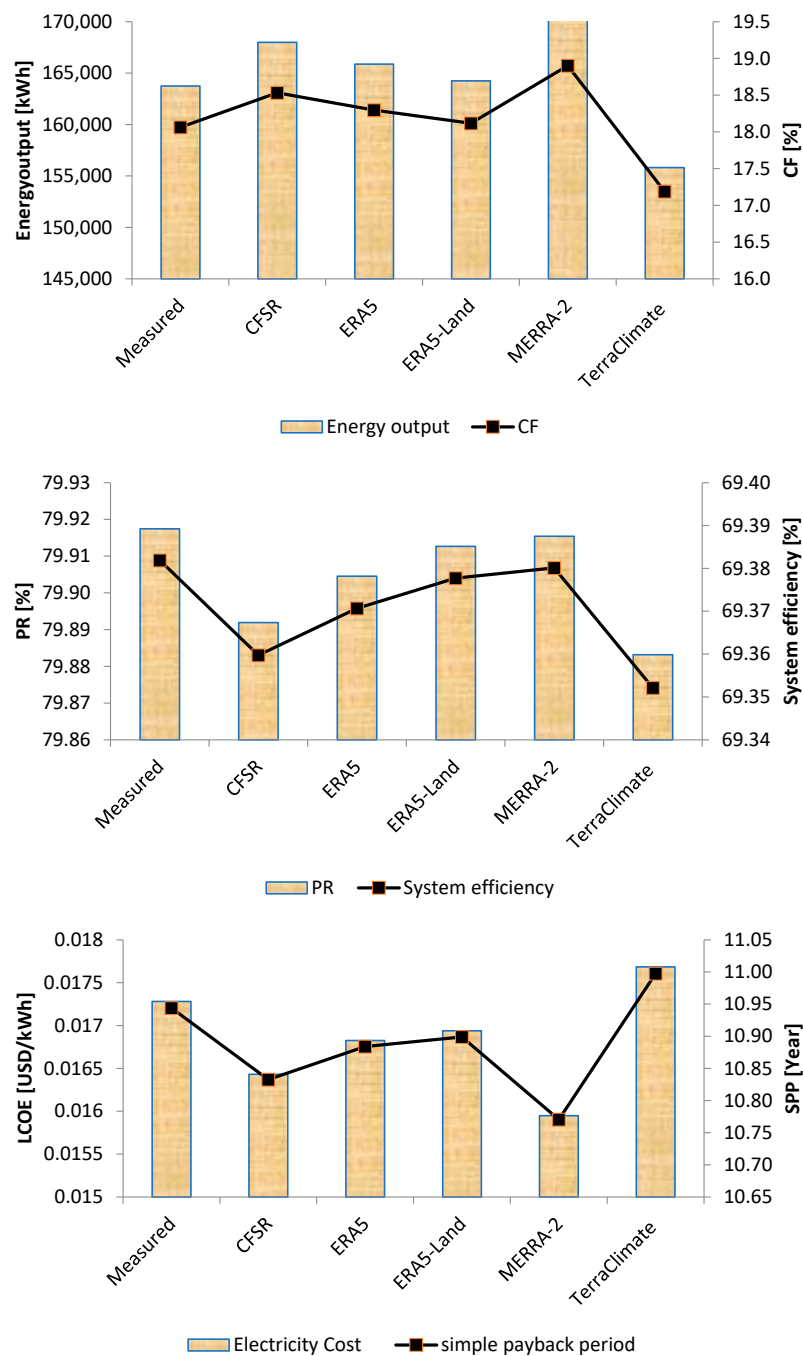


Figure 12. Performance of PV project in terms of EP, CF, LCO, and SPP for Farm 1.

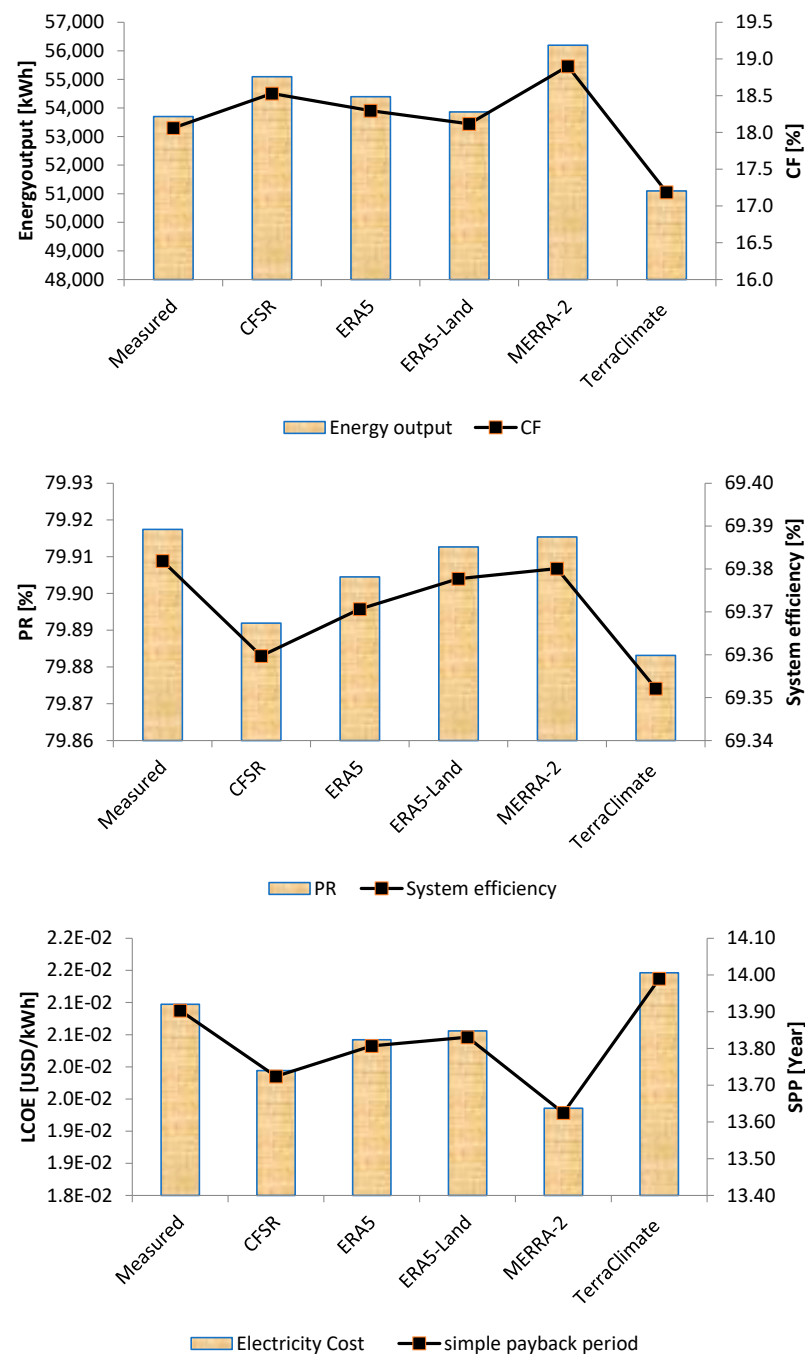


Figure 13. Performance of PV project in terms of EP, CF, LCO, and SPP for Farm 2.

Table 13. Performance of wind turbines in terms of EP, CF, LCO, and SPP for all selected locations.

Model	Parameter	Aljmail	Az-Zāwiyah	Castelverde	Msallatah	Sabratah
VAWT	EP [kWh]	136,984.92	136,181.38	140,164.78	143,662.34	141,862.04
	CF [%]	31.28	31.09	32.00	32.80	32.39
	SPP [Year]	10.5851	10.6476	10.3450	10.0931	10.2212
	LCOE [USD/kWh]	0.1033	0.1039	0.1009	0.0953	0.0965
HAWT	EP [kWh]	169,853.0	168,913.6	175,044.7	176,174.2	174,374.2
	CF [%]	38.78	38.56	39.50	40.22	39.92
	SPP [Year]	6.48	6.51	6.92	6.24	6.28
	LCOE [USD/kWh]	0.0632	0.0635	0.0653	0.0593	0.0609

Table 14 provides a comprehensive overview of the annual values associated with each farm. It encompasses key parameters such as EP, CF, PR, system efficiency, LCOE, and SPP. The analysis reveals that the annual EP (annual energy production) exhibits a variation across different family farms in Az-Zāwiyah and Aljmail. In Az-Zāwiyah, the minimum EP is recorded at 53,436.96 kWh for Farm 2, while the maximum EP is observed at 162,943.23 kWh for Farm 1. In Aljmail, Farm 2 has the minimum EP of 55,020.58 kWh, while Farm 1 demonstrates the maximum EP of 167,772.11 kWh. Moreover, the annual CF, PR, and system efficiency values are relatively similar across all regions. This indicates that the efficiency and performance of wind energy systems are consistently comparable, regardless of the specific location. Moreover, for Farm 1, the LCOE exhibits a range of 0.0164 to 0.0170 USD/kWh. On the other hand, for Farm 2, the LCOE varies between 0.0199 and 0.0206 USD/kWh. In terms of the SPP, Farm 1 has an estimated range of 10.83 to 10.91 years. This means that the investment in Farm 1 is expected to be recovered within this period. For Farm 2, the SPP falls within the range of 13.71 to 13.84 years.

**Table 14.** Performance of PV projects in terms of EP, CF, LCO, and SPP for all selected locations.

Family Farm	Parameter	Aljmail	Az-Zāwiyah	Castelverde	Msallatah	Sabratah
Farm 1	EP [kWh]	167,772.11	162,943.23	165,333.53	165,510.84	165,813.83
	CF [%]	18.51	17.97	18.24	18.26	18.29
	PR [%]	79.94	79.93	79.93	79.94	79.93
	System efficiency [%]	69.40	69.39	69.39	69.40	69.40
	LCOE [USD/kWh]	0.0164	0.0170	0.0167	0.0167	0.0166
	SPP [Year]	10.83	10.91	10.87	10.86	10.86
Farm 2	EP [kWh]	55,020.58	53,436.96	54,220.85	54,279.00	54,378.36
	CF [%]	18.51	17.97	18.24	18.26	18.29
	PR [%]	79.94	79.93	79.93	79.94	79.93
	System efficiency [%]	69.40	69.39	69.39	69.40	69.40
	LCOE [USD/kWh]	0.0199	0.0206	0.0203	0.0202	0.0202
	SPP [Year]	13.71	13.84	13.78	13.77	13.77

#### 4. Discussion

Understanding the variability of wind/solar energy potential serves as valuable guidance for policymakers and investors in determining the optimal locations and developing wind/solar projects in Libya. In the deployment stages of wind/solar energy systems, understanding the variability of wind speed and solar radiation variability becomes a vital factor in assessing the feasibility of these projects. However, due to the lack of measurement data, utilizing data derived from satellite measurements and various reanalysis becomes paramount in advancing the assessment and forecasting of next-generation wind and solar resources. These alternative data sources serve as crucial tools for evaluating the potential and economic viability of wind and solar energy in specific locations [60,85,87,89,92,122–124]. The reliability and suitability of these products need to be carefully evaluated before estimating wind and solar resources.

Considering the above, firstly, the present study aimed to investigate the performance of five satellite products with various resolutions against the average daily and monthly measured data (wind speed and solar radiation) for January 2022–December 2022 at Az-Zāwiyah, Libya. The results demonstrate that CFSR performed the best, whereas MERRA-2 was the weakest for average daily and monthly wind speed data. In general, the choice of satellite product for evaluating the wind energy potential depends on the spatial resolution and specific location. For instance, Jung and Schindler [95] found that utilizing wind speed data with higher resolution is imperative to enhance the prioritization of suitable sites for wind turbine installation at the local and global scale. Satyanarayana Gubbala et al. [125] confirmed that ERA (ECMWF ReAnalysis) wind data have proved to be valuable for accurately estimating the wind potential by validating the data against corresponding observations from automatic weather stations and wind turbine locations. Gualtieri [126]

concluded that ERA5 reanalysis data are sufficiently reliable in offshore locations as well as flat onshore areas. Yildirim et al. [127] found that ERA5 data exhibited stronger agreement with the onshore sites when compared to MERRA-2 dataset. Piasecki et al. [128] concluded that the wind speed data obtained from ERA5 demonstrated a closer alignment with the actual measurements taken on the ground, suggesting a higher level of accuracy and reliability compared to the wind speed data derived from MERRA. Khatibi and Krauter [129] found high correlation coefficients between MERRA-2 wind speed data and the measured data. Moreover, the findings of the study reveal a strong agreement between the estimations of solar radiation using ERA5-Land data and the ground measurements. Moreover, the results indicate that the solar radiation from the satellite products can be used for conducting preliminary assessments of solar resources, providing valuable insights for solar energy planning and implementation based on the RRMSE value. These results can be supported by previous scientific studies. Piasecki et al. [128] found strong agreement between solar radiation data from selected satellite products (ERA5 and CAMS) and ground measurements. Kassem et al. [116], Khatibi and Krauter [129], Gairaa and Bakelli [130], and Belgilani et al. [131] found close agreement between estimated (NASA, MERRA-2) and measured monthly global solar radiation data.

Secondly, this study examined the wind and solar potential and conducted an economic viability assessment for wind and solar energy systems in Az-Zāwiyah, Libya. Both measured data and the most reliable satellite products were utilized for wind speed and solar radiation analysis from January 2022 to December 2022. To assess the wind energy potential, 13 distribution functions were employed to analyze the wind characteristics in Az-Zāwiyah. The distribution parameters were calculated using the MLM method, and subsequently, the wind power density value was determined to classify the wind resources in the region. Additionally, solar energy resources are categorized based on calculation of the annual solar radiation. The findings indicated that the selected region exhibits a higher potential for solar energy compared to wind energy. This conclusion is consistent with previous scientific studies, as shown in Table 1.

The performance of wind and solar energy systems in terms of CF, LCOE, and SSP was investigated in selected locations. For the wind energy aspect, two distinct 50 kW wind turbines were selected for analysis. As for solar energy, two solar plants of varying capacities were proposed, considering the daily load requirements for family farms. The study aims to assess the effectiveness, cost-efficiency, and system feasibility of these renewable energy solutions in meeting the energy needs of family farms in the specified locations. The results showed that the annual CF value for both wind turbines was within the range of 16.9–41.2%, which varies based on the specific dataset employed in the analysis. Also, the results indicated that the LCOE and SSP for both wind turbines are within the range of 0.0675–0.138 USD/kWh and 9.98–19.59 years, respectively, depending on the dataset used. Other scientific researchers who analyzed the performance of a wind farm system in terms of CF and SPP can support these observations. For instance, Allouhi et al. [132] found that CF values were within the range of 31.1–49% and 37.3–56.6% for turbines with hub heights of 50 m and 75 m. Adeyeye et al. [123] found that SSP, LCOE, and CF for the BWT 61 m–800 kW wind turbine ranged from 1.9–27.3 years, 0.04 USD/kWh to 0.43 USD/kWh, and 4.5% to 37.2%, respectively. Alsaad [133] found that the payback period for different wind farms with a capacity of 100 MW ranged from 6.34 years to 19.9 years. Ucar and Balo [134] found that the values of CF and LCOE produced by various wind turbines were within the range of 32–38% and 0.255–0.306 USD/kWh, respectively. Ammari et al. [135] found that the CF values varied from 6.8% to 47.6% using various wind turbines with various characteristics. Moreover, according to the finding of Ref. [136], the CF values using different wind turbines are estimated to be within the range of 22.9–50.6%. Furthermore, the findings regarding the solar plants revealed that the annual CF for both farms fell within the range of 17.2% to 18.9%, depending on the specific dataset used in the analysis. Additionally, the results indicated that the LCOE and SSP for both farms ranged from 0.0159 USD/kWh to 0.0215 USD/kWh and from 10.99 years to 13.99 years,

respectively. These values were influenced by the dataset employed in the analysis. These results are supported by previous studies. For example, Kassem and Abdalla [108] determined that the LCOE for a 5 kW Vertical Axis Wind Generator-V ranged from 0.08703 to 0.01025 USD/kWh. In comparison, the LCOE for a 5 kW grid-connected PV system varied from 0.036 to 0.049 USD/kWh. The authors also found that the annual capacity factor (CF) for the PV system ranged from 18.72% to 19.1%, while for wind systems, it ranged from 2.58% to 56.10%. Moreover, according to Owolab et al. [124], the proposed PV system has an annual CF ranging from 20.70% to 21.70%. Additionally, the authors [124] determined that the SPP and LCOE for the developed PV system varied from 13.6 to 14.6 years and from 0.128 to 0.135 USD/kWh, respectively. Mohammadi et al. [137] found that the LCOE for the developed PV system was found to range between 112.3 and 125.6 USD/MWh. Moreover, the annual CF varied from 17.5% to 20.03%, and SPP was within the range of 6.38 to 7.00 years. Imam and Al-Turki [138] found that CF, PR, and LCOE are 22%, 78%, and 0.0382 USD/kWh, respectively, for 12.25 kW grid-connected PV systems. Kassem and Abdalla [108] determined that the LCOE for a 5 kW Vertical Axis Wind Generator-V ranged from 0.08703 to 0.01025 USD/kWh. In comparison, the LCOE for a 5 kW grid-connected PV system varied from 0.036 to 0.049 USD/kWh. The authors also found that the annual capacity factor (CF) for the PV system ranged from 18.72% to 19.1%, while for wind systems, it ranged from 2.58% to 56.10%.

Thirdly, the economic viability of the proposed PV and wind energy systems was evaluated using the best satellite products in five coastal agriculture areas. Monthly data from 2000 to 2022 were collected to assess the impact of the period on the performance and profitability of these systems. The results showed that the CF value is within the range of 31.09–32.80% and 17.97–18.29% for wind and solar systems, respectively. The findings indicate that the CF for the PV system remains consistent between the periods of January 2022 to December 2022 and 2000 to 2022. However, for the wind system, the CF for the period of 2000 to 2022 is higher compared to the period of January 2022 to December 2022. This difference may be attributed to the spatial variability. It should be noted that satellite and reanalysis data depend on spatial resolution. The spatial resolution of satellite and reanalysis data plays a significant role in determining their accuracy and level of detail. The data with higher spatial resolution provides more detailed information about the Earth's features and phenomena. High-resolution satellite data allow for a better understanding of spatial patterns and can capture fine-scale variations in variables. Moreover, the algorithms used to process satellite/reanalysis data can influence the accuracy of the final product. Differences in algorithms, data processing techniques, and assumptions can contribute to variations in accuracy. Additionally, the results showed that electricity cost generated from wind and solar systems remains constant for both periods. Similarly, the SPP is considered constant. This suggests that the electricity cost and simple payback period can remain relatively consistent over different periods due to technological stability, solar resource availability, and system efficiency.

## 5. Conclusions

The current study investigated the preliminary assessment of wind and solar energy potential in five coastal agricultural areas in Libya. The analysis relied on multiple data sources (measured data, reanalysis, and dataset analysis). The results revealed that these selected areas show significantly greater potential for solar energy generation than wind energy. Furthermore, the results confirmed the feasibility of implementing solar power plants of different scales. At the same time, small-scale wind energy systems can be used to generate electricity from wind energy in these locations. Wind and PV systems can offer a viable solution to meet the energy demands of family farms while also providing the potential for freshwater production to enhance agricultural productivity. It is important to note that the cost of electricity generated by these systems may be higher compared to conventional systems. However, their implementation holds significant benefits, particularly in addressing the chronic lack of electricity and water crises. Furthermore, wind and PV

systems contribute to reducing emissions, aligning with sustainable development goals. By harnessing the renewable energy potential of wind and solar power, these systems present an opportunity to alleviate the strain on conventional energy sources and mitigate environmental impacts. Despite the initial higher cost, the long-term advantages, such as energy security, reduced reliance on fossil fuels, and minimized greenhouse gas emissions, make wind and PV systems an attractive option for sustainable energy generation. Overall, the adoption of wind and PV systems not only offers a feasible means of meeting energy needs for family farms but also addresses critical issues of electricity scarcity, water crises, and environmental sustainability, promoting a pathway towards sustainable development in the country.

## 6. Future Work

In general, Libya's vast desert landscape and location in the Sun Belt provide ample exposure to the sun. The country's coastline also facilitates a steady flow of winds from both land and sea. As a result, some locations can have both a high potential for wind and solar energy generation due to a combination of geographic, meteorological, and climatic factors. Therefore, these areas present opportunities for diverse and reliable renewable energy generation, contributing to a cleaner and more sustainable energy mix. Therefore, future work should focus on implementing hybrid wind and solar systems that can take advantage of both sources, ensuring a constant supply of energy throughout the day and even during changing weather patterns as well as reducing the dependence on fossil fuels. Moreover, the suitability of specific sites for wind and solar installations with various scales should be studied by analyzing measured data and considering factors such as land availability, transportation infrastructure, and grid integration. In addition, making informed decisions about integrating wind and solar energy systems into Libya's energy matrix requires comprehensive studies. Hence, it is necessary to discuss the development of supportive policies, regulatory frameworks, and financial incentives to attract private investment and encourage the growth of future renewable energy projects to ensure a reliable and sustainable energy supply in Libya.

**Supplementary Materials:** The following supporting information can be downloaded at <https://www.mdpi.com/article/10.3390/en16186725/s1>, Table S1: Utilization of the satellite database for evaluating the potential of wind energy in various regions; Table S2: Model performance rating based on RRMSE; Table S3: Summary of reviewed studies on analyzing WSCs at different locations (worldwide) using various distribution functions (DFs); Table S4: Distribution parameters for all models used based on daily measured data; Table S5: Distribution parameters for all models used based on daily CFSR data; Table S6: Distribution parameters for all models used based on daily ERA5-Land data; Table S7: Distribution parameters for all models used based on whole-year data; Table S8: Distribution parameters for all models used based on monthly data; Table S9: Statistical estimators of the daily solar radiation in W/m<sup>2</sup> using various datasets for Az-Zāwiyah; Table S10: Distribution parameters for all models used based on monthly ERA5-Land dataset; Table S11: Distribution parameters for all models used based on monthly CFSR dataset; Table S12: Wind turbine characteristics; Table S13: Specification of selected PV panel; Figure S1: Libya map; Figure S2: Average daily solar radiation for Az-Zāwiyah during 2022; Figure S3: Characteristic machine power curves; Figure S4: Monthly variation in EP using VAWTs; Figure S5: Monthly variation in EP using HAWTs; Figure S6: Monthly variation in CF using VAWTs; Figure S7: Monthly variation in CF using HAWTs.

**Author Contributions:** Conceptualization, Y.K. and H.S.A.L.; methodology, Y.K. and H.G.; software, Y.K.; validation, Y.K. and H.S.A.L.; investigation, Y.K. and H.S.A.L.; writing—original draft preparation, Y.K., H.G. and A.K.; writing—review and editing, Y.K., H.G. and A.K.; supervision, A.K. All authors have read and agreed to the published version of the manuscript.

**Funding:** This research received no external funding.

**Data Availability Statement:** The data that support the findings of this study are available from the corresponding author.

**Acknowledgments:** The authors would like to thank the Ataturk Education Faculty, Engineering faculty, and Civil and Environmental Engineering Faculty at Near East University for their support and encouragement.

**Conflicts of Interest:** The authors declare no conflict of interest.

## References

1. Kavari, G.; Tahani, M.; Mirhosseini, M. Wind shear effect on aerodynamic performance and energy production of horizontal axis wind turbines with developing blade element momentum theory. *J. Clean. Prod.* **2019**, *219*, 368–376. [CrossRef]
2. Irfan, M.; Elavarasan, R.M.; Hao, Y.; Feng, M.; Sailan, D. An assessment of consumers' willingness to utilize solar energy in China: End-users' perspective. *J. Clean. Prod.* **2021**, *292*, 126008. [CrossRef]
3. Hossain, M.R.; Singh, S.; Sharma, G.D.; Apostu, S.A.; Bansal, P. Overcoming the shock of energy depletion for energy policy? Tracing the missing link between energy depletion, renewable energy development and decarbonization in the USA. *Energy Policy* **2023**, *174*, 113469. [CrossRef]
4. Olabi, A.G.; Abdelkareem, M.A. Renewable energy and climate change. *Renew. Sustain. Energy Rev.* **2022**, *158*, 112111. [CrossRef]
5. Potić, I.; Joksimović, T.; Milinčić, U.; Kićović, D.; Milinčić, M. Wind energy potential for the electricity production-Knjaževac Municipality case study (Serbia). *Energy Strategy Rev.* **2021**, *33*, 100589. [CrossRef]
6. Mohamadi, H.; Saeedi, A.; Firoozi, Z.; Zangabadi, S.S.; Veisi, S. Assessment of wind energy potential and economic evaluation of four wind turbine models for the east of Iran. *Heliyon* **2021**, *7*, e7234. [CrossRef] [PubMed]
7. Dehghani-Sanij, A.R.; Al-Haq, A.; Bastian, J.; Luehr, G.; Nathwani, J.; Dusseault, M.B.; Leonenko, Y. Assessment of current developments and future prospects of wind energy in Canada. *Sustain. Energy Technol. Assess.* **2022**, *50*, 101819. [CrossRef]
8. Kassem, Y.; Gökçekuş, H.; Güvensoy, A. Techno-economic feasibility of grid-connected solar PV system at Near East University hospital, Northern Cyprus. *Energies* **2021**, *14*, 7627. [CrossRef]
9. Maammour, H.; Hamidat, A.; Loukarfi, L.; Missoum, M.; Abdeladim, K.; Nacer, T. Performance investigation of grid-connected PV systems for family farms: Case study of North-West of Algeria. *Renew. Sustain. Energy Rev.* **2017**, *78*, 1208–1220. [CrossRef]
10. Ayadi, O.; Al-Assad, R.; Al Asfar, J. Techno-economic assessment of a grid connected photovoltaic system for the University of Jordan. *Sustain. Cities Soc.* **2018**, *39*, 93–98. [CrossRef]
11. Al-Najideen, M.I.; Alrwashdeh, S.S. Design of a solar photovoltaic system to cover the electricity demand for the faculty of Engineering-Mu'tah University in Jordan. *Resour. Effic. Technol.* **2017**, *3*, 440–445. [CrossRef]
12. Elnaggar, M.; Edwan, E.; Ritter, M. Wind energy potential of Gaza using small wind turbines: A feasibility study. *Energies* **2017**, *10*, 1229. [CrossRef]
13. Alsuessi, W. General electricity company of Libya (GECOL). *Eur. Int. J. Sci. Technol* **2015**, *4*, 61–69.
14. Rohouma, W.; Zubi, H.; Sannuga, S. Adoption of Smart Grid in Libya challenges and opportunities. In Proceedings of the 3rd International Conference on Automation, Control, Engineering and Computer Science, Hammamet, Tunisia, 20–22 March 2016.
15. Sorensen, B. *Renewable Energy: Physics, Engineering, Environmental Impacts, Economics and Planning*; Academic Press: Cambridge, MA, USA, 2017.
16. Alasali, F.; Saidi, A.S.; El-Naily, N.; Alsmadi, O.; Khaleel, M.; Ghirani, I. Assessment of the impact of a 10-MW grid-tied solar system on the Libyan grid in terms of the power-protection system stability. *Clean Energy* **2023**, *7*, 389–407. [CrossRef]
17. U.S. Energy Information Administration. Country Analysis Executive Summary: Libya. 2022. Available online: <https://www.eia.gov/international/analysis/country/LBY> (accessed on 10 April 2023).
18. Dagroum, A.; Assnoui, M.; Elhsaeshi, A. *Integration of Renewable Energy into Libyan Electrical Grid, General Electricity Company of Libya (GECOL)*; United Nations: New York, NY, USA, 2014.
19. Lochner, S.; Dieckhöner, C. Civil unrest in North Africa—Risks for natural gas supply? *Energy Policy* **2012**, *45*, 167–175. [CrossRef]
20. African Development Bank Group. Libya Renewable Energy. Available online: <https://www.afdb.org/en/countries/north-africa/libya/libya-renewable-energy> (accessed on 26 April 2023).
21. Al Jazeera. Libya Eyes Clean Energy with New Wind Farm. Available online: <https://www.aljazeera.com/economy/2018/11/13/libya-eyes-clean-energy-with-new-wind-farm> (accessed on 13 November 2022).
22. National Renewable Energy Authority. *Study on Solar Energy Potential in Libya*; Renewable Energy and Energy Efficiency Authority (REEEA): Golden, CO, USA, 2006.
23. Moner-Girona, M.; Szabo, S.; Caldés, N.; Bódis, K. *Assessment of the Rooftop Solar Potential in the Mediterranean Region*; European Commission, Joint Research Centre, Institute for Energy and Transport: Petten, The Netherlands, 2011.
24. IRENA. *Renewable Energy Prospects for North Africa: Summary for Policy Makers*; International Renewable Energy Agency: Abu Dhabi, United Arab Emirates, 2016. Available online: <https://www.irena.org/publications/2016/Sep/Renewable-Energy-Prospects-for-North-Africa> (accessed on 15 May 2023).
25. Solar Energy Solutions. Solar Energy Solutions Plans to Build Libya's First 50 MW Solar Power Plant. *PV Magazine*, 5 August 2019. Available online: <https://www.pv-magazine.com/2019/08/05/solar-energy-solutions-plans-to-build-libyas-first-50-mw-solar-power-plant/> (accessed on 12 April 2023).
26. PV Magazine. LEC Plans 500 MW Sebha Solar Power Plant. *PV Magazine*, 22 October 2020. Available online: <https://www.pv-magazine.com/2020/10/22/lec-plans-500-mw-sebha-solar-power-plant/> (accessed on 20 April 2023).

27. El-Osta, W.; Belhag, M.; Klat, M.; Fallah, I.; Kalifa, Y. Wind farm pilot project in Libya. *Renew. Energy* **1995**, *6*, 639–642. [[CrossRef](#)]
28. Kershman, S.A.; Rheinländer, J.; Gabler, H. Seawater reverse osmosis powered from renewable energy sources-hybrid wind/photovoltaic/grid power supply for small-scale desalination in Libya. *Desalination* **2003**, *153*, 17–23. [[CrossRef](#)]
29. El-Osta, W.; Kalifa, Y. Prospects of wind power plants in Libya: A case study. *Renew. Energy* **2003**, *28*, 363–371. [[CrossRef](#)]
30. Ibrahim, S. Prospects of Renewable Energy in Libya. Ph.D. Thesis, Al-Fateh University, Tripoli, Libya, 2006.
31. Abohedma, M.B.; Alshebani, M.M. Wind load characteristics in Libya. *Int. J. Civ. Environ. Eng.* **2010**, *4*, 88–91.
32. Abulqasem, K.; Alghoul, M.A.; Mohammed, M.N.; Mustafa, A.; Glaisa, K.; Amin, N.; Zaharim, A.; Sopian, K. Optimization of renewable power system for small scale seawater reverse osmosis desalination unit in Mrair-Gabis village, Libya. *Recent Res. Appl. Math. Simul. Model.* **2011**, *2011*, 155–160.
33. Mustafa, A.; Alghoul, M.A.; Asim, N.; Glaisa, K.H.; Abulqasem, K.H.; Mohammed, M.N. Potential of renewable system powering a mosque in Libya. *Models Methods Appl. Sci.* **2012**, *2012*, 139–144.
34. Ali, N.; Ramakumar, R. Impact of the penetration of wind power on the Libyan power system. In Proceedings of the 2012 IEEE Power and Energy Society General Meeting, IEEE, San Diego, CA, USA, 22–26 July 2012; pp. 1–8.
35. Mohamed, A.M.; Al-Habaibeh, A.; Abdo, H. An investigation into the current utilisation and prospective of renewable energy resources and technologies in Libya. *Renew. Energy* **2013**, *50*, 732–740. [[CrossRef](#)]
36. Ahwide, F.; Spena, A.; El-Kafrawy, A. Estimation of electricity generation in Libya using processing technology of wind available data: The case study in Derna. *APCBEE Procedia* **2013**, *5*, 451–467. [[CrossRef](#)]
37. Asheibe, A.; Khalil, A. The renewable energy in Libya: Present difficulties and remedies. In Proceedings of the 35th IAHR World Congress, Chengdu, China, 8–13 September 2013; pp. 34–44.
38. Glaisa, K.A.; Elayeb, M.E.; Shetwan, M.A. Potential of hybrid system powering school in Libya. *Energy Procedia* **2014**, *57*, 1411–1420. [[CrossRef](#)]
39. Elmabruk, A.M.; Aleej, F.A.; Badii, M.M. Estimation of wind energy in Libya. In Proceedings of the 2014 5th International Renewable Energy Congress (IREC), Hammamet, Tunisia, 25–27 March 2014; pp. 1–6.
40. Salem Elmnefi, M.; Bofares, A.M. An Analysis of Wind Speed Distribution at Benina, Benghazi, Libya. *Appl. Mech. Mater.* **2014**, *492*, 550–555. [[CrossRef](#)]
41. Al-Behadili, S.H.; El-Osta, W.B. Life cycle assessment of Derna (Libya) wind farm. *Renew. Energy* **2015**, *83*, 1227–1233. [[CrossRef](#)]
42. Khalil, A.; Asheibe, A. The chances and challenges for renewable energy in Libya. In Proceedings of the 4th International Conference on Renewable Energy Research and Applications, Palermo, Italy, 22–25 November 2015; pp. 1–8.
43. Mohamed, A.M.; Al-Habaibeh, A.; Abdo, H. Future prospects of the renewable energy sector in Libya. In Proceedings of the SBE16, Dubai, United Arab Emirates, 17–19 January 2016; pp. 1–8.
44. Ahwide, F.; Ismail, A. Wind Energy Resources Estimation and Assessment for AL-Maqrun Town-Libya. *Sol. Energy Sustain. Dev. J.* **2016**, *5*, 22–41. [[CrossRef](#)]
45. Gawedar, A.; Ramakumar, R. Impact of wind energy system integration on the Al-Zawiya refinery electric grid in Libya. *J. Power Energy Eng.* **2016**, *4*, 11. [[CrossRef](#)]
46. Mohamed, A.M.A. Investigation into the Feasibility of the Utilisation of Renewable Energy Resources in Libya. Ph.D. Thesis, Nottingham Trent University, Nottingham, UK, 2016.
47. Tjahjana, D.D.D.P.; Salem, A.A.; Himawanto, D.A. Wind energy potential analysis in Al-Fattaih-Darnah. In *Sustainable Energy and Advanced Materials: Proceeding of the 4th International Conference and Exhibition on Sustainable Energy and Advanced Materials 2015 (ICE-SEAM 2015)*, Solo, Indonesia, 11–12 November 2015; AIP Publishing: Long Island, NY, USA, 2016; Volume 1717.
48. Ahwide, F.; Aldali, Y. Wind Characteristics and Wind Energy Potential in Libya: The case study in Derna. *Al-Mukhtar J. Eng. Res.* **2017**, *9*, 1–13.
49. Rajab, Z.; Zuhier, M.; Khalil, A.; El-Faitouri, A.S. Techno-economic feasibility study of Solar Water Heating system in Libya. In Proceedings of the 2017 8th International Renewable Energy Congress (IREC), Amman, Jordan, 21–23 March 2017; pp. 1–6.
50. Belgasim, B.; Aldali, Y.; Abdunnabi, M.J.; Hashem, G.; Hossin, K. The potential of concentrating solar power (CSP) for electricity generation in Libya. *Renew. Sustain. Energy Rev.* **2018**, *90*, 1–15. [[CrossRef](#)]
51. Mohamed, O.A.; Masood, S.H. A brief overview of solar and wind energy in Libya: Current trends and the future development. *IOP Conf. Ser. Mater. Sci. Eng.* **2018**, *377*, 012136. [[CrossRef](#)]
52. Jenkins, P.; Elmnifi, M.; Younis, A.; Emhamed, A. Hybrid power generation by using solar and wind energy: Case study. *World J. Mech.* **2019**, *9*, 81–93. [[CrossRef](#)]
53. Teyabeen, A.; Akkari, F.; Jwaid, A.; Zaghwan, A.; Abodelah, R. Assessment of Wind Energy Potential in Zwara, Libya. *Sol. Energy Sustain. Dev. J.* **2019**, *8*, 34–49. [[CrossRef](#)]
54. Shreif, H.; El-Osta, W.; Yagub, A. Wind Resource Assessment for southern part of Libya: Case Study of Hun. *Sol. Energy Sustain. Dev. J.* **2019**, *8*, 12–33. [[CrossRef](#)]
55. Kassem, Y.; Çamur, H.; AbuGharara, M.A. Assessment of wind energy potential for selecting small-scale wind turbines in low wind locations in Libya: A comparative study. *Int. J. Eng. Res. Technol.* **2019**, *12*, 820–836.
56. Yahya, W.; Nassar, A.; Mansur, F.A.; Al-Nehari, M.; Alnakhliani, M.M. Future study of renewable energy in Libya. *Int. J. Adv. Eng. Res. Sci.* **2020**, *7*, 2561. [[CrossRef](#)]
57. Moria, H.; Elmnifi, M. Feasibility study into possibility potentials and challenges of renewable energy in Libya. *Int. J. Adv. Sci. Technol.* **2020**, *29*, 12546–12560.

58. Elshabli, A.; Hashem, G.; Hossin, K. Assessment of the potential for hydrogen production from renewable resources in Libya. In Proceedings of the 2020 Advances in Science and Engineering Technology International Conferences (ASET), Dubai, United Arab Emirates, 4 February–9 April 2020; pp. 1–9.
59. Asharaa, A. An Assessment of Renewable Energy Sources (RES) Potential in Libya: An Overview. In Proceedings of the 1st International Multi-Disciplinary Conference Theme: Sustainable Development and Smart Planning (IMDC-SDSP 2020), Online, 28–30 June 2020.
60. Kassem, Y.; Çamur, H.; Aateg, R.A.F. Exploring solar and wind energy as a power generation source for solving the electricity crisis in Libya. *Energies* **2020**, *13*, 3708. [[CrossRef](#)]
61. Kassem, Y.; Camur, H.; Abughinda, O.A. Solar energy potential and feasibility study of a 10MW grid-connected solar plant in Libya. *Eng. Technol. Appl. Sci. Res.* **2020**, *10*, 5358–5366. [[CrossRef](#)]
62. Almaktar, M.; Elbreki, A.M.; Shaaban, M. Revitalizing operational reliability of the electrical energy system in Libya: Feasibility analysis of solar generation in local communities. *J. Clean. Prod.* **2021**, *279*, 123647. [[CrossRef](#)]
63. Almaktar, M.; Shaaban, M. Prospects of renewable energy as a non-rivalry energy alternative in Libya. *Renew. Sustain. Energy Rev.* **2021**, *143*, 110852. [[CrossRef](#)]
64. Maka, A.O.; Salem, S.; Mehmood, M. Solar photovoltaic (PV) applications in Libya: Challenges, potential, opportunities and future perspectives. *Clean. Eng. Technol.* **2021**, *5*, 100267. [[CrossRef](#)]
65. Selimli, S.; Shtewi, F.A.; Fahed, A.K.A.; Koymatcik, Ç.Y.; Özkaymak, M. Investigation of Wind Energy Potential of Four Different Sites of Libya by Using Weibull Distribution. *Konya J. Eng. Sci.* **2021**, *9*, 766–786. [[CrossRef](#)]
66. Elmariami, A.; Elosta, W.; Elfleet, M.; Khalifa, Y. Assessment of Energy and Environment Footprint of a Proposed Wind Farm in Western Coast of Libya Using LCA. *Preprints*, 2021.
67. Jary, A.M.; Elmnifi, M.; Said, Z.; Habeeb, L.J.; Moria, H. Potential wind energy in the cities of the Libyan coast, a feasibility study. *J. Mech. Eng. Res. Dev.* **2021**, *44*, 236–252.
68. Mrehel, O.G.; Salama, A.G. Energy generation potential from wind power in the Southern Libyan Regions. In Proceedings of the 2021 IEEE 1st International Maghreb Meeting of the Conference on Sciences and Techniques of Automatic Control and Computer Engineering (MI-STA), Tripoli, Libya, 25–27 May 2021; pp. 548–553.
69. Salim, E.; Amar, A.A. Potential of Renewable Energy Resources in Aljofra-Libya. *Int. J. Eng. Res. Technol.* **2021**, *10*, 292–299.
70. Makken, S.; Shoai, N.; Abdall, A.B. A Comprehensive Economic Analysis of Solar and Wind Power and its Suitability to Libya. In Proceedings of the International Conference on Renewable and Sustainable Energy, Elbieda, Libya, 10–13 October 2021; pp. 1–8.
71. Badi, I.; Pamučar, D.; Stević, Ž.; Muhammad, L.J. Wind farm site selection using BWM-AHP-MARCOS method: A case study of Libya. *Sci. Afr.* **2023**, *19*, e01511. [[CrossRef](#)]
72. Badi, I.; Abdulshahed, A.; Alghazel, E. Using Grey-TOPSIS approach for solar farm location selection in Libya. *Rep. Mech. Eng.* **2023**, *4*, 80–89. [[CrossRef](#)]
73. Khan, Z.A.; Imran, M.; Altamimi, A.; Diemuodeke, O.E.; Abdelatif, A.O. Assessment of wind and solar hybrid energy for agricultural applications in Sudan. *Energies* **2021**, *15*, 5. [[CrossRef](#)]
74. Xydis, G. A wind energy integration analysis using wind resource assessment as a decision tool for promoting sustainable energy utilization in agriculture. *J. Clean. Prod.* **2015**, *96*, 476–485. [[CrossRef](#)]
75. Kumar, C.M.S.; Singh, S.; Gupta, M.K.; Nimdeo, Y.M.; Raushan, R.; Deorankar, A.V.; Kumar, T.A.; Rout, P.K.; Chanotiya, C.; Pakhale, V.D.; et al. Solar energy: A promising renewable source for meeting energy demand in Indian agriculture applications. *Sustain. Energy Technol. Assess.* **2023**, *55*, 102905. [[CrossRef](#)]
76. Kanwal, A.; Tahir, Z.U.R.; Asim, M.; Hayat, N.; Farooq, M.; Abdullah, M.; Azhar, M. Evaluation of reanalysis and analysis datasets against measured wind data for wind resource assessment. *Energy Environ.* **2022**, *4*, 1258–1284. [[CrossRef](#)]
77. Ben, U.C.; Akpan, A.E.; Mbonu, C.C.; Ufuafuonye, C.H. Integrated technical analysis of wind speed data for wind energy potential assessment in parts of southern and central Nigeria. *Clean. Eng. Technol.* **2021**, *2*, 100049. [[CrossRef](#)]
78. Sanz Rodrigo, J.; Buchlin, J.M.; van Beeck, J.; Lenaerts, J.; van den Broeke, M.R. Evaluation of the antarctic surface wind climate from ERA reanalyses and RACMO2/ANT simulations based on automatic weather stations. *Clim. Dyn.* **2013**, *40*, 353–376. [[CrossRef](#)]
79. Carvalho, D.; Rocha, A.; Gómez-Gesteira, M.; Santos, C.S. Offshore wind energy resource simulation forced by different reanalyses: Comparison with observed data in the Iberian Peninsula. *Appl. Energy* **2014**, *134*, 57–64. [[CrossRef](#)]
80. McKenna, R.V.; Hollnaicher, S.; van der Leye, P.O.; Fichtner, W. Cost-potentials for large onshore wind turbines in Europe. *Energy* **2015**, *83*, 217–229. [[CrossRef](#)]
81. Mentis, D.; Hermann, S.; Howells, M.; Welsch, M.; Siyal, S.H. Assessing the technical wind energy potential in Africa a GIS-based approach. *Renew. Energy* **2015**, *83*, 110–125. [[CrossRef](#)]
82. Mentis, D.; Siyal, S.H.; Korkovelos, A.; Howells, M. A geospatial assessment of the techno-economic wind power potential in India using geographical restrictions. *Renew. Energy* **2016**, *97*, 77–88. [[CrossRef](#)]
83. Arreyndip, N.A.; Joseph, E. Small 500 kW onshore wind farm project in Kribi, Cameroon: Sizing and checkers layout optimization model. *Energy Rep.* **2018**, *4*, 528–535. [[CrossRef](#)]
84. Onea, F.; Rusu, E. Sustainability of the reanalysis databases in predicting the wind and wave power along the European coasts. *Sustainability* **2018**, *10*, 193. [[CrossRef](#)]
85. Olauson, J. ERA5: The new champion of wind power modelling? *Renew. Energy* **2018**, *126*, 322–331. [[CrossRef](#)]

86. Carvalho, D.; Rocha, A.; Gómez-Gesteira, M.; Santos, C.S. WRF wind simulation and wind energy production estimates forced by different reanalyses: Comparison with observed data for Portugal. *Appl. Energy* **2014**, *117*, 116–126. [[CrossRef](#)]
87. Dabar, O.A.; Awaleh, M.O.; Kirk-Davidoff, D.; Olauson, J.; Söder, L.; Awaleh, S.I. Wind resource assessment and economic analysis for electricity generation in three locations of the Republic of Djibouti. *Energy* **2019**, *185*, 884–894. [[CrossRef](#)]
88. Boudia, S.M.; Santos, J.A. Assessment of large-scale wind resource features in Algeria. *Energy* **2019**, *189*, 116299. [[CrossRef](#)]
89. Gudo, A.J.A.; Deng, J.; Belete, M.; Abubakar, G.A. Estimation of Small Onshore Wind Power Development for Poverty Reduction in Jubek State, South Sudan, Africa. *Sustainability* **2020**, *12*, 1483. [[CrossRef](#)]
90. Arreyndip, N.A.; Joseph, E.; David, A. Wind energy potential assessment of Cameroon's coastal regions for the installation of an onshore wind farm. *Heliyon* **2016**, *2*, 1–19. [[CrossRef](#)]
91. Miao, H.; Dong, D.; Huang, G.; Hu, K.; Tian, Q.; Gong, Y. Evaluation of Northern Hemisphere surface wind speed and wind power density in multiple reanalysis datasets. *Energy* **2020**, *200*, 117382. [[CrossRef](#)]
92. Ruiz, S.A.G.; Barriga, J.E.C.; Martínez, J.A. Wind power assessment in the Caribbean region of Colombia, using ten-minute wind observations and ERA5 data. *Renew. Energy* **2021**, *172*, 158–176. [[CrossRef](#)]
93. Gualtieri, G. Reliability of ERA5 reanalysis data for wind resource assessment: A comparison against tall towers. *Energies* **2021**, *14*, 4169. [[CrossRef](#)]
94. Hiçsönmez, B.; Kassem, Y.; Gökçekuş, H. Techno-Economic Assessment of Wind Potential at Five Locations In Northern Cyprus Using Open Source Wind Data. *Int. J. Sci. Technol. Res.* **2021**, *10*, 294–299.
95. Jung, C.; Schindler, D. On the influence of wind speed model resolution on the global technical wind energy potential. *Renew. Sustain. Energy Rev.* **2022**, *156*, 112001. [[CrossRef](#)]
96. Fekih, A.; Abdelouahab, M.; Marif, Y. Evaluation of wind resource and mapping during 2009–2018 based on ERA5 reanalysis data: A case study over Algeria. *Int. J. Energy Environ. Eng.* **2022**, *14*, 15–34. [[CrossRef](#)]
97. Celik, A.N. A statistical analysis of wind power density based on the Weibull and Rayleigh models at the southern region of Turkey. *Renew. Energy* **2004**, *29*, 593–604. [[CrossRef](#)]
98. Hussain, I.; Haider, A.; Ullah, Z.; Russo, M.; Casolino, G.M.; Azeem, B. Comparative Analysis of Eight Numerical Methods Using Weibull Distribution to Estimate Wind Power Density for Coastal Areas in Pakistan. *Energies* **2023**, *16*, 1515. [[CrossRef](#)]
99. Serban, A.; Paraschiv, L.S.; Paraschiv, S. Assessment of wind energy potential based on Weibull and Rayleigh distribution models. *Energy Rep.* **2020**, *6*, 250–267. [[CrossRef](#)]
100. Ali, S.; Lee, S.M.; Jang, C.M. Statistical analysis of wind characteristics using Weibull and Rayleigh distributions in Deokjeok-do Island–Incheon, South Korea. *Renew. Energy* **2018**, *123*, 652–663. [[CrossRef](#)]
101. Ouarda, T.; Charron, C.; Shin, J.-Y.; Marpu, P.; Al-Mandoos, A.; Al-Tamimi, M.; Ghedira, H.; Al Hosary, T. Probability distributions of wind speed in the UAE. *Energy Convers. Manag.* **2015**, *93*, 414–434. [[CrossRef](#)]
102. Alayat, M.M.; Kassem, Y.; Çamur, H. Assessment of wind energy potential as a power generation source: A case study of eight selected locations in Northern Cyprus. *Energies* **2018**, *11*, 2697. [[CrossRef](#)]
103. Khan, M.A.; Çamur, H.; Kassem, Y. Modeling predictive assessment of wind energy potential as a power generation sources at some selected locations in Pakistan. *Model. Earth Syst. Environ.* **2019**, *5*, 555–569. [[CrossRef](#)]
104. Alavi, O.; Mohammadi, K.; Mostafaeipour, A. Evaluating the suitability of wind speed probability distribution models: A case of study of east and southeast parts of Iran. *Energy Convers. Manag.* **2016**, *119*, 101–108. [[CrossRef](#)]
105. Masseran, N. Evaluating wind power density models and their statistical properties. *Energy* **2015**, *84*, 533–541. [[CrossRef](#)]
106. Kassem, Y.; Gökçekuş, H.; Iravani, A.; Gökçekuş, R. Predictive suitability of renewable energy for desalination plants: The case of Güzelyurt region in northern Cyprus. *Model. Earth Syst. Environ.* **2021**, *8*, 3657–3677. [[CrossRef](#)]
107. Natarajan, N.; Vasudevan, M.; Rehman, S. Evaluation of suitability of wind speed probability distribution models: A case study from Tamil Nadu, India. *Environ. Sci. Pollut. Res.* **2022**, *29*, 85855–85868. [[CrossRef](#)]
108. Kassem, Y.; Abdalla, M.H.A. Modeling predictive suitability to identify the potential of wind and solar energy as a driver of sustainable development in the Red Sea State, Sudan. *Environ. Sci. Pollut. Res.* **2022**, *29*, 44233–44254. [[CrossRef](#)] [[PubMed](#)]
109. Aries, N.; Boudia, S.M.; Ounis, H. Deep assessment of wind speed distribution models: A case study of four sites in Algeria. *Energy Convers. Manag.* **2018**, *155*, 78–90. [[CrossRef](#)]
110. Wais, P. Two and three-parameter Weibull distribution in available wind power analysis. *Renew. Energy* **2017**, *103*, 15–29. [[CrossRef](#)]
111. Filom, S.; Radfar, S.; Panahi, R.; Amini, E.; Neshat, M. Exploring wind energy potential as a driver of sustainable development in the southern coasts of Iran: The importance of wind speed statistical distribution model. *Sustainability* **2021**, *13*, 7702. [[CrossRef](#)]
112. Kassem, Y.; Gökçekuş, H.; Zeitoun, M. Modeling of techno-economic assessment on wind energy potential at three selected coastal regions in Lebanon. *Model. Earth Syst. Environ.* **2019**, *5*, 1037–1049. [[CrossRef](#)]
113. Gökçekuş, H.; Kassem, Y.; Al Hassan, M. Evaluation of wind potential at eight selected locations in Northern Lebanon using open source data. *Int. J. Appl. Eng. Res.* **2019**, *14*, 2789–2794.
114. Khlaifat, N.; Altaee, A.; Zhou, J.; Huang, Y. Evaluation of wind resource potential using statistical analysis of probability density functions in New South Wales, Australia. *Energy Sources Part A Recovery Util. Environ. Eff.* **2020**, 1–18. [[CrossRef](#)]
115. Kassem, Y.; Gokcekus, H.; Essayah, A.M.S. Wind Power Potential Assessment at Different Locations in Lebanon: Best-Fit Probability Distribution Model and Techno-Economic Feasibility. *Eng. Technol. Appl. Sci. Res.* **2023**, *13*, 10578–10587. [[CrossRef](#)]

116. Kassem, Y.; Çamur, H.; Alhuoti, S.M.A. Solar energy technology for Northern Cyprus: Assessment, statistical analysis, and feasibility study. *Energies* **2020**, *13*, 940. [[CrossRef](#)]
117. Fazelpour, F.; Soltani, N.; Soltani, S.; Rosen, M.A. Assessment of wind energy potential and economics in the north-western Iranian cities of Tabriz and Ardabil. *Renew. Sustain. Energy Rev.* **2015**, *45*, 87–99. [[CrossRef](#)]
118. Fazelpour, F.; Markarian, E.; Soltani, N. Wind energy potential and economic assessment of four locations in Sistan and Baluchestan province in Iran. *Renew. Energy* **2017**, *109*, 646–667. [[CrossRef](#)]
119. Fornarelli, R.; Shahnia, F.; Anda, M.; Bahri, P.A.; Ho, G. Selecting an economically suitable and sustainable solution for a renewable energy-powered water desalination system: A rural Australian case study. *Desalination* **2018**, *435*, 128–139. [[CrossRef](#)]
120. WATTUNEED. Multisolar 30 kW Hybrid Inverter. Available online: <https://www.wattuneed.com/en/inverters-chargers/25737-multisolar-30kw-hybrid-inverter-0768563819032.html> (accessed on 20 April 2023).
121. WATTUNEED. Multisolar 10 kW Hybrid Inverter. Available online: <https://www.wattuneed.com/en/inverters-chargers/1177-ups-hybrid-10kw-injection-network-storage-multisolar-0712971128019.html> (accessed on 5 March 2023).
122. Rafique, M.M.; Rehman, S.; Alam, M.M.; Alhems, L.M. Feasibility of a 100 MW installed capacity wind farm for different climatic conditions. *Energies* **2018**, *11*, 2147. [[CrossRef](#)]
123. Adeyeye, K.A.; Ijumba, N.; Colton, J.S. A Techno-Economic Model for Wind Energy Costs Analysis for Low Wind Speed Areas. *Processes* **2021**, *9*, 1463. [[CrossRef](#)]
124. Owolabi, A.B.; Nsafon, B.E.K.; Roh, J.W.; Suh, D.; Huh, J.S. Validating the techno-economic and environmental sustainability of solar PV technology in Nigeria using RETScreen Experts to assess its viability. *Sustain. Energy Technol. Assess.* **2019**, *36*, 100542. [[CrossRef](#)]
125. Satyanarayana Gubbala, C.; Dodla, V.B.R.; Desamsetti, S. Assessment of wind energy potential over India using high-resolution global reanalysis data. *J. Earth Syst. Sci.* **2021**, *130*, 64. [[CrossRef](#)]
126. Gualtieri, G. Analysing the uncertainties of reanalysis data used for wind resource assessment: A critical review. *Renew. Sustain. Energy Rev.* **2022**, *167*, 112741. [[CrossRef](#)]
127. Yildirim, V.; Rusu, E.; Onea, F. Wind energy assessments in the northern Romanian coastal environment based on 20 years of data coming from different sources. *Sustainability* **2022**, *14*, 4249. [[CrossRef](#)]
128. Piasecki, A.; Jurasz, J.; Kies, A. Measurements and reanalysis data on wind speed and solar irradiation from energy generation perspectives at several locations in Poland. *SN Appl. Sci.* **2019**, *1*, 865. [[CrossRef](#)]
129. Khatibi, A.; Krauter, S. Validation and performance of satellite meteorological dataset MERRA-2 for solar and wind applications. *Energies* **2021**, *14*, 882. [[CrossRef](#)]
130. Gairaa, K.; Bakelli, Y. Solar energy potential assessment in the Algerian south area: Case of Ghardaïa region. *J. Renew. Energy* **2013**, *2013*, 496348. [[CrossRef](#)]
131. Belkilani, K.; Ben Othman, A.; Besbes, M. Assessment of global solar radiation to examine the best locations to install a PV system in Tunisia. *Appl. Phys. A* **2018**, *124*, 122. [[CrossRef](#)]
132. Allouhi, A.; Zamzoum, O.; Islam, M.R.; Saidur, R.; Kousksou, T.; Jamil, A.; Derouich, A. Evaluation of wind energy potential in Morocco's coastal regions. *Renew. Sustain. Energy Rev.* **2017**, *72*, 311–324. [[CrossRef](#)]
133. Alsaad, M.A. Wind energy potential in selected areas in Jordan. *Energy Convers. Manag.* **2013**, *65*, 704–708. [[CrossRef](#)]
134. Ucar, A.; Balo, F. Investigation of wind characteristics and assessment of wind-generation potentiality in Uludağ-Bursa, Turkey. *Appl. Energy* **2009**, *86*, 333–339. [[CrossRef](#)]
135. Ammari, H.D.; Al-Rwashdeh, S.S.; Al-Najideen, M.I. Evaluation of wind energy potential and electricity generation at five locations in Jordan. *Sustain. Cities Soc.* **2015**, *15*, 135–143. [[CrossRef](#)]
136. Bataineh, K.M.; Dalalah, D. Assessment of wind energy potential for selected areas in Jordan. *Renew. Energy* **2013**, *59*, 75–81. [[CrossRef](#)]
137. Mohammadi, K.; Naderi, M.; Saghafifar, M. Economic feasibility of developing grid-connected photovoltaic plants in the southern coast of Iran. *Energy* **2018**, *156*, 17–31. [[CrossRef](#)]
138. Imam, A.A.; Al-Turki, Y.A. Techno-economic feasibility assessment of grid-connected PV systems for residential buildings in Saudi Arabia—A Case Study. *Sustainability* **2020**, *12*, 262. [[CrossRef](#)]

**Disclaimer/Publisher's Note:** The statements, opinions and data contained in all publications are solely those of the individual author(s) and contributor(s) and not of MDPI and/or the editor(s). MDPI and/or the editor(s) disclaim responsibility for any injury to people or property resulting from any ideas, methods, instructions or products referred to in the content.